Comprehensive Vibration Assessment Program
for
US-APWR Reactor Internals

Non-proprietary Version

May 2009

ⓒ2009 Mitsubishi Heavy Industries, Ltd.
All Rights Reserved

Revision History

Revision	Date	Page	Description
0	December 2007	All	Original issued
1	May 2009	Section 1, 3,4 and 8 Appendixes	1. To reflect responses to Request for Additional Information No. 206-1576, 1577, 1578 and 1585 Revision 0 2. Composition of Chapter 3 was changed to correspond to the procedure in the validation of the analysis methodology, and add description to respond to the above RAI. 3. Replace the analysis results of the J-APWR SMT and US-APWR Prototype based on re-evaluated forcing functions for FIV and RCP loads. But the conclusion was not changed.

Abstract

A comprehensive vibration assessment program for the US-APWR reactor internals is established in accordance with the United States Nuclear Regulatory Commission Regulatory Guide 1.20 Revision 3.

The US-APWR reactor internals represent a first-of-a-kind design in its size, arrangement and operating conditions, although its components are based on a well-proven 4-loop plant design with long operational experience. Therefore the first operational US-APWR reactor internals are classified as a Prototype in accordance with Regulatory Guide 1.20. After the first US-APWR is qualified as a Valid Prototype, subsequent plants will be classified as Non-Prototype Category I.

Based on its "Prototype" classification, a comprehensive vibration assessment program is established as summarized below:
- Alternating stress levels of reactor internals due to flow induced vibrations are acceptably low in comparison with the limit for high cycle fatigue that is specified in the ASME Code.
- The difference in reactor internals vibration characteristics, such as the natural frequency of the core barrel, is very small with or without the core. The vibration responses without the core are the same or slightly larger than those with the core. These are because of the flow rate increase with the elimination of fuel assemblies and the subsequent pressure loss. Thus, in the preoperational test of the prototype plant, the results of vibration measurements after core loading are bounded by the measurements before core loading and only measurements before core loading will be necessary.
- Measurements will be performed during the pre-operational test to confirm the vibration characteristics and structural integrity of the Prototype US-APWR reactor internals.
- The reactor internals of all US-APWR plants will be inspected before and after the hot functional test. The reactor internals will not be considered adequate and pass the comprehensive vibration assessment program unless no indication of harmful sign, abnormally large vibration amplitudes or excessive wear is detected.

A comprehensive vibration assessment program for steam generator internals and the steam, feed water lines are not included in this report.

Table of Contents

List of Tables

List of Figures

List of Appendixes

<u>List of Acronyms</u>

APWR	Advanced Pressurized Water Reactor
BMI	Bottom Mounted Instrumentation
CB	Core Barrel
CHT	Cold Hydraulic Test
FEM	Finite Element Method
FIV	Flow Induced Vibration
FSI	Fluid Structural Interaction
GT	Guide Tube
HFT	Hot Functional Test
ICIS	In-core Instrumentation System
IHP	Integrated Head Package
IST	Initial Start-up Test
LCSP	Lower Core Support Plate
LDP	Lower Diffuser Plate
MHI	Mitsubishi Heavy Industries
NR	Neutron Reflector
NRC	United States Nuclear Regulatory Commission
PSD	Power Spectral Density
RCCA	Rod Cluster Control Assembly
RCP	Reactor Coolant Pump
Re	Reynolds Number
RMS	Root Mean Square
RV	Reactor Vessel
SMT	Scale Model Test
TSC	Top Slotted Column
UCP	Upper Core Plate
UDP	Upper Diffuser Plate
USC	Upper Support Column

1.0 INTRODUCTION

● **Back Ground and Objective**

A comprehensive vibration assessment program for the US-APWR reactor internals was established in accordance with the United States Nuclear Regulatory Commission Regulatory Guide 1.20 Revision 3 (Reference (1)).

The US-APWR reactor internals represent a first-of-a-kind design in its size, arrangement and operating conditions, although its components are based on a well-proven 4-loop plant design with long operational experience. Therefore the first operational US-APWR reactor internals are classified as a Prototype in accordance with the United States Nuclear Regulatory Guide 1.20 Revision 3 (Reference (1)). After the first US-APWR is qualified as a Valid Prototype, subsequent plants will be classified as the Non-Prototype Category I.

Based on its "Prototype" classification, a comprehensive vibration assessment program, consisting of four sub-programs, "Analysis, Measurement, Inspection and Evaluation", was set up for the US-APWR. This document summaries these programs.

A comprehensive vibration assessment program for the steam generator internals and the steam, feed water lines is not included in this report.

● **Description of Revision 1 of this Report**

The following modifications are included in Revision 1 of this report:

1. To reflect the responses to the following RAIs on the DCD and Revision 0 of this Vibration Assessment Program Report.

    (1) RAI206-1576
    (2) RAI206-1577
    (3) RAI204-1578
    (4) RAI272-1585

2. To reflect the latest analysis results including the following modifications after the completion of the Revision 0 analysis report

(1) Revision of the downcomer turbulent forcing functions based on the US-APWR test results

In Revision 0, measured data in the J-APWR scale model test was used for the forcing functions due to the downcomer flow turbulence. After the completion of Revision 0 of this report at the end of 2007, new data pertinent to the US-APWR configuration was obtained in the US-APWR Reactor Vessel Lower Plenum 1/7 Scale Model Flow Test (This test report has been submitted

to NRC in June of 2008 as MUAP-07022-P). MHI re-performed the analysis for the vibration assessment of the US-APWR with this new forcing function. The analysis result is reported in this Revision 1.

(2) Refinement of the vibration analysis caused by the RCP induced pressure pulsations

Two kinds of refinements were applied to the analysis of the vibration responses due to the RCP-induced pressure pulsations.

The first refinement was the re-evaluation of the RCP pulsation amplitude. In the Revision 0 analysis, the over all amplitude of the pressure fluctuation measured in the scale model test of the RCP for the APWR was applied. "Over all" means that the effect of local flow turbulence was included. In the Revision 1 analysis, the mean amplitude of the RCP pulsation was determined by additional study including spectral analysis of generic RCP data. This was still conservative because the over all pressure pulsation generated by the APWR RCP is lower than that generated by generic RCPs. As a result, the RCP pulsation amplitude was reduced to 1/5 of that in the Revision 0 analysis.

The second refinement was the justification in the time steps used in the time history analysis. The time increment was refined by an additional sensitivity study to simulate the maximum response. In the case of a perfect match of structural modal frequency with the RCP induced pressure pulsation frequency (at the shaft rotation, blade passing frequency, BPF and higher harmonics of them), the vibration amplitude increased by a factor of 5 from that without this refinement.

As a combined result of the above two refinements, the vibration responses due to RCP pulsation are about the same as those in Revision 0 of this report. Therefore, incorporation of the above two modifications has no impact on the conclusions in the assessment of the structural integrity and in the vibration measurement plan in Revision 0.

2.0 CLASSIFICATION OF REACTOR INTERNALS

2.1 Design Differences and Effects on Flow Induced Vibrations

The general design concept of the APWR is based on the current 4-loop, 193-fuel assembly plants, which have many years of operating experience both in the United States and in Japan. However, the core of the APWR was designed to accommodate 257 fuel assemblies. The US-APWR, with its 14-foot core, is a variant of the 12-foot core J-APWR developed for the Japanese utilities. As discussed in Appendix-A, the vibration characteristics of the US-APWR is similar to those of the J-APWR, the flow induced vibration of which has been verified in a scale model test. At this point there is no operational experience in any of the J-APWR plants. Therefore, the design differences and its effect on flow induced vibration are discussed with reference to the

current 4-loop plants, for the purpose of assessing the flow induced vibration characteristics of the US-APWR reactor internals, in the following subsection.

2.1.1 General Arrangement

The design concept of the US-APWR reactor internals is a normal evolution from the current 4-loop plant. Comparisons of the reactor vessel and internals between the US-APWR and the current 4-loop plant are shown in Figure 2.1-1. The general assembly of the US-APWR reactor internals is shown in Figure 2.1-2. The US-APWR reactor internal components are evolved from the well-proven 4-loop plant design currently operating in the United States and Japan. The differences are as follows;

- Design: neutron reflector instead of baffles to form the core cavity
- Size: increases in the diameters of the reactor vessel, core barrel and the secondary core support assembly.
- Arrangement: RCCA guide tubes and upper support columns in the upper plenum
- Operating conditions: increase in flow rate

The flow induced vibration characteristics of the US-APWR reactor internals are discussed and compared with the current 4-loop plant in what follows.

2.1.2 Flow Conditions

Flow paths in the US-APWR Reactor as shown in Figure 2.1-3 are similar to those in the current 4-loop plant. Both the total flow rates and the areas of flow paths in the vessel downcomer and the lower plenum of the US-APWR reactor are increased by about 30% from those in the current 4-loop plant. In the upper plenum, the diameter of the upper core support is increased by about 20% from that of the current 4-loop plant but the height of the upper plenum is maintained. Therefore, the cross-flow area is increased by about 20% from that of the current 4-loop plant. Because the flow rate is increased by about 30%, the rated cross-flow velocity is about 10% higher than that in the current 4-loop plant. Comparisons between typical flow velocities during normal operation with the current 4-loop plant are shown in Table 2.1-1.

2.1.3 Lower Reactor Internals

The Lower Reactor Internals Assembly is shown in Figure 2.1-4.

(1) Core Barrel / Lower Core Support Plate

The diameter of the core barrel of the US-APWR is about 20% larger than that of the current 4-loop design in order to accommodate an increase in the numbers of fuel assemblies from 193 to 257 to obtain a larger thermal output. The neutron reflector is a new component consisting of solid metal blocks instead of the baffle structures in the current 4-loop plant.

The core barrel stiffness is designed taking into consideration the included mass of the neutron reflector and the fuel assemblies to maintain the vibration characteristics of the current 4-loop plant. The bending stiffness of the core barrel is approximately twice that of the current 4-loop design and the vibratory response is estimated to be lower than that of the current 4-loop plant. The diameters of the core barrel and the lower core support plate are increased from those in the current 4-loop plants. This will affect the excitation force and the vibration characteristics of the lower internals assembly.

(2) Neutron Reflector / Tie Rod

Instead of the baffle structures, a new component, the neutron reflector consisting of perforated metal blocks, forms the core cavity.

(3) Lower Plenum Structures

The diffuser plate assemblies are placed in the lower plenum of the US-APWR. These assemblies are consisted of two ring plates and the support columns connecting to the lower core support plate. These constructions are similar to the tie plates and the bottom mounted instrumentation column used in the current 4-loop plant.

From the view point of flow induced vibrations, the main source of excitation is the cross-flow on the support columns. The cross-flow velocities in the lower plenum are the same as those in the current 4-loop plant. Because the shape of the reactor vessel lower plenum is semi-spherical, the support column is longer and the natural frequency of the assemblies is slightly lower but the diameter of the support column is much larger. As a result, the reduced velocity (U/fn D, where U is the flow velocity, fn is the fundamental frequency, and D is the diameter of the column), a key dimensionless parameter for flow induced vibration assessment, is reduced by 30% from that of the current 4-loop plant design. Thus sufficient margin of safety in the cross-flow induced vibration such as the fluid elastic instability is maintained.

2.1.4 Upper Reactor Internals

The Upper Internals assembly is shown in Figure 2.1-5.

The US-APWR upper internals design is based on the "Inverted top hat type upper internals" used in the current 4-loop plant. The diameter of the upper core support is enlarged by about 20% from that of the current 4-loop design as in the core barrel. The axial length remains the same as that in the current 4-loop plant.

The main flow induced vibration excitation source is cross-flow on the column structures such as the lower RCCA guide tube and the upper support column.

The diameter of the upper core support is increased by about 20% from that in the current 4-loop plant but the height of upper plenum is maintained, resulting in an increase of the cross-flow area near the outlet by about 20% from that in the current 4-loop plant. Because the flow rate is increased by about 30%, the rated cross-flow velocity in the upper plenum is about 10% higher than that in the current 4-loop plant,

(1) Upper Support Column (Standard Type)

The fundamental modal frequency of the upper support column is the same as that in the current 4-loop plant because the basic dimensions are not changed.

(2) Top Slotted Column

The top slotted column is another type of the upper support column located the core periphery, with the lager diameter and higher natural frequency than the standard type. With a stiffer body and smaller reduced velocity (U/fn D), the top slot column has improved margin against cross-flow induced vibration compared with the standard type upper support column.

(3) Upper Core Support / Upper Core Plate

The diameters of the upper core support and the upper core plate are increased from those of the current 4-loop plant. This will affect the vibration characteristics of the upper internals assembly.

(4) RCCA Guide Tube

The RCCA guide tube design in the US-APWR has been changed from that of the current plants in the following aspects:

  - Adoption of a square pipe for the lower guide tube enclosure,
  - Extension of the upper guide tube height to fit extended RCCA travel length for the 14ft core.

But the stiffness, width and length of the lower guide tube which is subject to the cross-flow in the upper plenum, are the same as those in the current 4-loop plant. Therefore any change in the fundamental modal frequency is negligible.

Table2.1-1 Comparison of Typical Flow Velocities between the US-APWR and the Current 4-loop Plant

	Typical Flow Velocities (ft/s)		Ratio
	US-APWR	Current 4-loop	
Vessel Inlet Nozzle			
Down Comer			
Lower Plenum[1]			
Core			
Upper Plenum[2]			
Vessel Outlet Nozzle			

(1) Assumed same in the down comer
(2) Maximum velocities of the RCCA guide tube location considering blockage factor
(3) Values in (   ) are velocities at the neutron panel areas.

US-APWR   **Current 4-loop Plant**
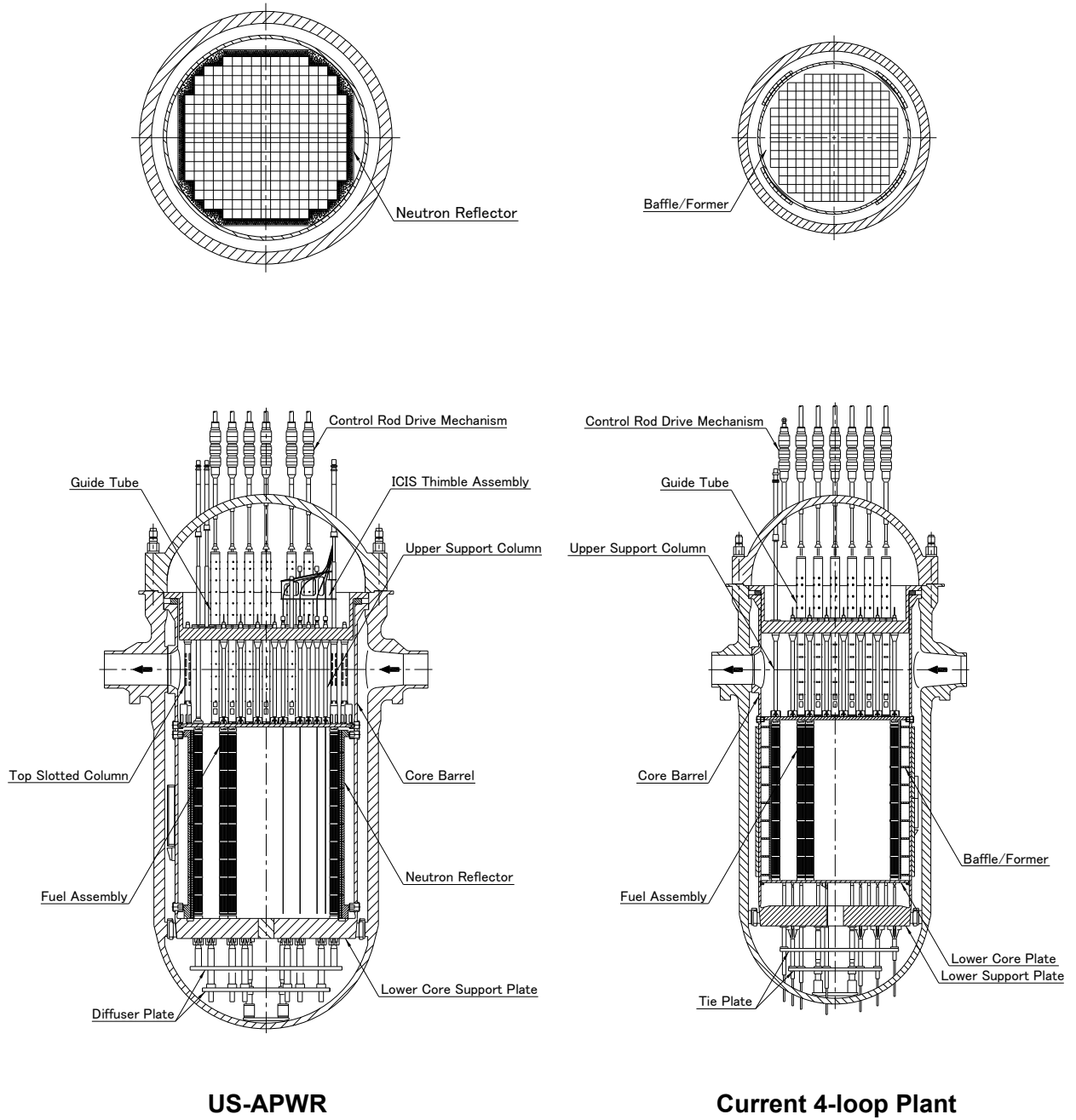
Figure 2.1-1 Comparison between the US-APWR and the Current 4-loop Reactor
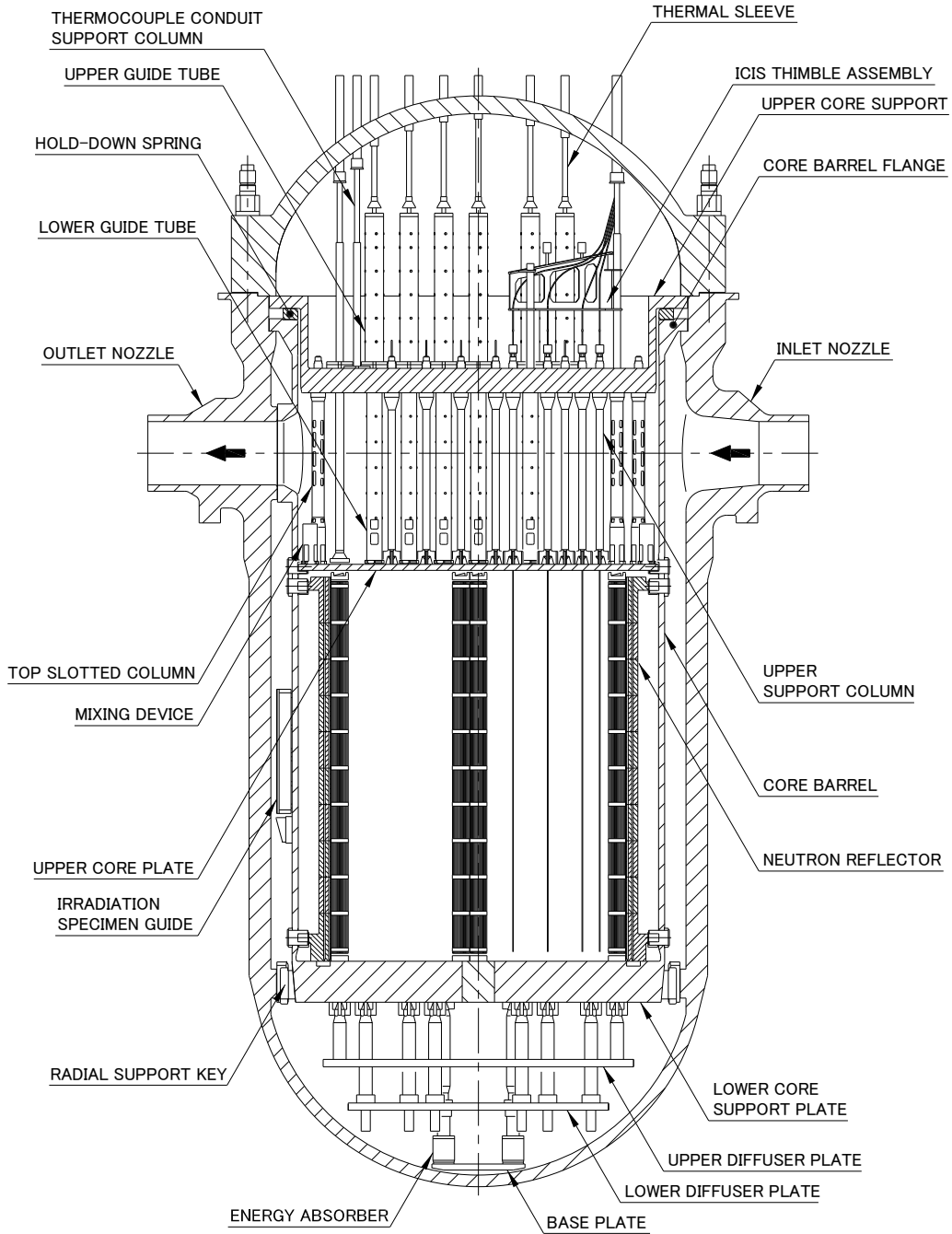
Figure 2.1-2 Reactor Internals General Arrangement
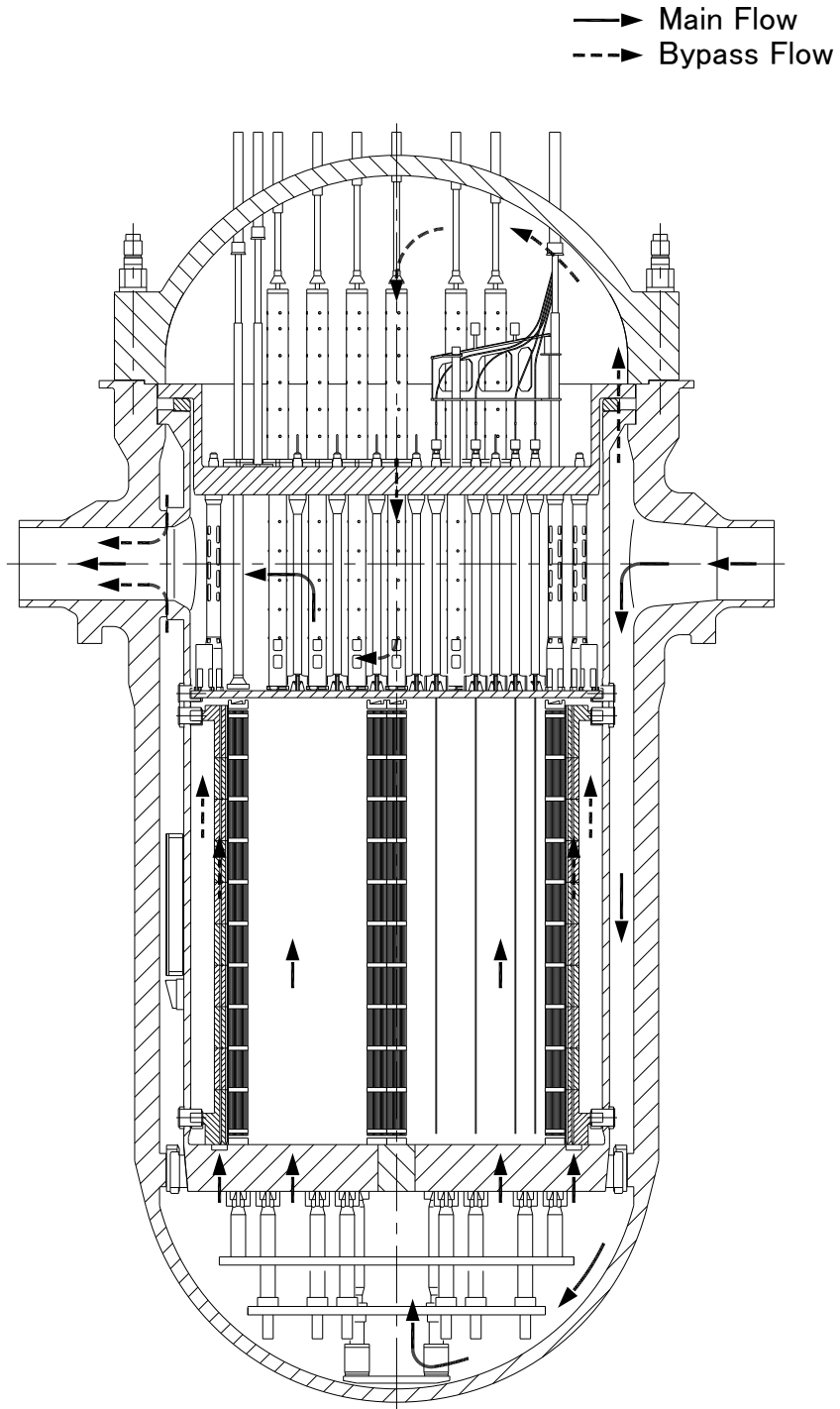
Figure 2.1-3 Reactor Internals RCS Flow and Bypass Flow Paths
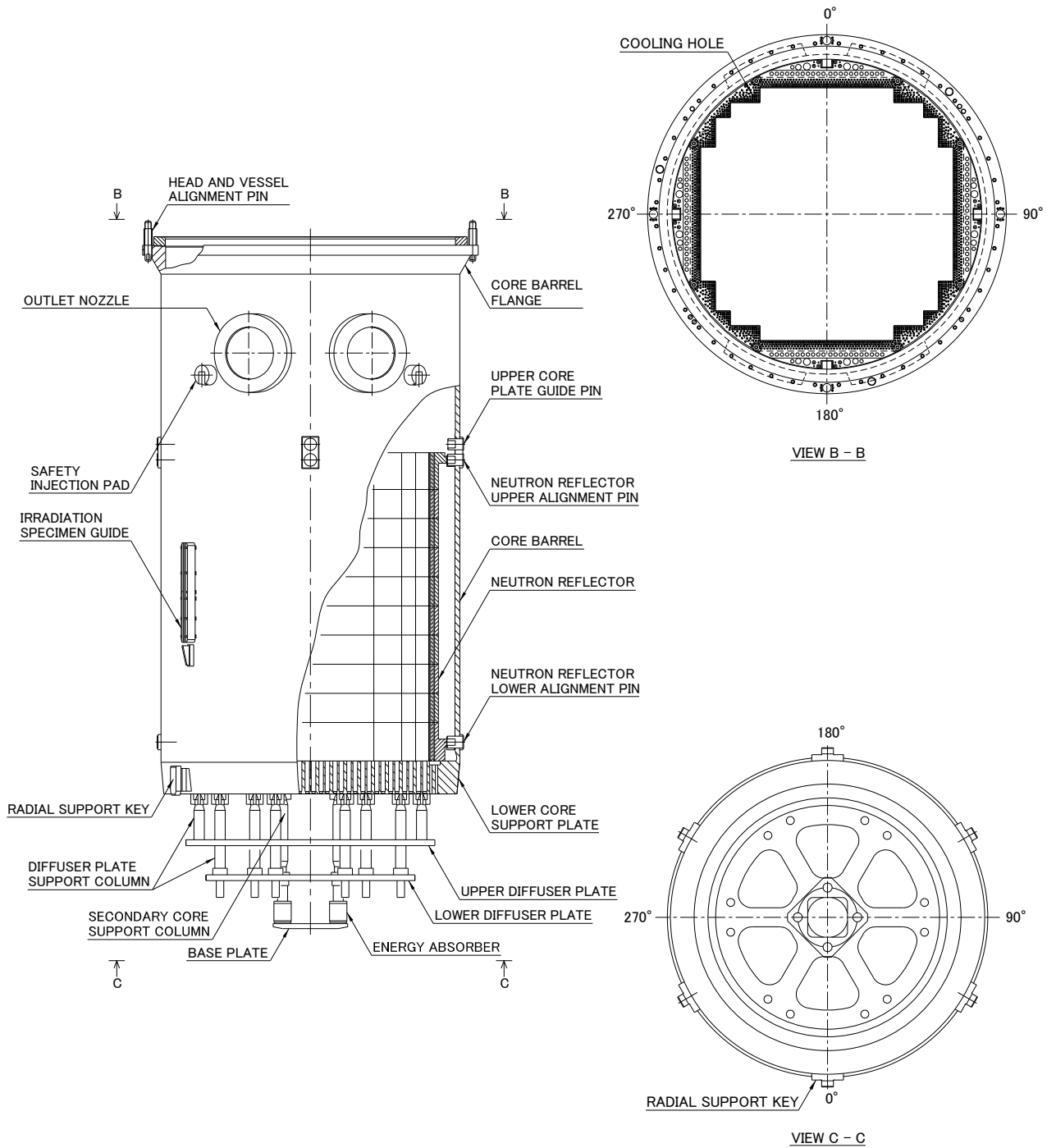
Figure 2.1-4 Lower Reactor Internals Assembly
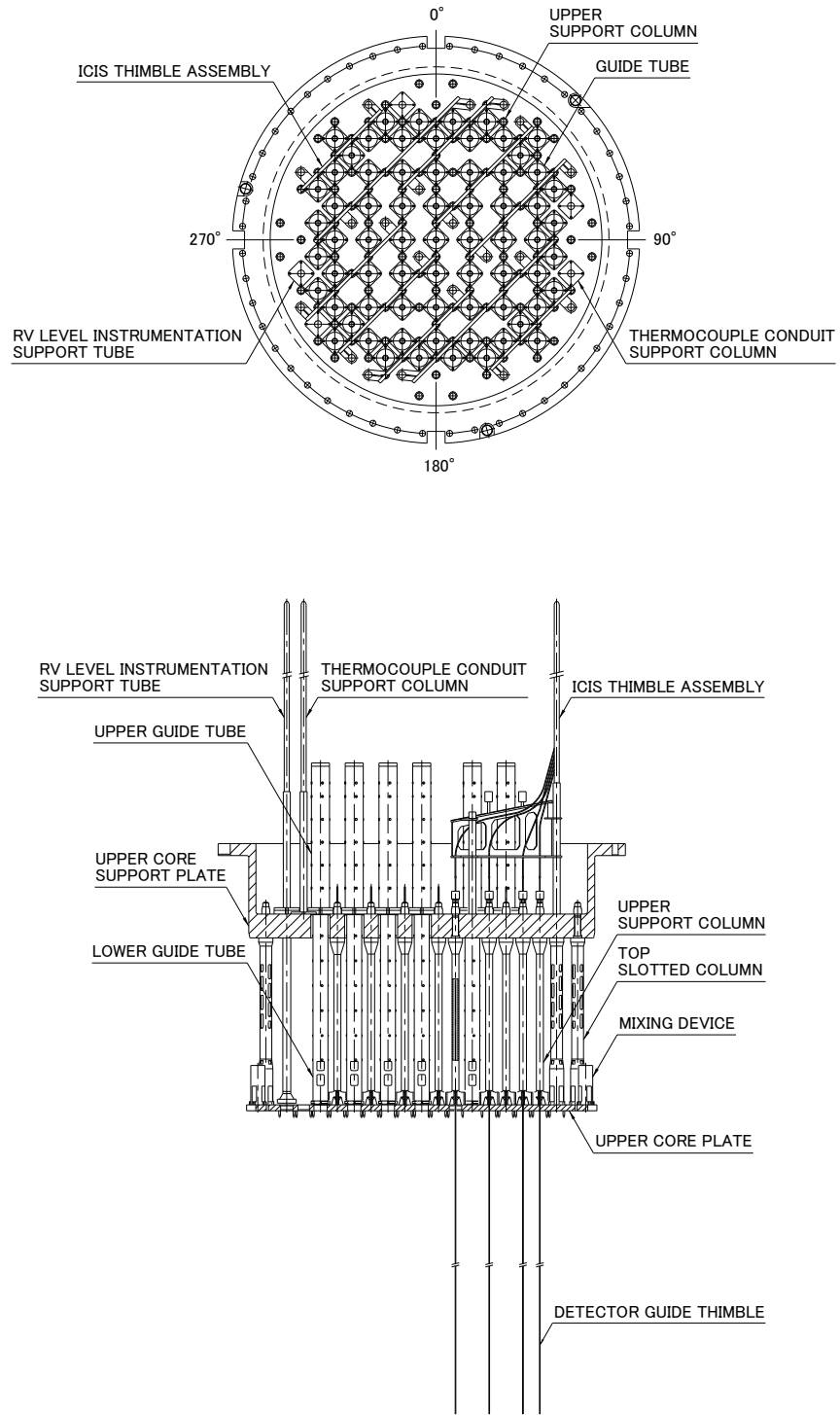
Figure 2.1-5 Upper Reactor Internals Assembly

2.2 Classification of Reactor Internals in Accordance with the Comprehensive Vibration Assessment Program

a. The first plant

The US-APWR reactor internals represent a unique, first-of-a-kind design because of its design, size, arrangements and operating conditions. Therefore, the first US-APWR will be classified as a Prototype in accordance with Regulatory Guide 1.20 Rev.3 (Reference (1)).

b. Subsequent plants

Upon qualification of the first US-APWR as a valid prototype, subsequent plants will be classified as Non-Prototype Category I.

3.0 VIBRATION AND STRESS ANALYSIS PROGRAM

In this section, the prediction analysis of the flow induced vibration response and stress of the US-APWR reactor internals are reported. At first, the procedure of the analysis is described in Subsection 3.1. Verification of the analysis method through a benchmark analysis the scale model used in the flow test is described in Subsection 3.2. The analysis results and evaluations for the US-APWR reactor internals and the predicted vibration responses under the hot functional test condition are also included are discussed in Subsection 3.3. The design margin for the adverse flow effects are discussed in Subsection 3.4 and the acceptance criteria for comparison between the analysis results and test data are given in Subsection 3.5.

3.1 Analysis Method

3.1.1 Analysis Procedure

Figure 3.1.1-1 shows the flowchart for flow induced vibration analysis of the US-APWR reactor internals. The analysis consisted of the following two tasks. Table 3.1.1-1 shows three kinds of FEM Models Used for FIV Response Analysis in the following two tasks.

Task 1: Verification of the vibration analysis methodology

The verification of the vibration analysis methodology was demonstrated using the results of the J-APWR reactor internals 1/5 scale model flow test (J-APWR 1/5 SMT) as described in Reference (7).

The J-APWR 1/5 SMT was conducted using a 1/5 scale model that simulated the reactor vessel and the reactor internals of the 12 ft-core APWR (J-APWR). In this test, the vibration characteristics of each component, the pressure fluctuations due to flow turbulence, and the vibration responses were measured (Reference (7)). The test was performed under ambient temperature and pressure.
Comparisons of dimensionless parameters between the J-APWR SMT and the US-APWR plant are discussed in Appendix-A. The J-APWR and the US-APWR of MHI APWR series have the same basic structure such as reactor vessel, core barrel, neutron reflector and upper reactor internals and similar flow rates.   On the other hand, they differ from each other in the following aspects:
(1) Increasing fuel effective length from 12ft (J-APWR) to 14ft in the US-APWR.
(2) Change in the top structure array by inserting an ICIS detector from the top of the reactor vessel (3) Simplification of the structure in the lower plenum by eliminating the Bottom Mounted Instrumentation (BMI).
Therefore, the benchmark analysis of J-APWR SMT is appropriate for the verification of the analysis methodology due to their similar flow vibration characteristics.

An alternative way of validating the analytical method is to use an operating plant as a benchmark and compare the calculated vibration responses with field test data. MHI however, does not believe this is a better way of validation due to the following reasons.

a. The vibration characteristics of the US-APWR reactor internals are close to those of the J-APWR rather than to the current 4-ioop plant, as discussed in Appendix - A.
b. This method cannot be applied to fist-of-a-kind design with significantly different dimensions or configurations, such as the neutron reflector or the core barrel.

All properties in the benchmark analysis model (the J-APWR SMT model) were adjusted to 1/5 scale. The structural model of the reactor internals was developed based on the full scale J-APWR drawings and scaled down following the scaling laws for each parameter. The stiffness of the test vessel support in the J-APWR SMT analytical model, which was not intended to simulate the vessel support stiffness in the J-APWR plant, was determined based on the measured natural frequency in the tapping test.

Two finite element (FE) models--a 3D solid system model and 3D beam system model-- were made. The modal analyses were carried out to check the validity of the structural model by comparing the computed natural frequencies with the measured frequencies in the J-APWR SMT.

The forcing functions were generated and input into the FEM models, and the vibration response analyses were conducted. The computed responses of the reactor internals for the J-APWR SMT were compared with the measured values to verify the analysis methodology and forcing function derivation. If the difference between a calculated response and measured one is not acceptable, the forcing function relate to the response should be corrected.

Task 2: US-APWR response analysis

The FEM models of the US-APWR prototype reactor internals were constructed in the same manner as the model for the J-APWR 1/5 scale model. All properties in the US-APWR prototype analysis model were developed to a full scale, based on the US-APWR drawings. The stiffness of the reactor vessel support and primary coolant loops in the US-APWR analytical model was simulated to the actual plant. In addition, two kinds of 3D beam elements were used to simulate the Control Rod Drive Mechanism (hereafter CRDM) and Integrated Head Package (IHP). The latter supports the structure of the CRDM. These were added at top of the reactor vessel model. The forcing functions for the US-APWR were modified taking into consideration the differences between the J-APWR and US-APWR in the dimensions, flow rate, fluid temperature and mass density, elasticity of the material and so on. The details of the conversion for the flow induced vibration forcing functions from the J-APWR 1/5 SMT to US-APWR prototype conditions are described in Appendix-B. In addition, the forcing function due to the RCP induced pressure pulsation in the US-APWR was included in the analysis.

The analysis results were used to predict the responses, such as displacements, strains and accelerations, at the transducer locations and to confirm the structural integrity against high cycle fatigue in each component.

3.1.2 Structural Modeling

As described in 3.1.1, after verifying the methodology with the benchmark analysis of the J-APWR 1/5 SMT (Task-1), this same methodology of structure modeling was applied to the full-scale US-APWR (Task-2). The same calculation procedure and finite element codes used in Task 1 were also used in Task 2. Here, outlines for the modeling of the J-APWR SMT and the US-APWR are described. In the benchmark analysis of the J-APWR model, the model geometry data and physical properties were based on the dimensions and materials of the 1/5 SMT and under ambient conditions. On the other hand, materials and water properties and flow rates corresponding to the general drawings of the reactor components and temperature under actual operating conditions were inputted in the full-scale US-APWR model.

(1) FEM Code and Analysis Scheme

ANSYS computer code version 11.0 was used in constructing all structure models for this analysis. The finite elements types such as solid, shell and beam elements used in this analysis, including the fluid element, have been verified by benchmark analyses of simple problems and comparing the results with theoretical values, and in the benchmark analysis of the J-APWR 1/5 SMT.

The direct time integration method was used in all vibration response analysis because of the non-linearity of the fluid element.

(2) FE Model

Three FE models were used as summarized in Table 3.1.1-1. Two kinds of system models, the 3D solid system model and the 3D beam system model were used in both the benchmark analysis of the J-APWR SMT and in the prediction analysis of the US-APWR. The third FE model was the single beam model which simulated individual components in the upper plenum of the US-APWR

a. 3D solid system model,

The reactor vessel, core barrel and neutron reflector form a triple co-axial system with fluid coupling between them. To compute the beam and shell mode responses of this system, the core barrel and the neutron reflector were modeled with solid elements. 3D-Fluid elements were used to simulate the fluid structural interaction (FSI) between the reactor vessel and the core barrel, and between the core barrel and the neutron reflector. And the reactor vessel wall was simulated with shell elements.

Mitsubishi Heavy Industries, LTD.

The beam mode natural frequencies of the core barrel and the neutron reflector, obtained from the 3D solid element model, were used to determine the added mass matrices in the 3D beam and shell element models discussed below.

b. 3D beam system model

The 3D beam element system model consisting of the reactor vessel and the entire reactor internals was used to evaluate the fundamental beam mode responses to the flow loads and RCP pulsation loads. The shell element was used only for the diffuser plates with this model. This model had beam elements for the CRDM and the IHP to simulate the proper vibration characteristics of the reactor vessel. The nodal point degrees of freedom and damping ratios of the reactor internals and surrounding structures were selected such that the most dominant frequencies were represented in the flow induced vibration and seismic-LOCA response. This formed the basis for establishing any directional decoupling and system structural partitioning in the model.

To simulate fluid structure interaction, hydrodynamic mass matrices at the following three locations were included.

(a) Between the RV and the core barrel (CB) in two horizontal directions

(b) Between the CB and the neutron reflector (NR) in two horizontal directions

(c) Between the upper core support (UCS) and the RV head in the vertical direction

The mass properties in the horizontal directions, (a) and (b) above, were determined to simulate the beam mode natural frequencies obtained in the 3D solid element model. The mass property in the vertical direction (c) was derived from a hand calculation. The 3D beam and shell element model were also applied to LOCA and seismic analyses with different boundary conditions which were justified for larger responses.

c. Single beam element models

The single beam models for the upper plenum structures such as the GT, USC and TSC which simulate the higher modal natural frequency of each structure were used to perform the response analysis with the RCP pulsations related to the blade passing frequency (NZ) or its second harmonics (2NZ). If an estimated natural frequency of the vibration mode was within 10% of the NZ or 2NZ of the RCP, the natural frequency was adjusted to coincide with the NZ or 2NZ. This was to ensure conservative results in the analysis.

(3) Force loading on the model

The combination of the analysis model types and forcing functions are summarized in Table 3.1.1-1.Each of the forcing function was generated as a time history of a distributed load. For example, the downcomer forcing functions for the 3D Solid System Model were determined as the force per unit area and applied to all of the elements surface of the core barrel and the inner surface of the reactor vessel. Vertical loads on the core support plates were applied in the same manner.

The forcing functions on the beam elements, such as the cross flow loads in the upper plenum were determined as force per unit length and applied as distributed element loads. The downcomer forcing functions on the core barrel and on the reactor vessel in the 3D beam and shell element model were applied in the same manner.

Table 3.1.1-1 FEM Models Used for FIV Response Analysis

	RV/CB/NR Solid Model	Beam System Model	Single Beam Model (GT / USC / TSC)
Applied Elements	Solid + Fluid Element	Beam + Shell	Single Beam
Output	1. CB / NR beam and shell mode natural frequency with FSI 2. CB / NR beam / shell mode response	1. Beam mode and vertical mode frequency with FSI 2. RV and reactor internals response due to flow turbulence and RCP pulsation	1. Higher beam modal frequencies 2. Response to RCP pulsation harmonics
Target Frequency Range			
Forcing Functions			
Flow Induced (Downcomer) (Lower Plenum) (Upper Plenum) (Vertical)			
RCP Pulsation (Downcomer) (Upper Plenum) (Vertical)			

TASK 1

Develop FEM Model for
J-APWR 1/5 SMT (12ft core)
First   : Solid model
Second: Beam model

J-APWR 1/5 SMT

Revise FEM Model

Frequencies / mode agree?

NO

YES

➢ Vibration characteristics
- Natural frequencies of the fundamental modes
- Damping ratio

Calculation of J-APWR SMT Response

Excitation Force

Determine correction factor of forcing function

Responses agree ?

NO

YES

➢ Vibration responses
- Displacements
- Moments

Excitation Force under actual plant conditions

TASK 2

Develop US-APWR model using same procedure
14ft core
Increase number of the USC, NR blocks
Delete lower core plate

US-APWR analysis and Evaluation
・Response: Displacement, loads
・Hi-Cycle Fatigue Evaluation

Figure 3.1.1-1 US-APWR Reactor Internals FIV Response Analysis Procedure

3.2 Verification of the vibration analysis methodology

Following the Task 1 procedure as described in 3.1.1, the vibration analysis methodology was verified by carrying out an analysis using the J-APWR 1/5 scale model as a benchmark and then comparing the computed results with the corresponding measured values in the J-APWR 1/5 SMT, as described in Reference (7)

3.2.1 Validation of Structural Models

The J-APWR SMT was conducted using a 1/5 scale model that simulated the reactor vessel and the reactor internals of the 12 ft-core APWR (J-APWR). The test was performed under ambient temperature and pressure. In this test, the vibration characteristics of each component, the pressure fluctuations due to flow turbulence, and the vibration responses were measured (Reference (7).

(1) Benchmark model analysis

As described in 3.1.2 (2), two different system models, the 3D solid system model (Figure 3.2.1-1) and the 3D beam system (Figure 3.2.1-2)   were used to simulate the scale model test.
All properties of the benchmark analysis model in the J-APWR SMT were adjusted to a 1/5 scale. The structural model of the reactor internals was developed based on the full scale J-APWR drawings and scaled down following the scaling laws for each parameter. The stiffness of the test vessel support, which did not simulate the vessel support stiffness of the actual plant, was determined based on the measured natural frequency in the tapping test. A modal analysis was carried out to check the validity of the structural model by comparing the computed natural frequencies with measured ones.

(2) Natural Frequencies of J-APWR 1/5 SMT

a.   Results

The natural frequencies of the J-APWR 1/5 SMT are shown with the J-APWR SMT results in Table 3.2.1-1. Typical mode shape of the Neutron Reflector and Core Barrel in the lower reactor internals, and the lower and upper diffuser plate support column in the lower plenum are shown in Figures 3.2.1-3 through 3.2.1-12.

b. Uncertainties and bias errors of FEM Model and analysis

A typical value of the uncertainties and bias errors of the structural natural frequencies was [   ] %, which was obtained from averaging the errors in a total of 12 pairs of natural frequencies as shown in Table 3.2.1-1.

The effect of the [   ] % error in the structural natural frequencies on the vibration response was estimated by considering the mode shapes and the frequency response functions.
It lead to [   ] % error in the random vibration response, with a conservative assumption that the [   ] % error in the natural frequency was totally caused by the uncertainty in the stiffness of structures. However the error in the mass of the model had little effect in the vibration response.

c. Validity of Structural Models

The validity of the FEM structural models were evaluated from the correlation of measured results and the frequency analysis results based on the 1/5-scale model. Category 2 acceptance criteria described in subsection 3.5 were applied as follows.

- Natural frequency for the fundamental beam mode and the lowest shell mode: with in 10%.

The results in Table 3.2.1-1 show the beam mode and shell mode natural frequencies of the core barrel and the neutron reflector with the 3D Solid System model were within the 10% criterion. The beam modes of these structures in the 3D Beam System Model with added mass matrices also satisfied this criterion.

And the beam mode frequencies of the structures in the lower plenum or the upper plenum for 3D beam system model were also within the 10% criterion except the [   ] % for the lower tie plate assembly and [   ] % for the RCCA guide tube. As for the RCCA guide tube, the analysis result is rather reliable than the measured one because of the uncertainties to simulate the support condition with alignment pins in a scale model. For the lower tie plate assemblies, analysis model was refined to simulate all columns with beam elements and the tie plate with the shell element for the US-APWR, as discussed in 3.3.1.

Therefore, the FEM modeling methodology confirmed that the physical properties and fluid elements of the structure are appropriately modeled, and can be used for the calculation of vibration response of reactor internals.

Table 3.2.1-1 Comparison of Frequencies with Test Results (J-APWR 1/5 SMT)

	Vibration Mode		Fundamental Modal Frequency (Hz)	
			Analysis	Measured
Core Barrel	Beam			
	Shell	n=2		
		n=3		
		n=4		
Neutron Reflector	Beam			
	Shell	n=2		
		n=2,diagonal		
		n=3		
		n=4		
Lower Tie Plate Assembly	Transverse			
Upper Tie Plate Assembly	Transverse			
RCCA Guide Tube (Lower Guide Tube)	Beam			
Upper Support Column	Beam			
Top Slotted Column	Beam			
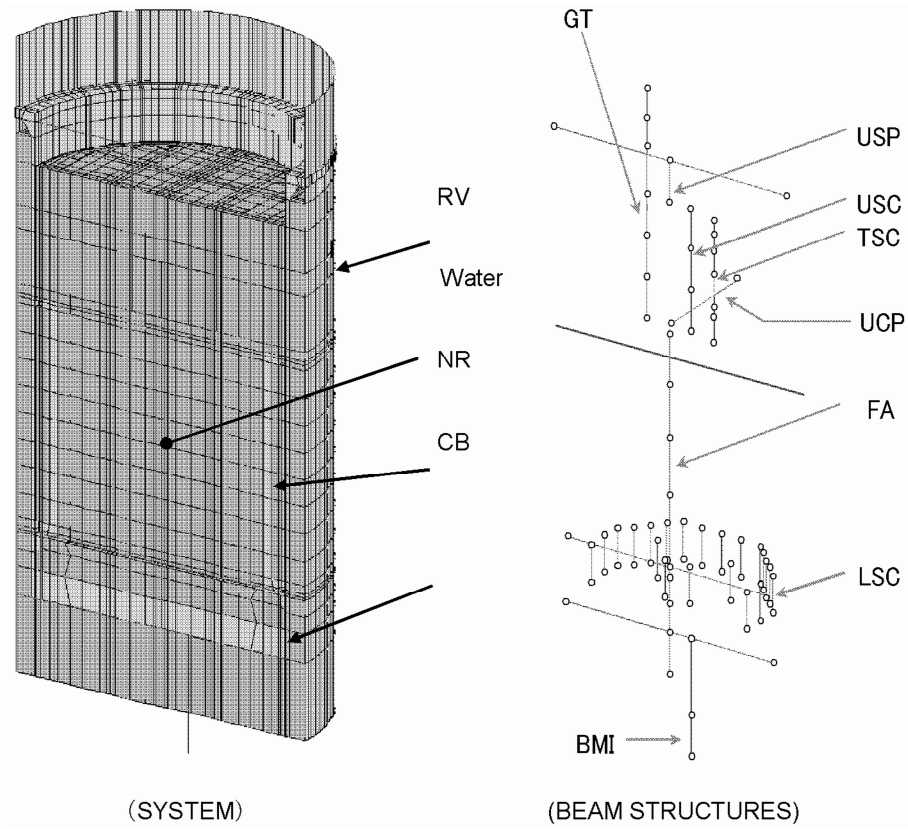
Figure 3.2.1-1 Solid System Model for J-APWR SMT Benchmark Analysis (1/2)

Reactor Vessel   Core Barrel   Neutron Reflector
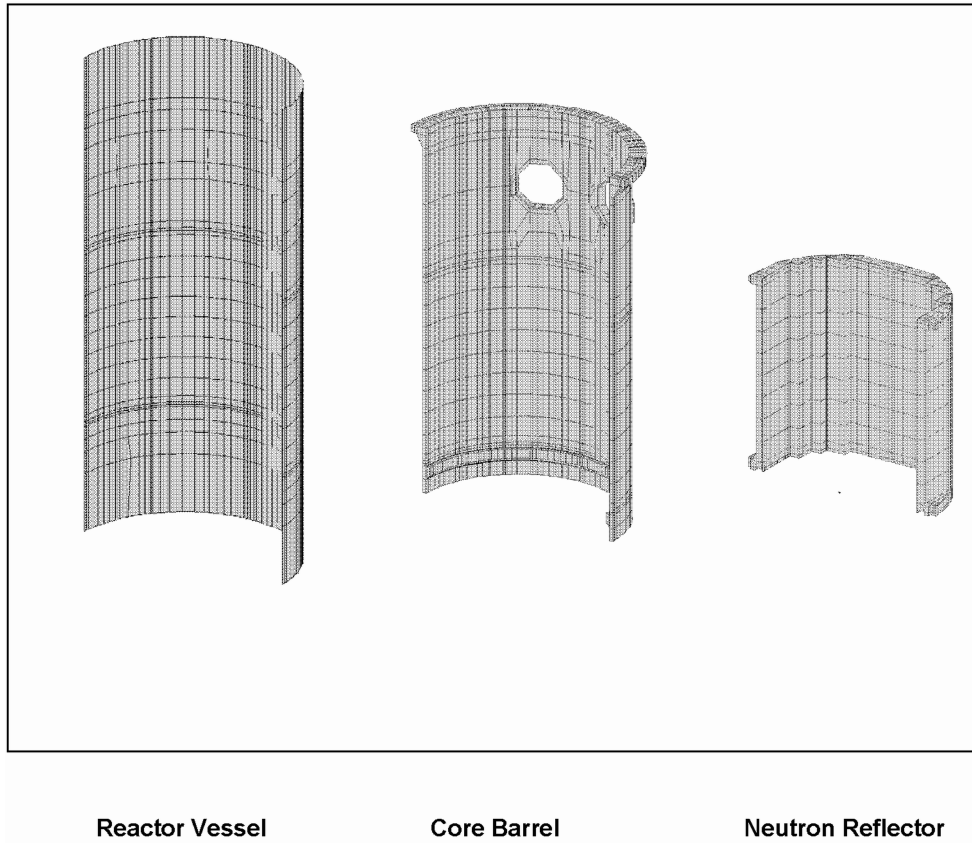
Figure 3.2.1-1 Solid System Model for J-APWR SMT Benchmark Analysis (2/2)
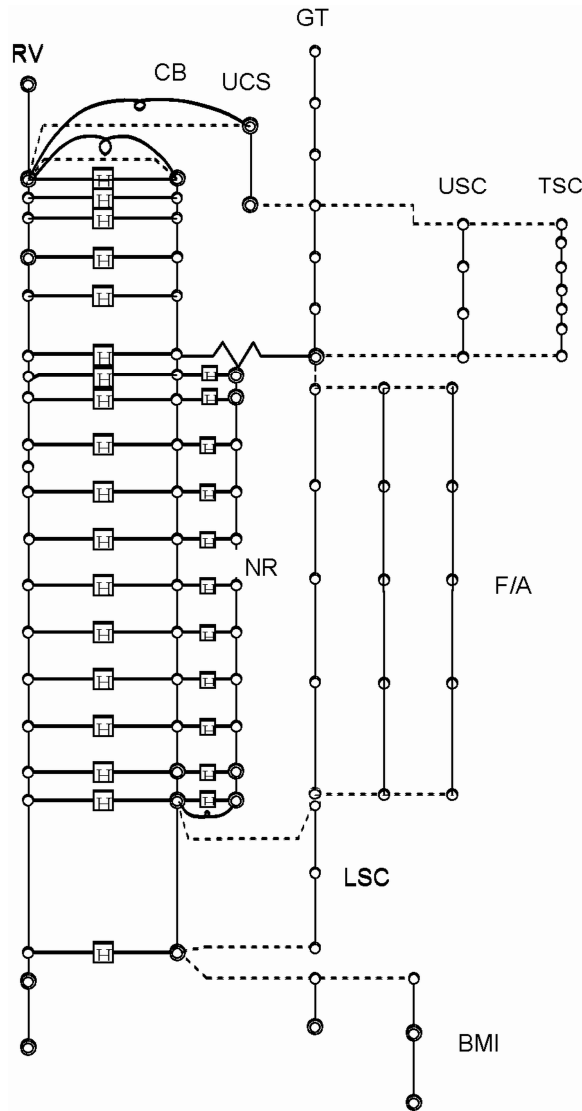
Figure 3.2.1-2   Beam System Model for J-APWR 1/5 Scale Model Analysis

Figure 3.2.1-3 Core Barrel 1ˢᵗ Beam Mode

(J-APWR SMT benchmark analysis, scaled to actual dimensions)

Figure 3.2.1-4 Neutron Reflector Beam Mode

(J-APWR SMT benchmark analysis, scaled to actual dimensions)

Figure 3.2.1-5 Neutron Reflector Shell Mode (n=2)

(J-APWR SMT benchmark analysis, scaled to actual dimensions)

Figure 3.2.1-6 Neutron Reflector Shell Modes (n=2, diagonal)

(J-APWR SMT benchmark analysis, scaled to actual dimensions)

Figure 3.2.1-7 Neutron Reflector / Core Barrel Shell Mode (n=3)
(J-APWR SMT benchmark analysis, scaled to actual dimensions)

Figure 3.2.1-8 Neutron Reflector / Core Barrel Shell Mode (n=4)
(J-APWR SMT benchmark analysis, scaled to actual dimensions)

Figure 3.2.1-9 Core Barrel

(J-APWR SMT benchmark analysis, scaled to actual dimensions)

Figure 3.2.1-10 Bottom Mounted Instrumentation

(J-APWR SMT benchmark analysis, scaled to actual dimensions)

Figure 3.2.1-11 RCCA Guide Tube

(J-APWR SMT benchmark analysis, scaled to actual dimensions)
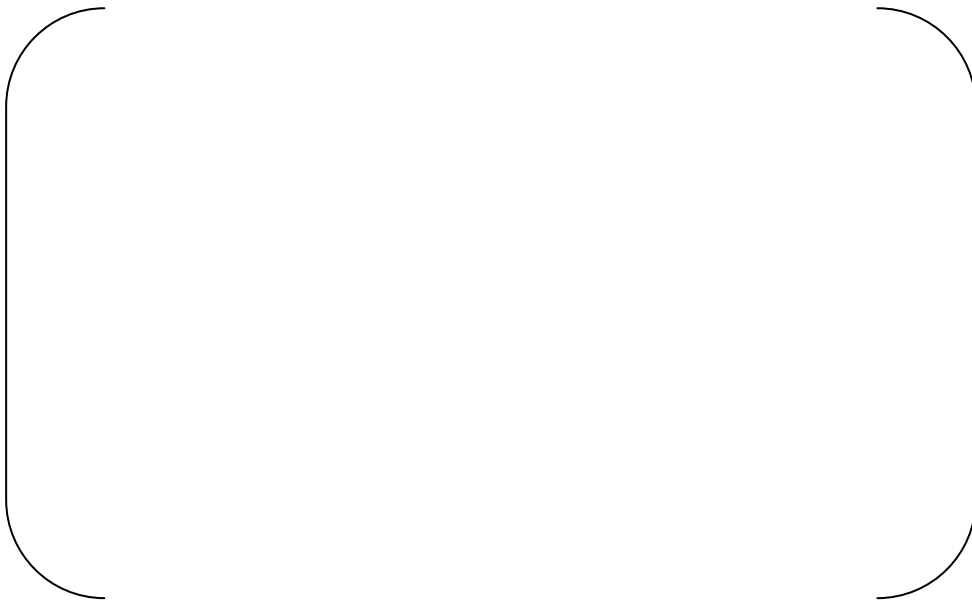
Figure 3.2.1-12 Top Slotted Column

(J-APWR SMT benchmark analysis, scaled to actual dimensions)

3.2.2 Forcing Functions for J-APWR 1/5 SMT model

In this section, two different flow induced forcing functions, which were input into the J-APWR 1/5 scale model benchmark analysis are described. The first one is from the axial flow turbulence in the downcomer. This is the main source of the vibrations of the reactor vessel, the core barrel, the neutron reflector is excited because it is coupled with the core barrel both in beam mode and shell modes. The 2nd one is the cross flow turbulence and vortex shedding loads on the structures in the lower plenum and the upper plenum.

3.2.2.1 Axial Flow Turbulence in the Downcomer

(1) Formula of the forcing function

The turbulent pressure fluctuation has been identified as the main forcing function on the reactor internals during normal operation. The methodology of the turbulence force generation was proposed by Au-Yang (Reference (4)) was followed. The Joint acceptance is a function to determine the relationship between the turbulent pressure forcing function and the displacement response. As a result, the joint acceptance integral involves both the coherence function of the pressure field and the structural mode shapes. The coherence function of the pressure field includes a convection velocity term with flow velocities in x and y directions. When the flow is in one direction (eg, x-direction), the convection term disappears in the cross-stream direction (in this case the y-direction).

MHI simplified the Joint acceptance integral as follows:
a. Assumed constant mode shape functions inside the acceptance integral.
b. Assumed the downcomer flow is purely axial so that the convection term in the pressure
   coherence function in the circumferential direction could be eliminated.

Because the joint acceptance involves integration over the entire mode shape, Assumption 1 has only a secondary effect on the joint acceptance. An example of this is shown in Figure 8.5 in Reference (4). Assumption 2 is generally valid over most of the downcomer flow surface. Since neither assumption involved the modal frequencies, the modal transfer functions were not affected. Therefore, the above two assumptions had no significant impact on the validity of the original method.

The formulas of the forcing functions are described in equations 3.2-1 through 3.2-7.

$$P_{RMS} = \frac{1}{2} C_P \rho U^2 \quad\quad\quad \text{3.2-1}$$

$$PSDP(f) = (P_{RMS})^2 \cdot \frac{PSD0(f)}{\int PSD0(f)df} \quad\quad\quad \text{3.2-2}$$

$$PSDF(f) = PSDP(f) \cdot J_X J_Y \cdot (L_X)^2 (L_Y)^2 \quad\quad\quad \text{3.2-3}$$

$$J_x = \left(1/L_x{}^2\right)\cdot \iint \Gamma(f, x_1, x_2) dx_1 dx_2 \quad\text{3.2-4}$$

$$J_y = \left(1/L_Y{}^2\right)\cdot \iint \Gamma(f, y_1, y_2) dy_1 dy_2 \quad\text{3.2-5}$$

$$\Gamma(f, x_1, x_2) = \exp(- ABS(x_1 - x_2)/\lambda_x)\cos(2\pi f(x_1 - x_2)/U) \quad\text{3.2-6}$$

$$\Gamma(f, y_1, y_2) = \exp(- ABS(y_1 - y_2)/\lambda_y) \quad\text{3.2-7}$$

where

P_{RMS}	: rms amplitude of pressure fluctuation
PSDP (f)	: power spectral density of pressure fluctuation
PSD0 (f)	: reference PSD shape
PSDF (f)	: power spectral density of force

and

J_x	: joint acceptance in axial direction
J_y	: joint acceptance in lateral direction
L_x	: length of force calculation area in axial direction
L_y	: length of force calculation area in lateral direction
$\Gamma(f, x_1, x_2)$	: coherence between 2 points x_1, x_2 in axial direction
$\Gamma(f, y_1, y_2)$	: coherence between 2 points y_1, y_2 in lateral direction
λ_x	: correlation length in axial direction
λ_y	: correlation length in lateral direction
U	: axial flow velocity (in/s)
F	: frequency (Hz)
ρ	: fluid mass density (lb/in3)
C_P	: rms pressure coefficient

(2) Measured pressure fluctuation

Normalized pressure PSD was obtained from the measured pressure fluctuation in a scale model test. In the Revision 0 analysis, results from the 1/5 scale model test of J-APWR were used. After the completion of the Revision 0 analysis, data based on the US-APWR configurations became available from US-APWR 1/7 scale model lower plenum test. After detailed analysis of this new set of data, including a sensitivity analysis, this new data from the US-APWR lower plenum model test were selected for the Revision 1 analysis. More details on the effect of replacing the downcomer pressure PSD data with this new data set are described in Appendix- C.

The measurement locations of the pressure fluctuation are summarized in Table 3.2.2-1.The rms pressure fluctuation amplitudes are summarized in Table 3.2.2-2. Figure 3.2.2-1 shows the fluctuating pressure measurement locations in the 1/7 scale test model. Figure 3.2.2-2 shows the measured pressure fluctuation in the 1/7 scale model test, and Figure 3.2.2-3 shows the downcomer pressure PSD. They show typical characteristics of turbulence spectra, which decline exponentially with increase of frequency. The spectrum at the upper part and 90 degree

from the reference point was remarkably larger because this point was located close to the inlet nozzle of the reactor vessel. This high forcing function was caused by jet impingement.

The local normalized dynamic pressure PSD as functions of the reduced frequency are shown in Figure 3.2.2-3 in semi-log scales and in Figure 3.2.2-4 in log-log scales. At the upper 90- degree location, the reactor vessel inlet nozzle velocity was used for the normalization. At the other 3 locations, the average downcomer velocity was used for normalization. The typical turbulence spectral trend is observed from the log-log plot. These logarithmic plots show that the amplitude declines did not reach the noise floor level, thus confirming that high S/N ratio was maintained in the measurement. The slope of the decline in the log-log scale plots shows the ratio of around 5 to 3 which is consistent with the 5/3rd power law of turbulence energy. This suggests that the data were physically reasonable.

(3) Correlation length

In general, the correlation length is larger in the lower frequency region. For the US-APWR analyses the following equations are defined based on the flow test data in Reference (6). The relationship between the correlation length normalized by the downcomer width and the reduced frequency is shown in Figure 3.2.2-5.

$$\lambda_x/d = 0.6(fd/U)^{-1} \quad \cdots\cdots\cdots 3.2\text{-}9$$
$$\lambda_y/d = 0.24(fd/U)^{-1} \quad \cdots\cdots\cdots 3.2\text{-}10$$

or

$$\lambda_x = 0.6\,U/f \quad \cdots\cdots\cdots 3.2\text{-}9'$$
$$\lambda_y = 0.24\,U/f \quad \cdots\cdots\cdots 3.2\text{-}10'$$

where,
- λ_x : correlation length in axial direction
- λ_y : correlation length in lateral direction

- U   : axial flow velocity (m/s)
- f   : frequency (Hz)
- d   : downcomer width (m)

(4) Sample of generated forcing function

Samples of generated time histories of the downcomer turbulent forcing function at for the typical locations are shown in Figure 3.2.2-6

3.2.2.2 Cross-Flow Turbulence and Vortex Shedding

(1) Evaluation of the cross flow velocity

The cross flow velocities distribution around the structures in the lower and upper plenum of the reactor vessel were evaluated in the following manner.

(a) Upper plenum

a. The cross flow velocities in the upper plenum were calculated based on the potential flow theory without structures in the plenum.

b. The Cross flow velocity distribution between the structures were determined based on the equation of continuity and the pitch-to-diameter ratio of the structures

c. When the cross flow is not uniform along the axis of the structure in the upper plenum, the maximum cross flow was used for vortex shedding and fluid elastic instability evaluation.

(b) Lower plenum

a. The cross flow velocity in the lower plenum was assumed to be equal to the downcomer average velocity.

b. The cross flow velocity distribution between the diffuser plate support columns was determined based on the equation of continuity and the pitch-to-diameter ratio of the support columns.

c. When the cross flow is not uniform along the axis, the maximum cross flow was used in vortex shedding and fluid elastic instability evaluations.

(2) Formula of the forcing function

The equations for the cross-flow induced loads are based on ASME Sec. III APPENDIX N (Reference (2)), "N-1300 FLOW-INDUCED VIBRATIONS OF TUBES AND TUBE BANKS" and Chapter 9 in Reference (5). These equations are applied to the column structures in the lower plenum and the upper plenum as follows.

$$\text{PSDP}(f) = \left(1/2\,\rho U^2\right)^2 \cdot (D/U) \cdot \text{PSD0} \quad \cdots\cdots\cdots\cdots\cdots\cdots\cdots\cdots\cdots\cdots\cdots\cdots 3.2\text{-}11$$

$$\begin{aligned}
\text{PSD0} &= 0.01 \text{ for } f\,D/U < 0.1 \quad \cdots\cdots\cdots\cdots\cdots\cdots\cdots\cdots\cdots 3.2\ 12\text{-a} \\
&= 0.2 \quad \text{for } 0.1 \leq f\,D/U \leq 0.4 \quad \cdots\cdots\cdots\cdots\cdots\cdots 3.2\text{-}12\text{-b} \\
&= 5.3\text{E-4 } (f\,D/U)^{(-7/2)} \text{ for } 0.4 < f\,D/U \quad \cdots\cdots\cdots\cdots 3.2\text{-}12\text{-c}
\end{aligned}$$

$$\text{PSDF}(f) = \text{PSDP}(f) \cdot J \cdot (D)^2 (L)^2 \quad \cdots\cdots\cdots\cdots\cdots\cdots\cdots\cdots\cdots 3.2\text{-}13$$

$$J = \left(1/L_x^2\right) \cdot \iint \Gamma(f, x_1, x_2)\, dx_1 dx_2 \quad \cdots\cdots\cdots\cdots\cdots\cdots\cdots\cdots 3.2\text{-}14$$

$$\Gamma(f, x_1, x_2) = \exp(-ABS(x_1 - x_2)/\lambda) \cdots\cdots\cdots\cdots\cdots\cdots\cdots 3.2\text{-}15$$

$$\lambda = 0.2P(1 + P/2D) \cdots\cdots\cdots\cdots\cdots\cdots\cdots\cdots\cdots 3.2\text{-}16$$

where,

       PSDP (f) : power spectral density of pressure fluctuation
       PSD0 (f) : normalized pressure PSD in Figure 3.2.2-7
       PSDF (f) : power spectral density of force

       J   : joint acceptance
       L   : length of force calculation area in axial direction (in)
       Γ(f, x_1,x_2) : coherence between points 1, 2 in axial direction
       λ : correlation length (in)
       U   : flow velocity (in/s)
       P   : column pitch (in)
       D   : column diameter (in)
       F   : frequency (Hz)
       ρ : fluid mass density (lb/in^3)

(3) Sample of the forcing function

Samples of generated time histories of the cross-flow turbulence induced loads for the typical locations are shown in Figure 3.2.2-8

Table 3.2.2-1 List of the Pressure Measurements in the US-APWR 1/7 Scale Model Vessel Lower Plenum Test

Measurement Item	Measuring Parts	Circumferential Location	Transducer ID	Number of Transducers
Pressure Fluctuation	Core barrel wall face to the downcomer			
Pressure Fluctuation	Vessel lower head			
Static Pressure	Along the main flow path			

Table 3.2.2-2 Rms Pressure Fluctuation of the Downcomer
(Measured in the US-APWR 1/7 Scale Lower Plenum Flow Test)

Measured Locations			Rms Pressure Fluctuation (1-100Hz in actual plant scale) (psi)	Remarks
Elevation	Direction	Transducer ID		
upper	90º	PD2	1.88	nearest to the inlet nozzle
	0º	PD1	0.70	
lower	90º	PD4	0.58	
	0º	PD3	0.49	
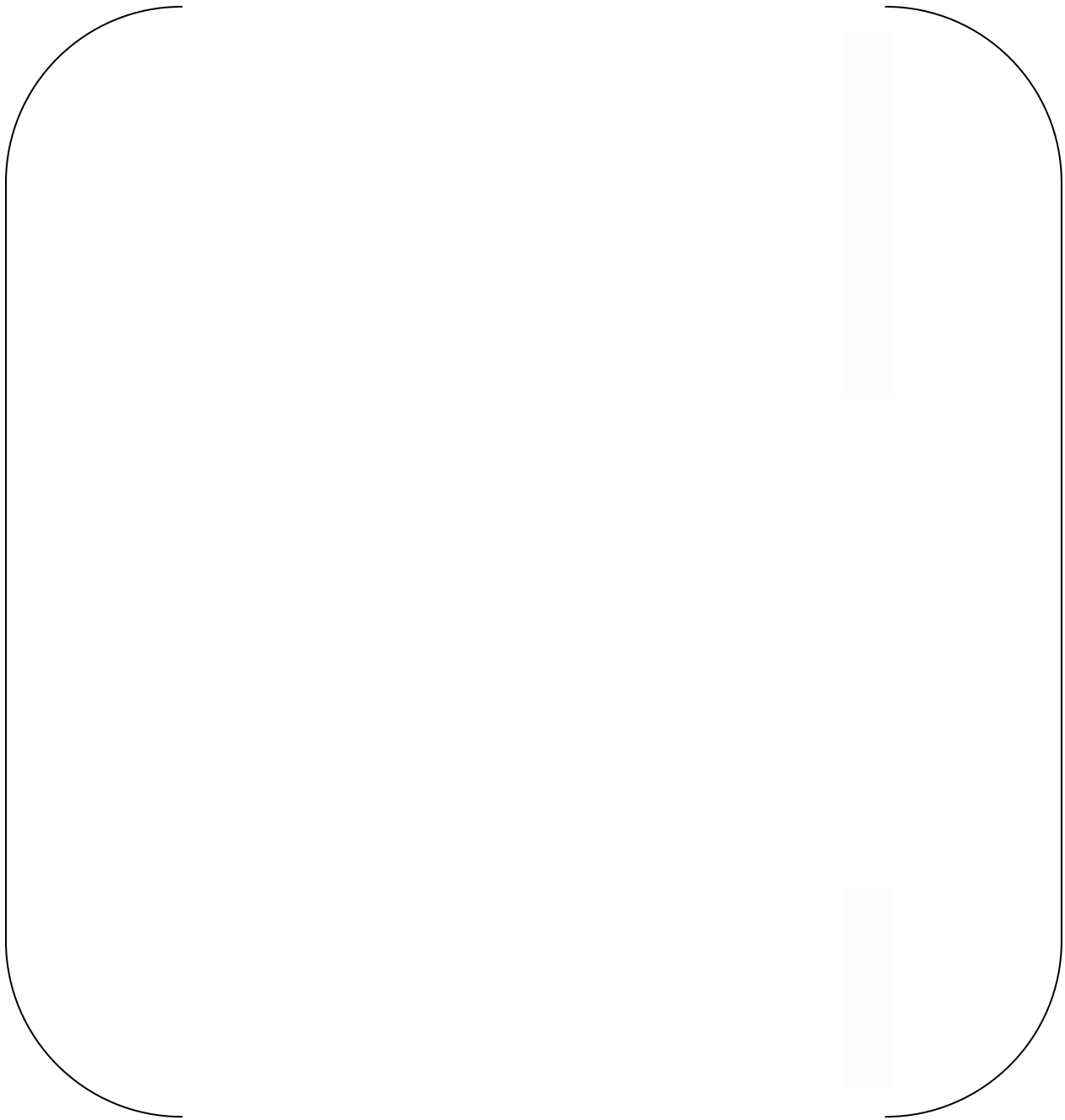
Figure 3.2.2-1   Pressure Measurement Locations in the US-APWR 1/7 Scale Vessel Lower Plenum Test
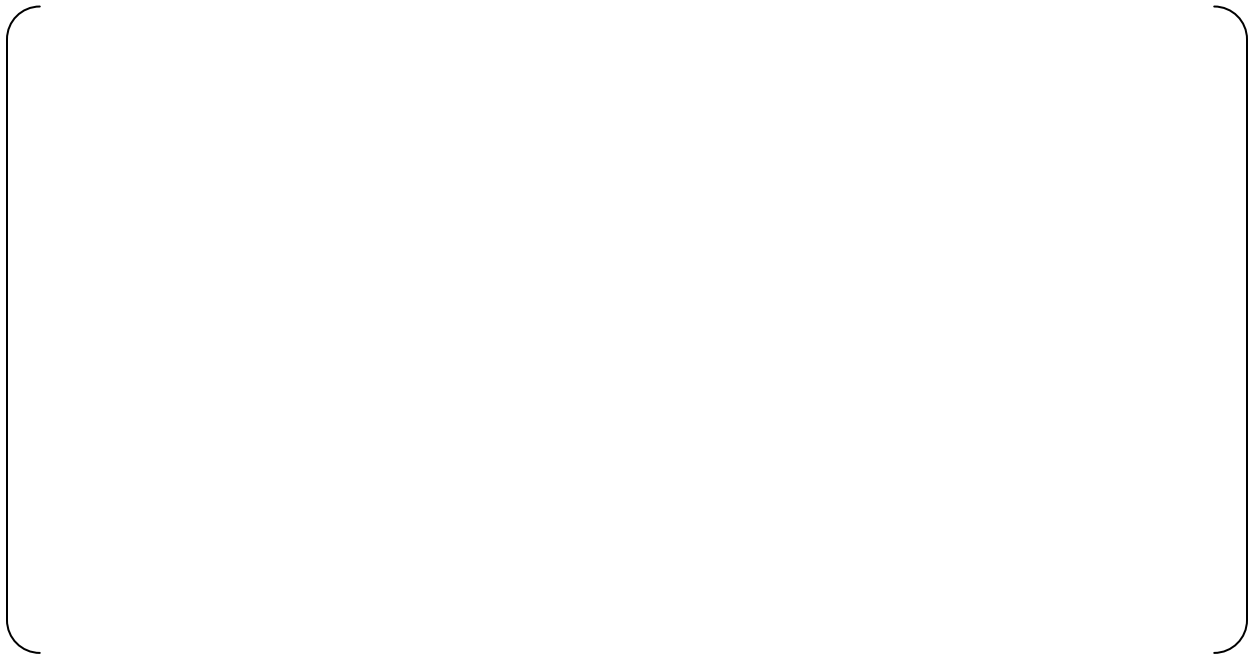
Figure 3.2.2-2 Measured Downcomer Pressure PSD vs. Frequency
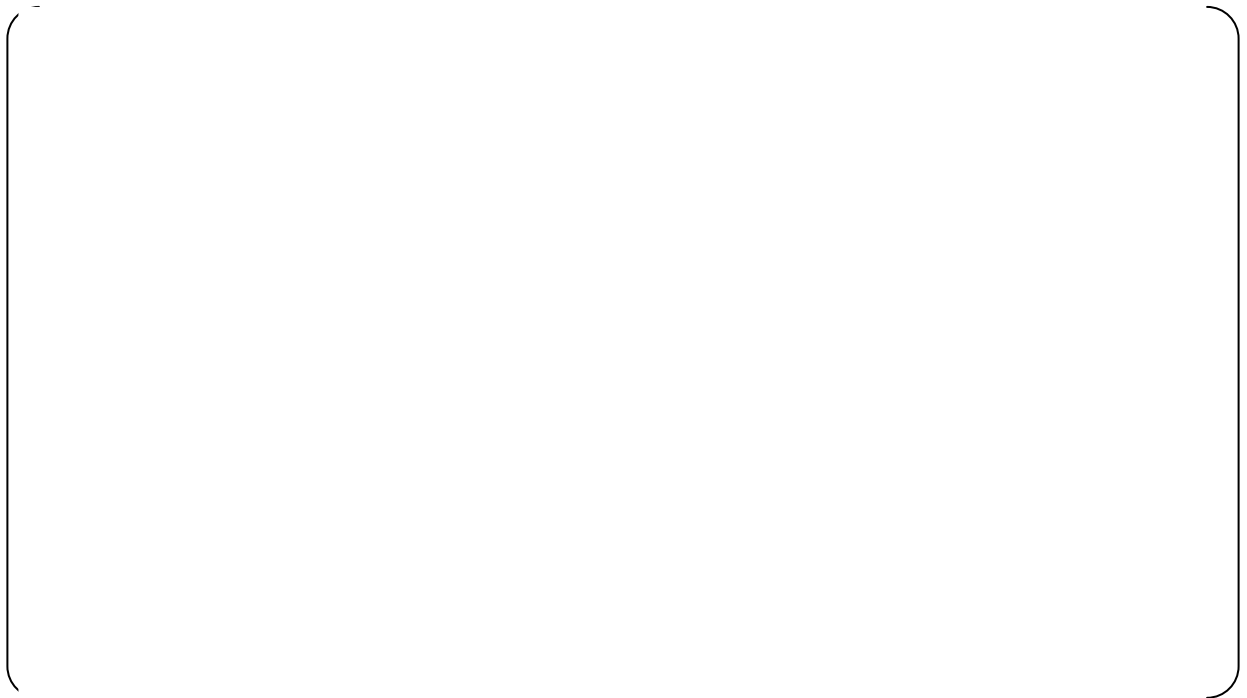
Figure 3.2.2-3 Normalized Pressure PSD vs. Reduced Frequency (Semi-log Scales)

Figure 3.2.2-4 Normalized Pressure PSD vs. Reduced Frequency (Log-log Scales)

Reference (6): M.K. Au-Yang & B. Brenneman,
Flow induced Vibration ASME 1994

f   : frequency (Hz)
λ   : correlation length (m)
d   : annulus gap (m)
U   : flow velocity (m/s)
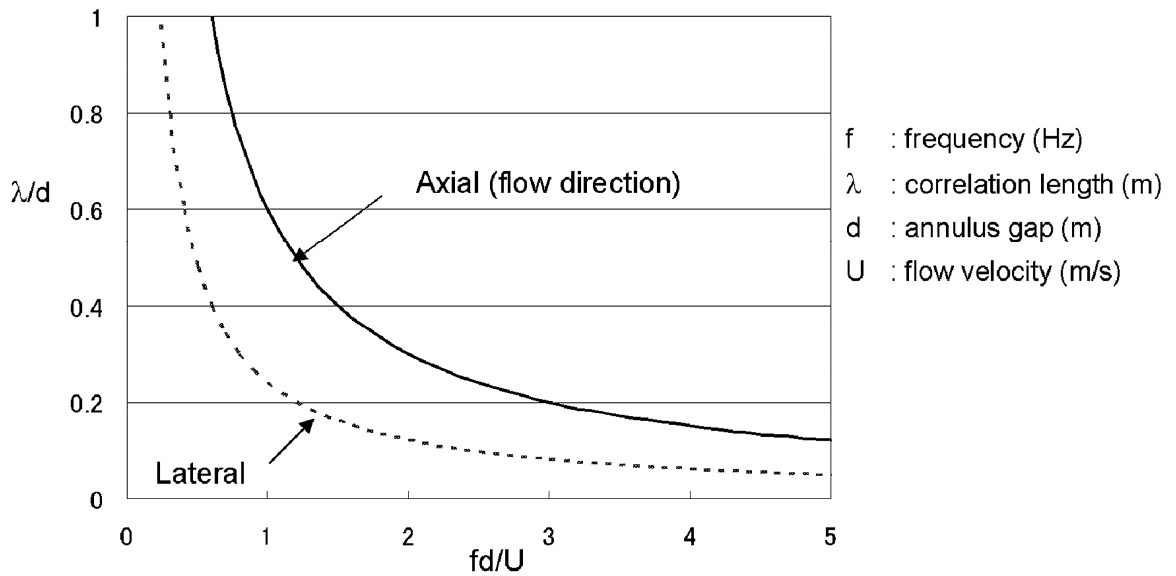
Figure 3.2.2-5 Correlation Length for the Downcomer

Figure 3.2.2-6 Downcomer Turbulent Forcing Functions
(Input of J-APWR SMT Benchmark Analysis)
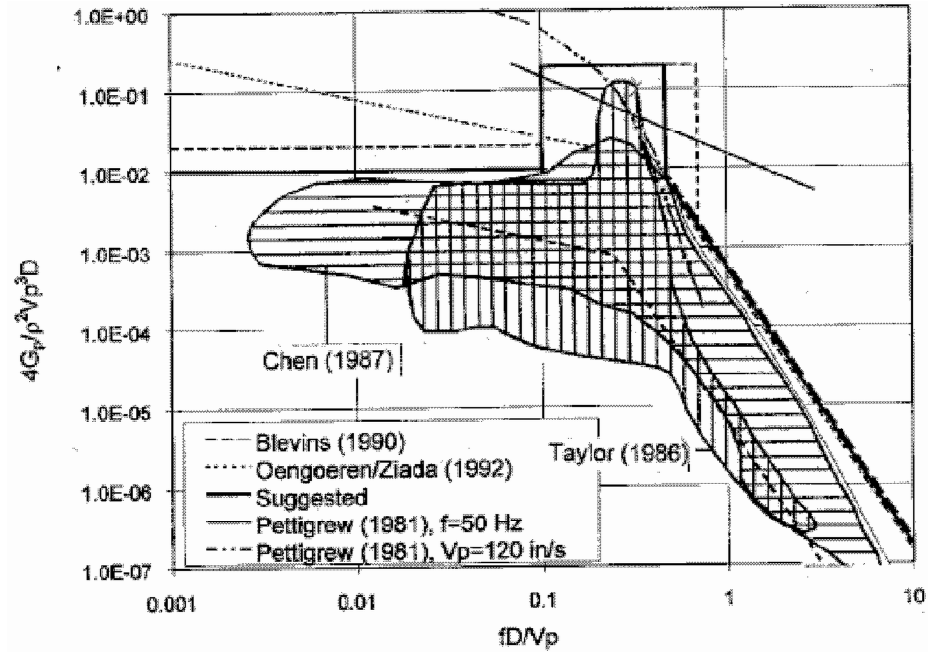
Figure 3.2.2-7 Normalized PSD for Cross Flow Turbulence from Reference (5)
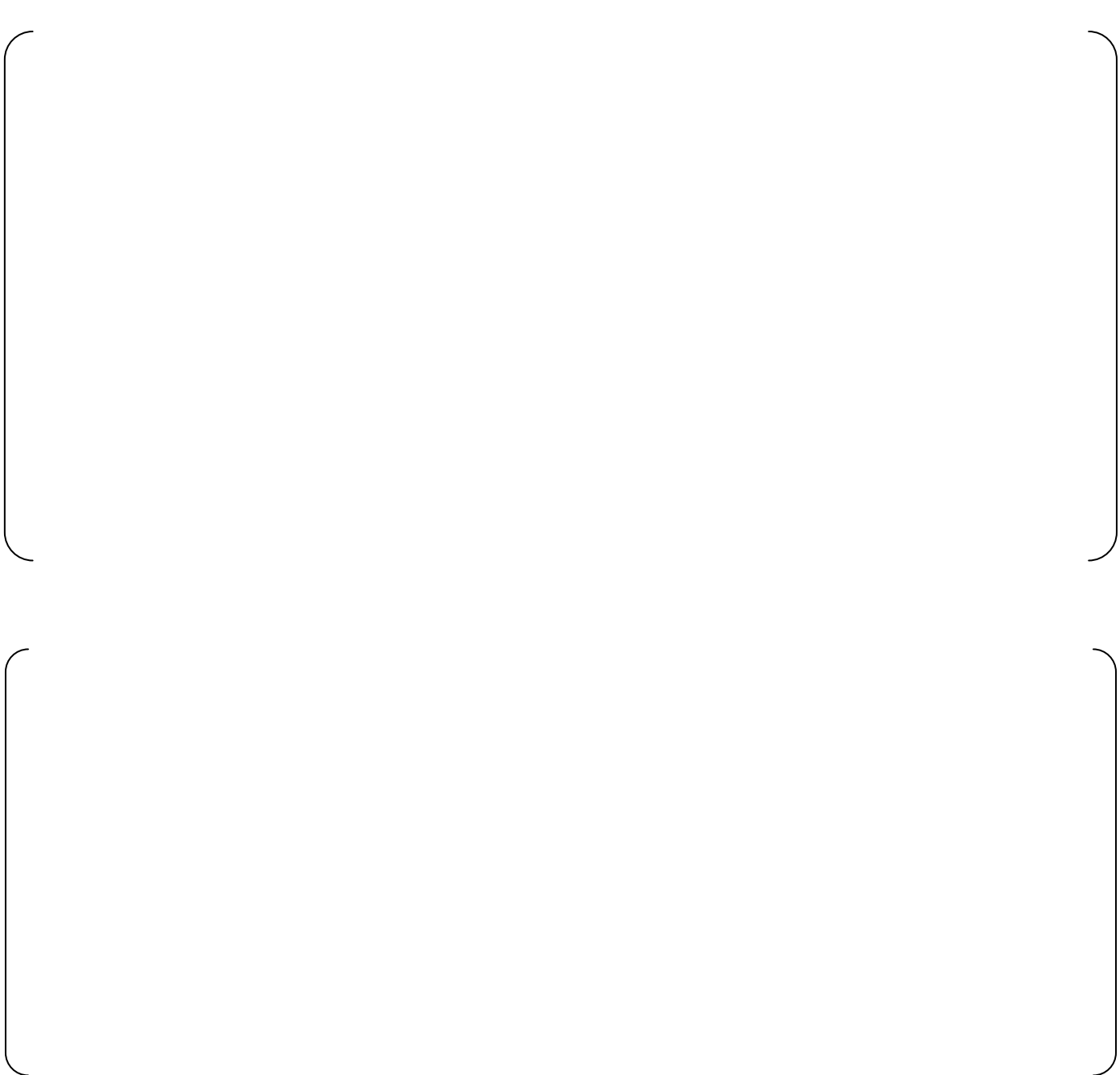
Figure 3.2.2-8 Cross Flow Vibration Load on Columns

(Input for J-APWR SMT Benchmark Analysis)

3.2.3 Response Results of the J-APWR Benchmark Analysis

(1) Analysis conditions

The response analyses were performed under the J-APWR SMT conditions as described in Table 3.2.3-1. For the support conditions at the key supports, such as the bottom of the core barrel and top of the radial reflector, are assumed to be free to simulate the maximum displacement. In the scale model test, these the key supports were not supported such as "open gap condition". The time histories of the forcing functions were generated and applied on the model elements as described in 3.1.2 (3).

(2) Criteria for the comparison with measured response

The validity of the flow induced forcing functions was verified by comparison with measured responses. The following two criteria were applied for the validity check of the benchmark analysis which is based on the category 2 acceptance criteria as described in subsection 3.5.

a. Natural frequency for the fundamental beam mode and the lowest shell mode: with in 10%

b. The ratio of the analysis response (displacement or moment) to measured one should be in the factor of 3.0 as the acceptance criteria with the random response discussed in 3.5.

(3) Response Results

Response results of the J-APWR benchmark analysis are summarized as below.

The results are shown in Table 3.2.3-2, Table 3.2.3-3, Figure 3.2.3-1 and Figure 3.2.3-2. The response of the core barrel and the neutron reflector due to the downcomer turbulences were adjudged acceptable based on the following rationale:

(a) The Core barrel / Reactor vessel relative displacement

i) The ratio of the rms relative displacement from the analysis results to the measured one is [   ] which satisfies the acceptance criterion of 1.0-2.0.

ii) In Figure 3.2.3-1, the dominant frequency of the displacement response for the core barrel is observed around [   ] Hz both in the analysis and measured data. The difference was in the 10% as the acceptance criterion for the natural frequency.

iii) The peak of the response in the spectrum for the relative displacement between the bottom of the core barrel and the reactor vessel was around [   ] Hz in the measurement was identified to

be related to the test vessel mode.

(b) The core barrel and neutron reflector relative displacement

i) The ratio of the computed rms relative displacement between the core barrel and the neutron reflector to the measured value was [   ] which satisfies the acceptance criterion of within 1.0-2.0 for the random forcing functions,

ii) In Figure 3.2.3-2, the dominant peak in the frequency of the neutron reflector in the response spectrum is observed to be around [   ] Hz both in the analysis and measured data. The difference was within the 10% as the acceptance criteria for the natural frequency.

iii) The peak of the response in the spectrum for the core barrel and neutron reflector relative displacement was around [   ] Hz in the measurement and was identified to be related to the test vessel mode.

From above discussions the analysis method is adequate for FIV response analysis.

(c) Responses due to the cross flow

The validity of cross flow forcing functions was confirmed by comparison of the dynamic moment for the columns in lower and upper plenum as shown in Table 3.2.3-3. For all the column structures in the lower plenum and the upper plenum, the ratio of analysis results to the measurement results were in the range of [   ] to [   ]. The maximum ratio [   ] was obtained for the RCCA guide tube in the upper plenum. This value does not satisfy the acceptance criteria for the random forcing function, factor of 2.0. The minimum ratio [   ] was obtained for the response of the support column of the upper tie plate. This one is acceptable because it is not conservative.

3.2.4 Validity of the Analysis Methodology

Incorporating with the discussions in subsections 3.2.1 and 3.2.3, the validity of the modeling methodology and formulation of the forcing functions is summarized as follows:

(1) Validity of the modeling

a. The computed results using this model in which the components in the J-APWR 1/5 SMT were modeled with solid and fluid elements agreed well with the in-water measured results.

b. The computed natural frequencies of the fundamental mode of the J-APWR 1/5 SMT model agreed with the test results to within ±10% except for the RCCA guide tube and the lower tie

plate assembly in the lower plenum. As for the guide tube, the analysis result is rather reliable than the measured one because of the uncertainty of the pin support benchmark in the scale model. And the model for the lower plenum structures, the model refinement was reflected to the US-APWR modeling.

(2) Validity of the forcing functions

a. The formulation of the turbulent forcing functions in the downcomer was adequate because the rms vibration amplitude of the core barrel and the neutron reflector are in a factor of [   ]-[   ] of the corresponding measured values and met the acceptance criterion factor of 3.0 for the random response.

b. The formulation of the cross flow loads in the lower plenum and upper plenum was adequate because the rms response of the bending moment on the upper plenum and lower plenum structures were in the ratio of [   ] to [   ] and satisfied the acceptance criterion factor of 3.0 for the random response. One under estimated value [   ] for the upper tie plate BMI column was also acceptable because the moment and stress of the BMI column can be represented by those of the lower tie plate assembly.

Table 3.2.3-1 J-APWR SMT Benchmark Analysis Conditions

Case ID	Configuration	Model Type	Forcing Functions[1]	Damping Ratio
A1	1/5 scale test model	Solid	DC	[ ]%
A2	Ditto	Beam System	Ditto	Ditto
A3	Ditto	Ditto	DC+LP+UP	Ditto

Note 1)   DC   : Downcomer Turbulence
LP   : Lower Plenum Cross Flow
UP   : Upper Plenum Cross Flow
V   : Vertical Load
RCP : RCP Pulsation

Table 3.2.3-2 Correlation of Test Results of CB / NR Rms Response

with Results from the J-APWR SMT Benchmark Analysis

Components	Rms Response (mil rms)		Analysis /Measured
	Measured*	Analysis*	
CB bottom –RV relative displacement			
NR top –CB relative displacement			

*Both results are converted to actual plant scale.

Table 3.2.3-3 Correlation of Test Results in Cross Flow Induced Vibration,

with Computed Results from the J-APWR SMT Benchmark Analysis

Components	Rms Response (column moment in Lb-in rms)		Analysis /Measured
	Measured* (Reference (7))	Analysis*	
Lower Tie Plate BMI Column			
Upper Tie Plate BMI Column			
RCCA Guide Tube			
Upper Support Column			
Top Slotted Column			

*Both results have been converted to actual plant condition.

Figure 3.2.3-1 CB Bottom / RV Relative Displacement Linear Spectral (Test Scale)

(J-APWR SMT Measured and Analysis Results)

Figure 3.2.3-2 NR Top / CB Relative Displacement Linear Spectral (Test Scale)

(J-APWR SMT measured and analysis results)

3.3 US-APWR Response Analysis

In this section, the prediction analysis of the US-APWR reactor internals vibration response as the Task-2 is described in Section 3.1. The analysis methods which were verified through the benchmark analysis in 3.2 were applied. Additional information on the analysis models and the conversion of the forcing functions from J-APWR SMT benchmark model to US-APWR normal operating condition are described in 3.3.1 and 3.3.2. The results of vibration response under the US-APWR normal operating conditions and the assessments for the high cycle fatigue are discussed in 3.3.3. In Subsection 3.3.4, vibration response under the HFT conditions are described. Based the comparison with the vibration responses under the normal operating condition, the needs of the vibration measurements after the core loading are discussed.

3.3.1 Structural Model

(1) Model definition for the US-APWR

Two structural system models, a 3D solid system model consisting of the reactor vessel, the core barrel and the neutron reflector, and a 3D beam system model were constructed similar to those in the benchmark analysis as described in Subsection 3.1.2. In the analytical model for the full-scale prototype model, the 3D solid and 3D beam system model were made based on the following actual structural properties and operating conditions and with the same modeling methodology as in the J-APWR analysis. This methodology has been verified in the previous section. The following are high lights in the US-APWR analytical model.
a. Full-scale dimensions
b. RV support stiffness of the US-APWR
c. Addition of CRDB and IHP models
d. Average temperature at inlet and outlet of the reactor vessel for the physical properties of the structure
e. Analytical conditions without fuel assemblies to allow prediction analysis under HFT conditions

After the above changes and addition, the 3D solid and 3D beam system model was made. The single beam element model for RCP pulses was made for the pole-structure placed on the upper plenum. The 3D solid system model, 3D beam system model, and single beam model are shown in Figures 3.3.1-1 through 3.

(2) Vibration characteristics of the US-APWR reactor internals

The fundamental modal frequencies of the US-APWR reactor internals obtained by the FEM modal analysis using the solid system model both with and without the core to simulate the operating condition and hot functional test condition are shown in Table 3.3.1-1 and Figures 3.3.1-4 through 3.3.1-15. The results confirmed that the loading of the fuel assemblies has little effect on the reactor internals vibration characteristics.

Table 3.3.1-1 Natural Frequencies of US-APWR Reactor Internals

（**US-APWR Analysis Results**）

	Vibration Mode		Natural Frequency (Hz)		Ratio
			With Core	Without Core	
Core Barrel	Beam				
	Shell	n=2			
		n=3			
		n=4			
Neutron Reflector	Beam				
	Shell	n=2			
		n=2, diagonal			
		n=3			
		n=4			
Core Barrel	Beam				
Lower Diffuser Plate Assembly	Transverse / Rotational				
Upper Diffuser Plate Assembly	Transverse				
RCCA Guide Tube (Upper / Lower)	Beam				
Upper Support Column	Beam				
Top Slotted Column	Beam				
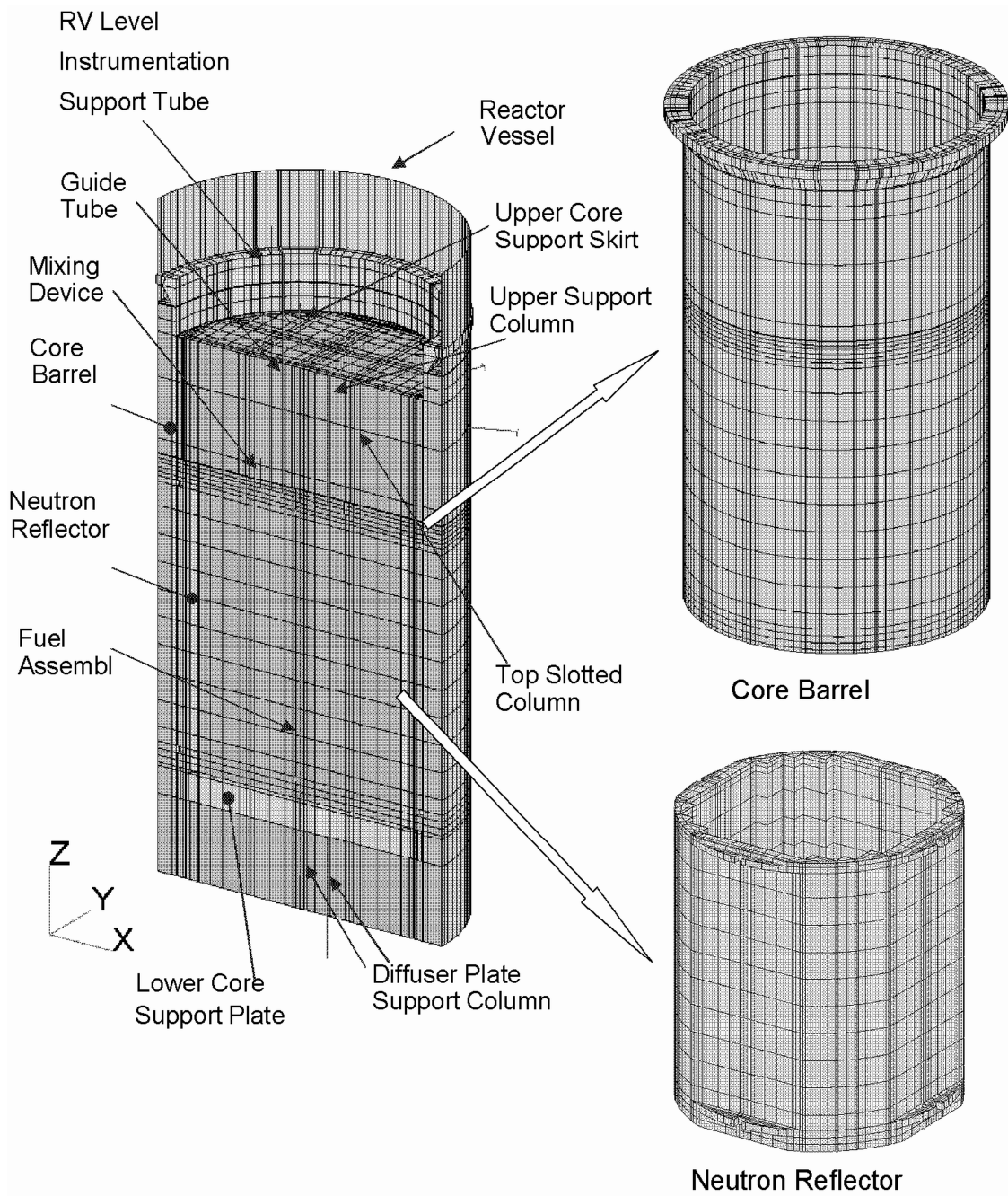
Figure 3.3.1-1 Solid Model for Core Barrel / Neutron Reflector

(US-APWR Analysis Model)

Control Rod Drive Mechanism

Integrated Head Package

Guide Tube

Upper Core Support Skirt

RV Level Instrumentation Support Tube

Upper Support Column

Upper Core Support Plate

Top Slotted Column

Core Barrel

Mixing Device

Reactor Vessel

Upper Core Plate

Neutron Reflector

Fuel Assembly

Lower Core Support Plate

Diffuser Plate

⟷ : Hydraulic Dynamic Mass Matrices
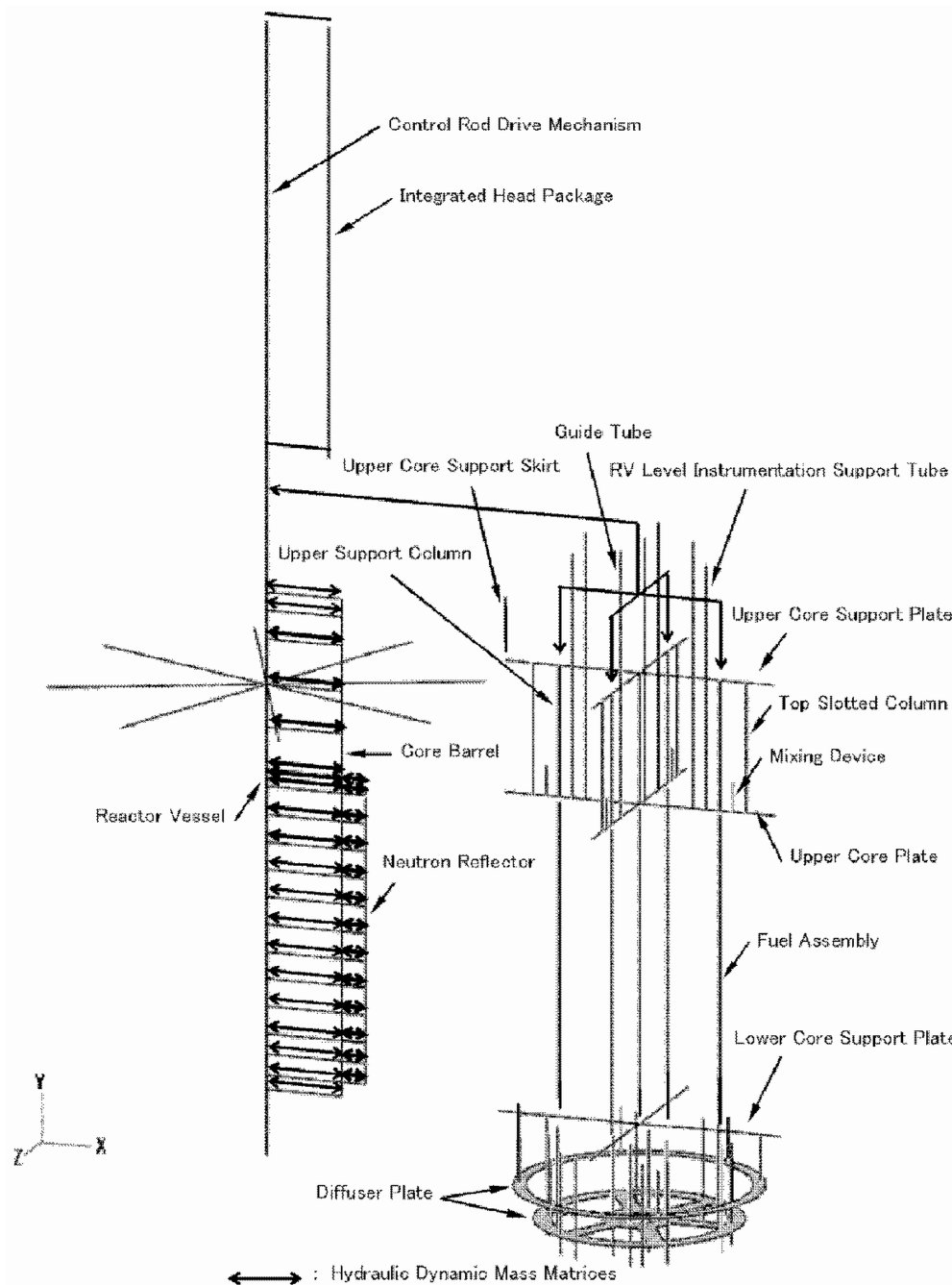
Figure 3.3.1-2 Beam Elements System Model for Reactor Vessel / Internals
(US-APWR Analysis Model)
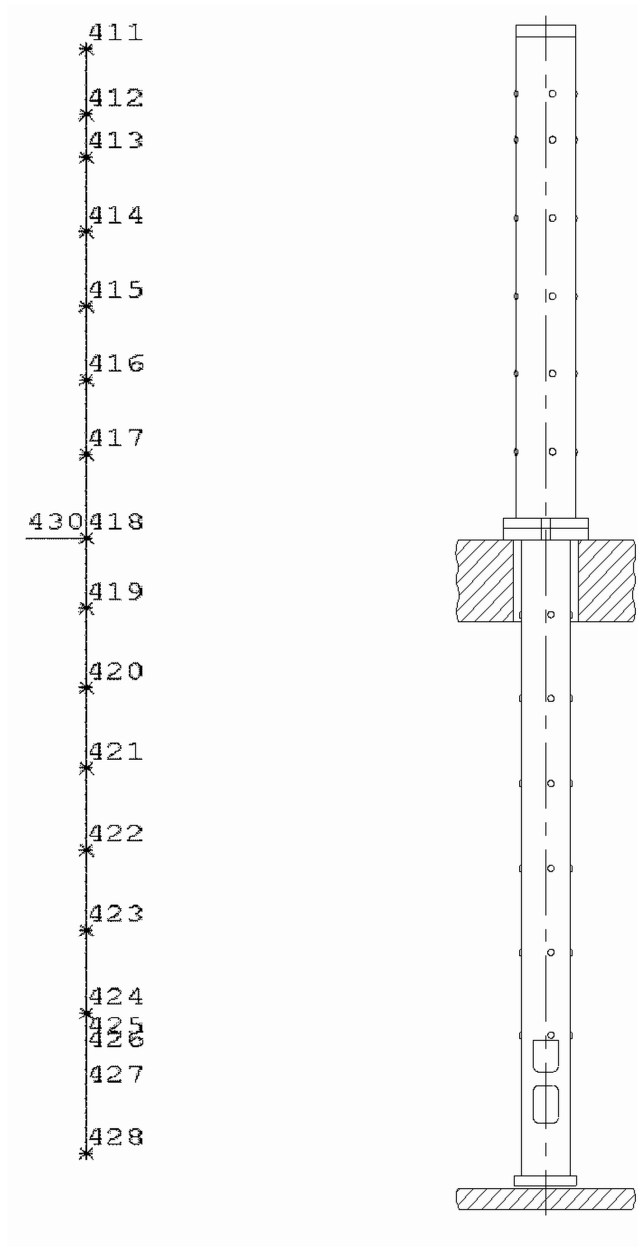
Figure 3.3.1-3 Single Beam Element Model for the Components in the Upper Plenum (US-APWR RCCA Guide Tube Analysis Model)
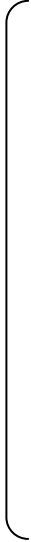
Figure 3.3.1-4 Core Barrel 1st Beam Mode
(US-APWR Analysis Results)

Figure 3.3.1-5 Neutron Reflector Beam Mode
(US-APWR Analysis Results)

Figure 3.3.1-6 Neutron Reflector Shell Mode (n=2)

(US-APWR Analysis Results)

Figure 3.3.1-7 Neutron Reflector Shell Mode (n=2, diagonal)

(US-APWR Analysis Results)

Figure 3.3.1-8 Neutron Reflector / Core Barrel Shell Mode (n=3)
(US-APWR Analysis Results)

Figure 3.3.1-9 Neutron Reflector / Core Barrel Shell Mode (n=4)
(US-APWR Analysis Results)

Figure 3.3.1-10 Core Barrel Beam Mode by 3D Beam System Model
(US-APWR Analysis Results)
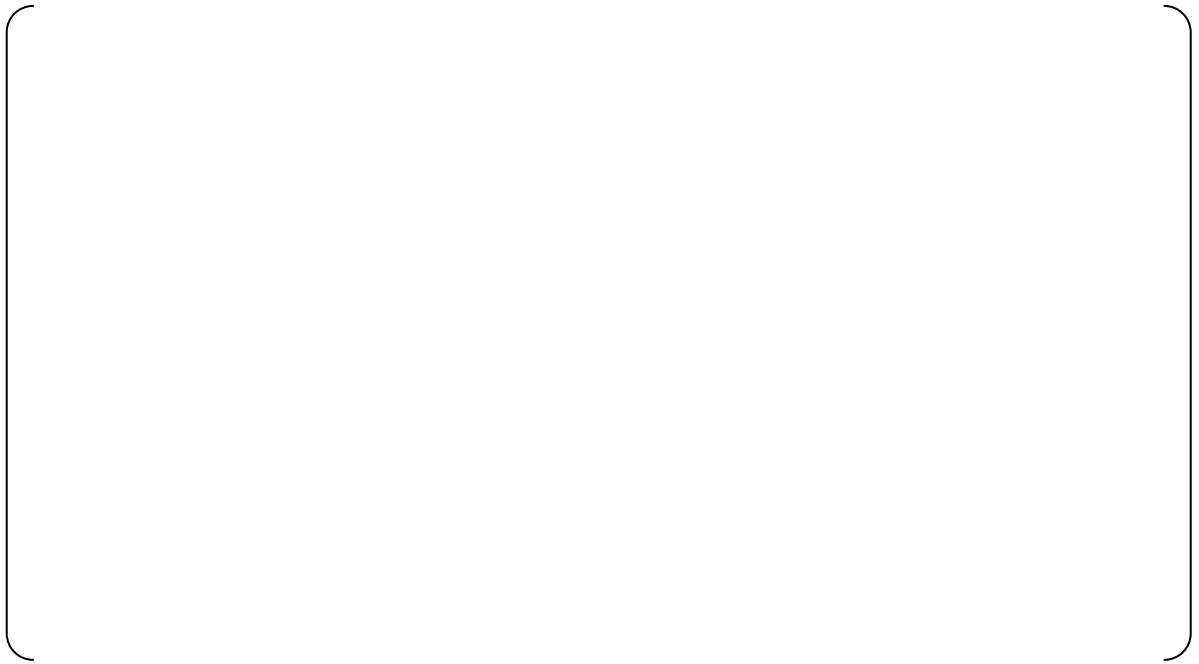
Figure 3.3.1-11 Lower Diffuser Plate Assembly Transverse Mode
(US-APWR Analysis Results)

Figure 3.3.1-12 Lower Diffuser Plate Assembly Rotational Mode
(US-APWR Analysis Results)

**Figure 3.3.1-13 Upper Diffuser Plate Assembly Transverse Mode
(US-APWR Analysis Results)**
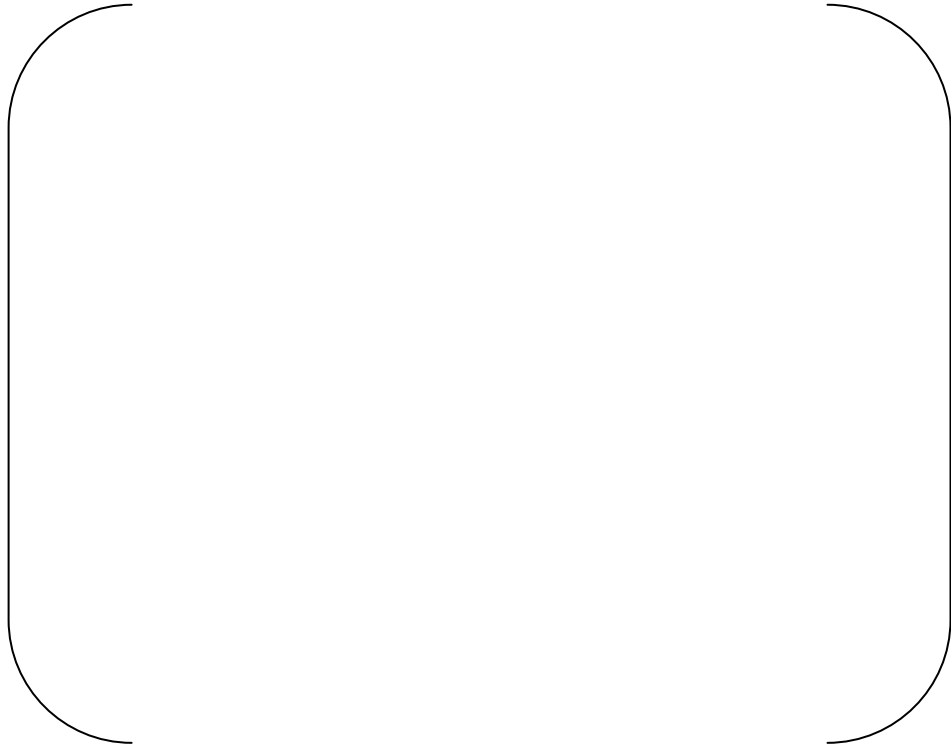
Figure 3.3.1-14 Lower RCCA Guide Tube Beam Mode

(US-APWR Analysis Results)
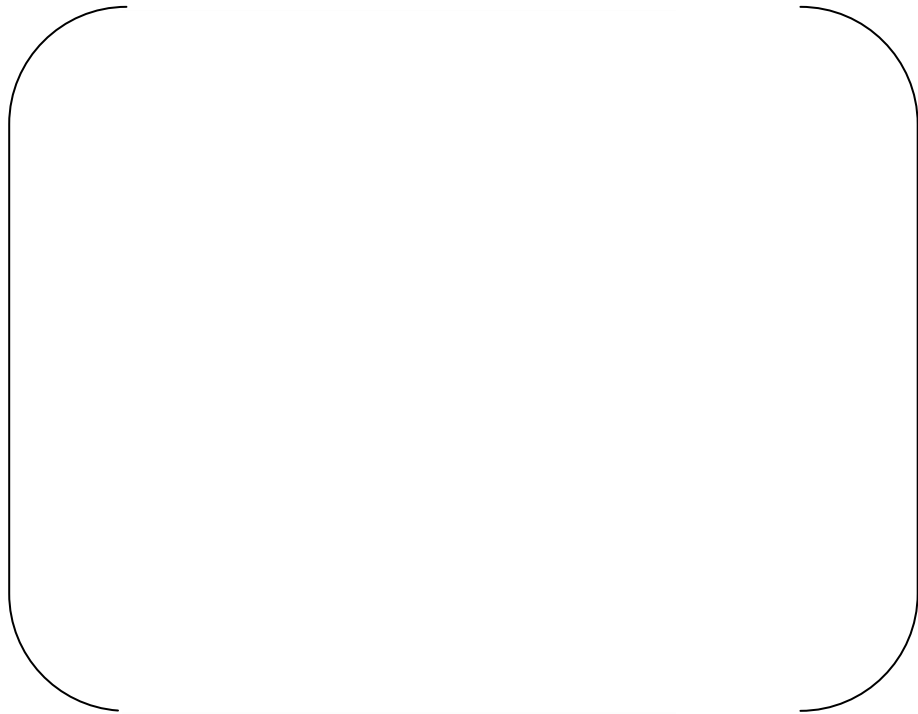
Figure 3.3.1-15 Top Slotted Column Beam Mode
(US-APWR Analysis Results)

3.3.2 Forcing Functions for the US-APWR

The US-APWR and J-APWR SMT have similar geometries for the downcomer turbulent flow and the cross flow in the upper plenum. Therefore, the time history data of these forcing functions, which had been verified in the benchmark analysis of the J-APWR 1/5 SMT, were used after scaling up to the conditions for the full-scale US-APWR. The detailed conversion methodology is discussed in Appendix-B. Because the dimension and location of the columns in the US-APWR are different from those in the J-APWR, the cross flow loads on the structures in the lower plenum were derived specifically for the US-APWR using the same method used in establishing the loads for the J-APWR. In addition, the vertical vibration of the perforated plates and loads induced by the RCP pulsations were derived. These loads are described below.

3.3.2.1 Flow Induced Vibration Loads

(1) Downcomer turbulence

The time histories of the downcomer flow turbulence for the US-APWR were converted from those of the J-APWR SMT benchmark analysis as described in 3.2.2.1, considering with the scaling law and the following differences of conditions on the coolant density and flow rates. The details are shown in Appendix-B.

a.   Reference temperature of coolant density

     With the core   : Temperature at the inlet of the reactor vessel during normal operation was used

     Without the core   : Temperature at the inlet of the reactor vessel at hot standby was used

b.   Coolant flow rates

     With the core   :   Mechanical Design Flow

     Without the core :   Mechanical Design Flow x [   ]

Some samples of the downcomer flow turbulence loads for US-APWR analysis are shown in Figure 3.3.2-1.

(2) Cross flow loads

The time histories of the cross flow induced loads on the upper plenum structures of the US-APWR were converted from those of the J-APWR SMT benchmark analysis as described in Subsection 3.2.2.2, considering with the scaling law and the following differences of conditions on the coolant density and flow rates. The details are shown in Appendix-B.

a.   Reference temperature of coolant density

With the core   : For the lower plenum, temperature at the inlet of the nuclear reactor vessel during normal operations was used.
For the upper plenum, temperature at the inlet of the nuclear reactor vessel during normal operations was used.

Without the core: Temperature at the inlet of the reactor vessel at hot standby was used

b.   Coolant flow rates

With the core   : Mechanical Design Flow
Without the core: Mechanical Design Flow x [   ]

For the lower plenum structures, because of the difference of support column diameter, the PSD of the cross flow loads are not in proportion with the J-APWR. Therefore, cross flow loads for the US-APWR were originally made with the US-APWR configurations using the same method as preparing the load of the J-APWR.

Some samples of the cross flow vibration loads for US-APWR analysis are shown in Figure 3.3.2-2.

(3) Vertical vibration load

The vertical vibration loads were estimated from the integral of random pressure fluctuation through the flow holes in the lower core support plate and the upper core plate, respectively. The same PSD function in the downcomer (Figure 3.2.2-4) was assumed, but the downcomer width was replaced with the diameter of flow hole. The justification for this premise is based on the assumption that the pressure fluctuation close to the RPV inlet nozzle is caused by the jet flow turbulence exiting from the inlet nozzle and, therefore is assumed to be similar to the jet flow turbulence through the lower core support plate and upper core plate flow holes. The adequacy to use the downcomer pressure data as the vertical loads on the perforated plate is discussed in Appendix-E.

An example of measured pressure PSD of the vertical loads on the lower core support plate and the upper core plate are shown in Figure 3.3.2-3, and the samples of generated time histories of vertical vibration loads are shown in Figure 3.3.2-4.

The joint acceptance and the correlation length were not known. The total force on the plate was calculated as the SRSS due to the flow through all the holes in the plate. This is because the Jet flow turbulence in each flow hole is statistically independent of the others.

Figure 3.3.2-1 Downcomer Turbulent Forcing Functions (US-APWR)

(Input for US-APWR Analysis)
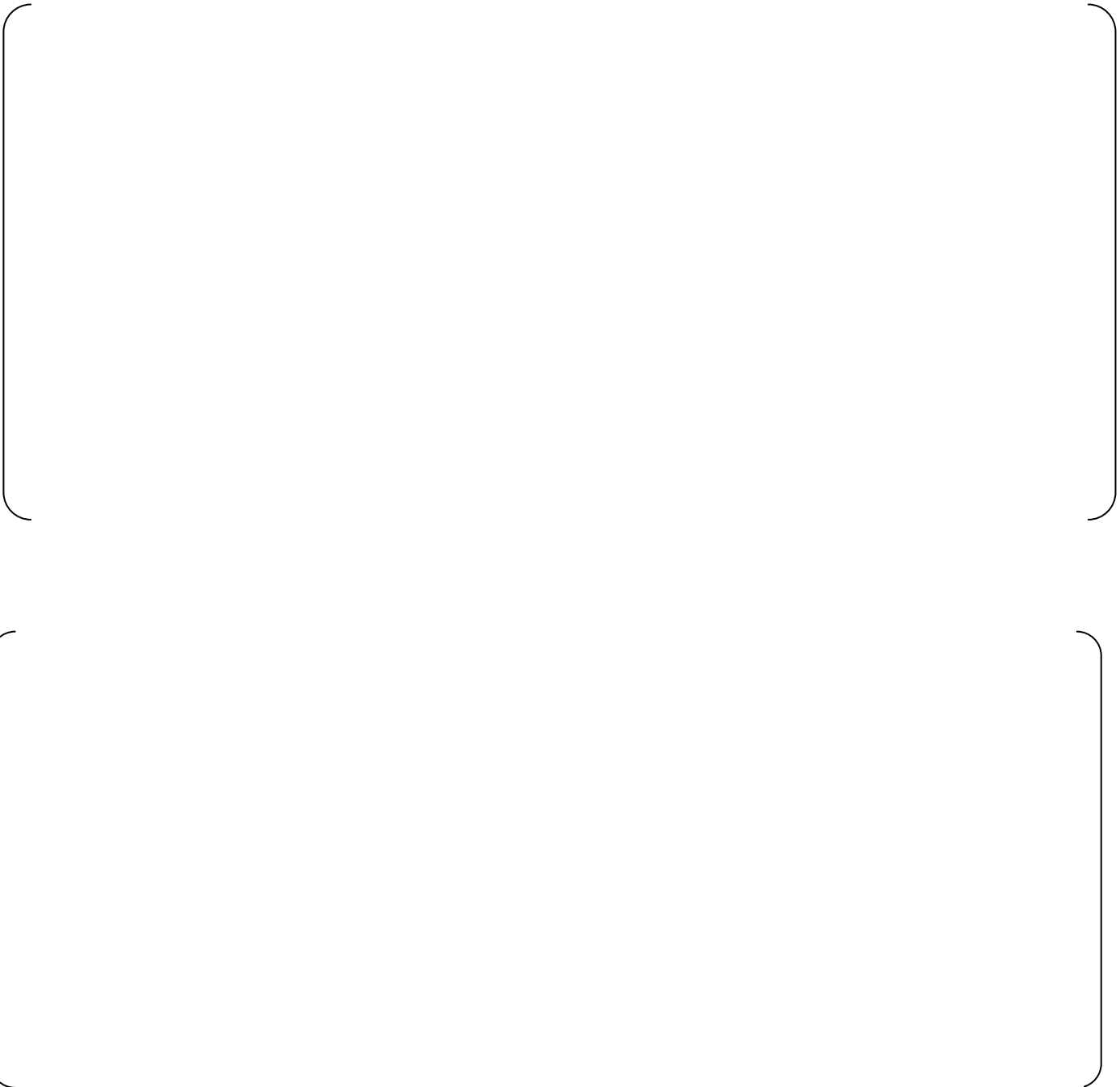
Figure 3.3.2-2 Cross Flow Vibration Load on Columns (US-APWR Analysis)
(Input for US-APWR Analysis)

Figure 3.3.2-3 PSD of Vertical Vibration Force on the Lower Core Support Plate and Upper Core Plate   (Input for US-APWR Analysis)

Figure 3.3.2-4 Vertical Vibration Force Time Histories on Lower Core Plate and Upper Core Plate   (Input for US-APWR Analysis)

3.3.2.2 Pump Pulsation Load

(1) RCP characteristics

The specifications related to the RCP pulsation characteristics, such as the rotational speed and the number of impellers are same as those of the generic RCP as shown in Table 3.3.2-1. Therefore the frequencies of RCP pulsation do not changed from those generated by the generic RCP. The difference in the hydraulic head was accounted for in determining the absolute amplitude of the RCP pulsation.

(2) Estimation of the US-APWR RCP pulsation

Pressures fluctuations were measured at the outlets of both generic and APWR-specific RCPs, as discussed in Appendix. D.

In the Revision 0 analysis, the amplitude of the RCP pulsation was determined based on the pressure fluctuation at the outlet in the APWR test. Note that this measured pressure fluctuation included not only the RCP induced acoustic pulsation but also the fluctuating pressure due to local turbulence.

In the Revision 1 analysis, the ratios of the acoustic pulsations at the shaft rotation and at each blade passing frequency were determined based on spectral analysis of acoustic pulsations generated by generic RCPs.

The RCP pulsation amplitudes at the shaft rotation and the first two blade passing frequencies were determined as shown in Table 3.3.2-2.

(3) Acoustic analysis

a. Analysis code

Acoustic resonance modes in the reactor vessel and their gains of the amplification with the RCP pulsations were determined by the acoustic analysis with the FEM code 'SYSNOSE '.

b. Code verification

The SYSNOISE code was verified with two kinds of the bench mark calculations as follows.

The downcomer and the upper plenum were selected for the verification of the SYSNOISE acoustic analysis because there are high possibilities of acoustic resonance induced by the RCP.

The downcomer was analyzed as an annulus while the upper plenum was analyzed as a cylinder to compare with the theoretical results.

The results of the verification analysis are summarized in Table3.3.2-3. The computed acoustical modal frequencies were within 1.0 %, of the corresponding theoretical values and met the acceptance criterion.

c. Acoustic analysis model of the US-APWR.

The outlines of the US-APWR acoustic model is shown in Table 3.3.2-4, Figure 3.3.2-5 and Figure 3.3.2-6. The analytical model for the SYSNOISE code was composed of the RCP, RV, inlet plenum of the steam generators and the main coolant piping.

In the reactor vessel, the downcomer and the upper plenum have high possibilities of acoustic resonance induced by the RCP. The lower plenum and the reactor core connecting the above region were added. The head plenum was excluded from the model because it is an acoustically-isolated closed space. In addition, a sensitivity analysis was conducted for the effect of reactor internals in the lower plenum and the upper plenum. The internals of the lower plenum was omitted because the presence of the internal components there has insignificant effect on its acoustic characteristics. On the other hand, in the upper plenum, the presence of internal components alters its acoustic characteristics. Therefore they were included in the model to keep the uncertainty and bias errors of the calculated resonance frequencies to within [   ] %, even with uncertainties in the sound speed

d. Acoustic damping (Sound attenuation)

Sound attenuation included in the SYSNOISE model is discussed in the analysis of acoustic loading in the reactor internals of the US-APWR.

Table 3.3.2-5 shows the mechanisms causing sound attenuation in the reactor vessel. Test data for the validation of sound attenuation are limited. Therefore, for obvious reasons, only attenuation through the perforated plates (spray nozzles, lower core support plate, and upper core plate) was conservatively included in the model. The derivation of acoustic attenuation through perforated plates is described in Reference (9). The acoustic resistance was obtained with an equivalent the diameter of hole, plate thickness, opening ratios in the spray nozzle, lower core support plate, and upper core plate respectively. At this time, steady flow along the perforated plates was ignored for a conservative evaluation. Table 3.3.2-6 shows values for the acoustic resistance in each perforated plate derived as shown above.

(4) RCP pulsation forcing functions related to structures

The forcing functions due to RCP pulsation for reactor internals were defined considering with the possibility of resonant vibration of structural components.

a.   Core barrel and neutron reflector

In the RCP pulsations, the shaft rotational speed [   ] Hz is nearest to the fundamental beam or shell modes of the core barrel or neutron reflector as discussed in 3.3.
In addition, from the acoustic analysis by SYSNOISE code, an acoustic resonance mode with the RCP blade passing frequency [   ] Hz is identified in the downcomer. Although this frequency is much higher than the fundamental mode beam or shell mode frequencies of the core barrel or the neutron reflectors, some vibration response with higher shell mode may be induced.
Therefore, the RCP pulsation forcing functions on the core barrel and the neutron reflector are the sum of the sine waves of [   ] Hz and [   ] Hz as equation 3.3-17. The amplitudes and phase angles related to the locations are determined from the SYSNOISE acoustic analysis.

$$F(x, y, z, t) = A \ \Sigma \ \{P \ (f, x, y, z) \sin (2\pi \ ft + \phi(x, y, z))\} \ \cdots\cdots\cdots\cdots\cdots\cdots \ 3.3\text{-}17$$

Where,
   F : force on the core barrel or the neutron reflector (lb)
   P : amplitude of standing wave pressure fluctuation (psi) with the function of the
         frequency f and location   x, y, z.
   A : area where the force is defined (in^2)
   t : time (s)
   ϕ : phase angle (rad)
   f   : RCP shaft rotational speed (Hz)

The maximum pressure amplitudes on the core barrel and the neutron reflector are shown in Table 3.3.2-7. The RCP forcing function time history waves on the Core Barrel and the Neutron Reflector are shown in Figure 3.3.2-8 and Figure 3.3.2-9.

b.   Upper plenum structures

The modal frequencies of components in the upper plenum--the RCCA guide tubes, the upper support columns, and the top slotted columns—were are much higher than the RCP shaft rotational speed [   ] Hz, but the beam modal frequencies were close to the higher harmonics of the RCP blade passing frequency. Thus, exact resonance with the RCP pulsation harmonics was assumed to be conservative. The forcing functions on these structures were defined in the form of equation 3.3-18.

$$F (z, f) = D \ (D \ grad \ P \ (z)) \sin (2\pi \ ft + \phi \ (z)) \ L \ \cdots\cdots\cdots\cdots\cdots\cdots\cdots\cdots \ 3.3\text{-}18$$

Where,

        D   : diameter of the structures (in)
        ϕ : phase angle (rad)
        z   : elevation (in)
        grad P : pressure gradient in the force acting direction (psi/in)
        f   : RCP pulsation frequency (Hz)
        L   : length of force calculation area in axial direction (in)

The RCP pulsation loads on the upper plenum structures are summarized in Table 3.3.2-8. The RCP pulsation time history wave on the RCCA Guide Tube is shown in Figure 3.3.2-10.

c.   Vertical force on support plates

The dynamic vibration force on the lower core support plate and the upper core support plate were determined from the pressure difference across each plate for [   ] Hz which was closest to the vertical natural frequencies of these components. The pressure difference on each plate is shown in Table 3.3.2-9.

Table 3.3.2-1 Comparison of RCP Specification of US-APWR / Current 4-loop

	US-APWR	Current 4-loop
RCP Model	Type MA25S	Type 93A-1
Shaft Power	8200 HP	6000 HP
Head	306.9 ft	276.9 ft
Flow Rate(TDF)	112000 gpm/loop	88500 gpm/loop
Shaft Rotational Speed		
Number of Impeller Blades		

Table 3.3.2-2 US-APWR RCP Pulsation Amplitude for the Vibration Analysis

	Shaft Rotational Speed (N)	Blade Passing Frequency (NZ)	2nd Harmonic of Blade Passing (2NZ)
Frequency(Hz)			
Amplitude(psi)			

Table 3.3.2-3 SYSNOISE Code Verification Analysis

		Boundary Condition	Application for PWR Reactor	Resonance mode frequency error with theoretical value	Judgment
1	Annulus	Top closed Bottom open	Down Comer		Acceptable
2	Cylinder	Top closed Bottom open	Upper Plenum		Acceptable
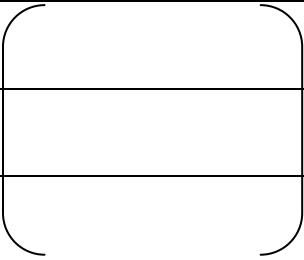
Table 3.3.2-4 SYSNOISE US-APWR Acoustic Model

Components	Use of Simplified method	Remarks
RCP	Simulated as a point source of pressure wave	Figure 3.3.2-6
Inlet Pipe	(Not Simplified)	
Vessel Down Comer	(Not Simplified)	
Lower Plenum	(Not Simplified)	
Lower Support Plate	Damping matrix for Pressure loss model	Figure 3.3.2-5
Core (Fuel Assembly)	Not Simulated	
Neutron Reflector	Not simulated. (Considered as core boundary walls)	
Upper Core Plate	Damping matrix for Pressure loss model	Figure 3.3.2-5
Upper Plenum	Number reduction of column structures (GT / USC / TSC)	
Outlet Pipe	(Not Simplified)	
Steam Generator	Simulated to the inlet of SG Plenum	

Table 3.3.2-5 Mechanism by Sound Attenuation in Reactor

(Input for US-APWR Analysis)

Sound attenuation mechanism	Description	Analysis in DCD
Perforated plate	Attenuation of acoustic energy is caused by resistance during passing through holes of perforated plates.	Considered ;spray nozzle, lower core support plate, and upper core plate
Viscosity of fluid itself	Acoustic energy is converted to thermal energy during shear deformation due to viscosity of fluid itself.	Not considered
Friction between fluid and wall	Acoustic energy is converted to thermal energy when fluid moves contacting the wall.	Not considered
Coupling of eddy	Acoustic energy is converted to eddy energy by eddy in fluid with steady flow.	Not considered
Attenuation due to vibration of internals	Converted to kinetic energy of internals	Not considered

Table 3.3.2-6 Value of Sound Attenuation with SYSNOISE Input

(Input for US-APWR Analysis)

Location	Value of acoustic resistance $\mathrm{Re}[Z/(\rho c)]$	Remarks
Spray nozzle		Acoustic impedance has an effect on frequency response.
Lower core support plate		
Upper core plate		

Table 3.3.2-7 RCP Pulsation Loads on Core Barrel and Neutron Reflector
(Input for US-APWR Analysis)

Components	Frequency (Hz)	Pressure Amplitude (psi)
Core Barrel (down comer)		
Neutron Reflector (core)		

Table 3.3.2-8 RCP Pulsation Loads on the Upper Plenum Structures
(Input for US-APWR Analysis)

Components	Beam Mode Nodal Number	Pressure Gradient (psi/in)		
RCCA Guide Tube				
Upper Support Column				
Top Slotted Column				

Table 3.3.2-9 RCP Pulsation Loads on Core Support Plates
(Input for US-APWR Analysis)

Components	Frequency (Hz)	Pressure Difference (psi)
Lower Core Support Plate		
Upper Core Support Plate		

Figure 3.3.2-5 SYSNOISE Acoustic Analysis Model
(Modeling of Components)
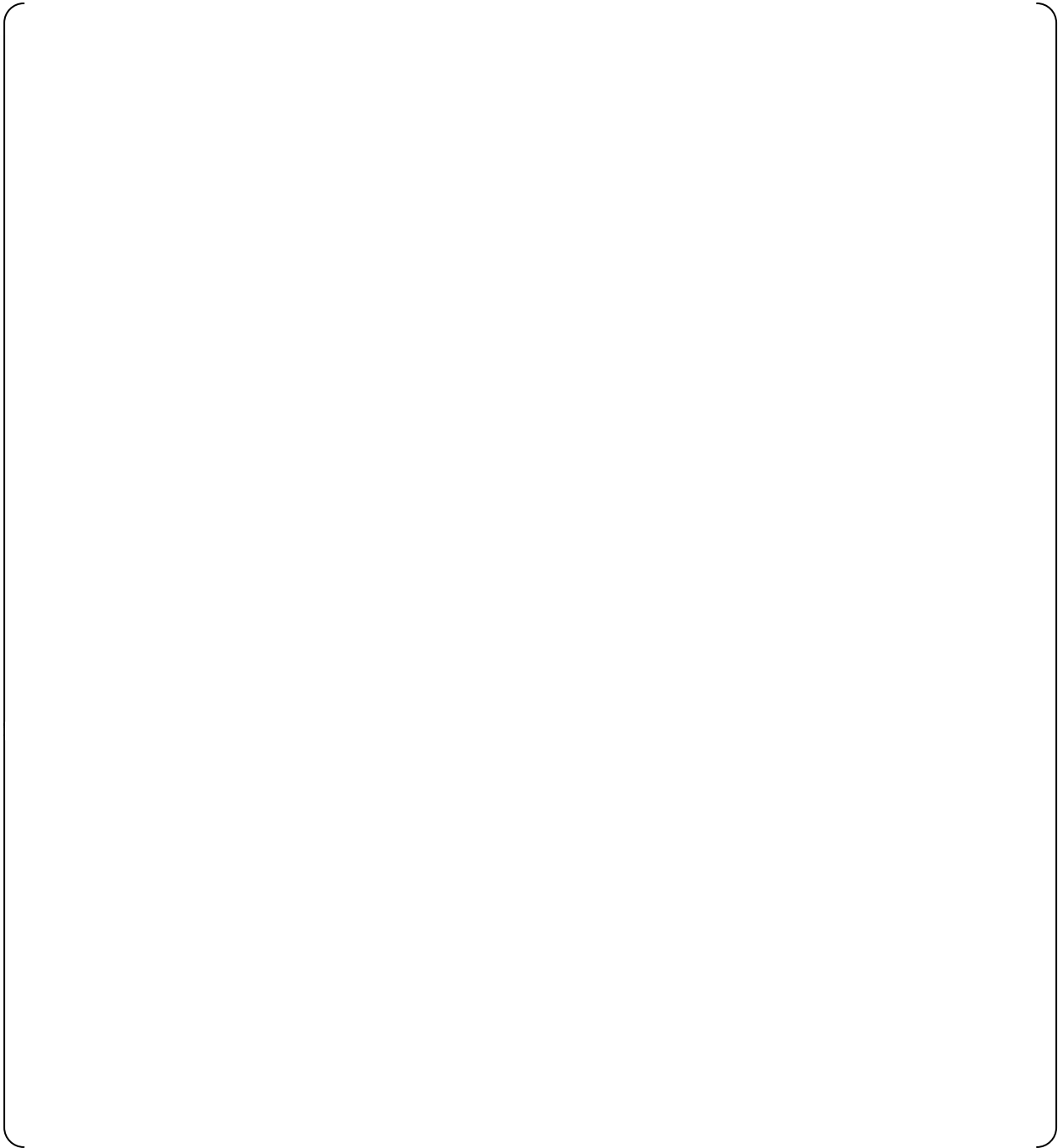
Figure 3.3.2-6 SYSNOISE Acoustic Analysis Model

(Boundary Condition)

a. Downcomer standing wave mode close to RCP NZ

b. Upper plenum standing wave mode close to RCP 2NZ

Figure 3.3.2-7 Samples of the SYSNOISE Acoustic Analysis Result

Figure 3.3.2-8 RCP Pulsation Wave on the Core Barrel (N+NZ)

Figure 3.3.2-9 RCP Pulsation Wave on Inside of the Neutron Reflector (N+NZ)

Figure 3.3.2-10 RCP Pulsation Wave on a RCCA Guide Tube (2NZ)

3.3.3   Results of the US-APWR Vibration Analysis

3.3.3.1 Response Analysis Conditions

The vibration response analysis conditions for the US-APWR reactor internals are summarized in Table 3.3.3-1. Cases identified as B1 to B6 are analyses for the US-APWR normal operating conditions with fuel assemblies, and cases C1 to C6 are those for the HFT conditions.

The vibration responses of the core barrel and the neutron reflector including shell modes due to the downcomer flow turbulence are obtained from Case A1 or C1 with the 3D solid system model. There is no account of the effect of cross flow loads because the core barrel and the neutron reflector vibration response have been verified with the downcomer flow turbulence alone in the benchmark analysis case A1 in Table 3.2.3-1 of J-APWR 1/5 SMT, as discussed in 3.2.3 (3) b.

The flow induced vibration responses of the structures in the lower and the upper plenum were determined from the case B3 or C4 with the 3D beam system model with all of the flow induced loads. Case B2 or C3, the system beam model with the downcomer flow turbulence, were referred to separate the effect of the base excitation from the results of B3 or C4.

The vibration responses due to the RCP pulsations were represented by analyses case C2, C5 and C6 under without core conditions, because the fuel assemblies act as acoustic absorbers.

In discussed above, the all of the key supports, such as the radial keys on the bottom of the core barrel, the upper radial reflector alignment pins and the upper core plate alignment pins were assumed to be free for the larger response. The design loads for these key supports were determined the case B5 and B6 by the 3D beam system model with the spring elements to represent the key supports.

3.3.3.2 Vibration Responses under the Full Power Conditions

(1) Vibration Response

(a) Responses due to the Flow Induced Vibration

The flow induced response by the analysis of the US-APWR reactor internals are shown in Table 3.3.3-2.
The relative displacement between the core barrel and the reactor vessel with the downcomer turbulence was about twice of that in J-APWR SMT benchmark results scaled to actual dimensions. It is supposed by the effect of the decrease of the damping ratio from 3% with J-APWR SMT benchmark analysis to 1% with the US-APWR analysis.

(b) Responses due to the RCP pulsation

The RCP induced vibration responses by the analysis of the US-APWR are shown in the Table 3.3.3-3. For the RCP induced vibration, the response level depends on the vibration characteristics of the each component. For the core barrel, and structures in the upper or lower plenum, the RCP induced response (0-peak) was not larger than flow induced responses (4.5 rms). But for the neutron reflector, the RCP induced vibration response was equivalent with the FIV response in displacement. Note that this RCP induced response was based on the acoustic analysis with empty the core cavity without fuel assemblies. In the US-APWR operating condition after core loading, the RCP induced response will be reduced by the acoustic damping with the fuel assemblies between the inside walls of the neutron reflector.

(2) High Cycle Fatigue Evaluation

a.　Evaluation method

The evaluation was performed considering the maximum displacement (strain) or components with the maximum values in dynamic response results with combination of the loads caused by the flow turbulence and the RCP pulsation response (horizontal and vertical), which were obtained from the above.

High cycle fatigue was evaluated by obtaining of the stresses and caused by the largest dynamic responses and considering stress concentration factors were applied in the calculation of the peak stresses. Since the uniform cross sections of the core barrel and column structures have lower stress, a stress concentration factor 5 was used. The cross-shaped legs in the fixed parts of the column structures, however, have higher stress due to large loads. Therefore, a stress concentration factor 2 was used to calculate the peak stress according to FE model analysis.

The alternating peak stress due to the flow turbulence and due to the RCP pulsation is determined from the FEM response as following equations.

$$Sa_{FIV} = [\quad](\sigma\, rms_{FIV})\, K\, (E/E\, p)$$

$$Sa_{RCP} = (\sigma\, 0\text{-}P_{RCP})\, K\, (E/E\, p)$$

Where,
Sa_{FIV}　　: alternating peak stress due to the flow
Sa_{RCP}　　: alternating peak stress due to the RCP pulsation
$\sigma\, rms_{FIV}$　: rms amplitude of alternating stress due to the flow
$\sigma\, 0\text{-}p_{RCP}$　: zero to peak amplitude of the alternating stress due to the RCP
K　　　　: stress index for the structural discontinuous

  E   : Young's modulus in the room temperature
  Ep   : Young's modulus in the plant operating condition
  [   ]   : ratio between 0-peak and rms value for random vibration response

The combined alternating peak stress was assumed to be the simple sum of those due to the flow turbulence and the RCP induced pulsation as shown in the following equation.

$$Sa_{total} = Sa_{FIV} + Sa_{RCP}$$

b. Evaluation results

The evaluation results of the high cycle fatigue analysis are summarized in Table 3.3.3-4. The minimum margin of safety [   ] was obtained with the structures in the upper plenum. Considering with the conservative assumption on damping ratio (3% is used for force correction and 1% for response analysis) this margin is sufficient.

As the conclusion, the reactor internals of the US-APWR have the sufficient margin of safety against high cycle fatigue as specified in ASME Code Section III, Subsection NG.

(3) Interface load

The vibration load acting on the alignment key supports are summarized in Table 3.3.3-5.
These are applied for the stress or functional analysis combined with other design loads.

3.3.4 Structural Responses in the Preoperational Test Conditions

The analysis simulating the hot functional testing condition was performed. Because the hot functional test is conducted before core loading, the fuel assemblies were excluded from the analysis models for the normal operating conditions. The increase of flow rate (2.5% is assumed) by the effect of the reduction of the flow resistance in the core was reflected to the flow induced forcing functions with the square of flow rates from those in the normal operating conditions.

The vibration responses in the hot functional test are used for following assessments.
a. Needs of the vibration measurement after the core loading by comparison with the vibration responses under the normal operating conditions
b. Selection of the transducer type and locations in the hot functional test as discussed in Section 4.

(1) Comparison with Normal Operation Response

The typical vibration responses in the preoperational hot functional testing condition (without core) are compared with the normal operating conditions (with core) at the initial startup testing condition of the US-APWR as shown in Table 3.3.3-2, Figure 3.3.3-1 and Figure 3.3.3-2.

The ratio of vibration responses in the hot functional test conditions to those in the normal operating condition are within 1.0 to 1.4. It is concluded that the vibration responses in the hot functional test conditions are the equivalent or slightly larger than those in normal operating conditions. These are because of the flow rate increase with the elimination of fuel assemblies and the subsequent pressure loss. As discussed with Table 3.3.3-1, the effect on the vibration characteristics of the core loading is also small.

Thus, in the preoperational test of the prototype plant, the results of vibration measurements after core loading are bounded by the measurements before core loading and only measurements before core loading will be necessary.

(2) Vibration Responses on the each Transducer Location

The transducer type and locations for the vibration measurement are discussed in Section 4 of this program. The responses on each transducer were predicted from the analysis results as follows.

a. Accelerometers: The time history of acceleration at the transducer location was obtained by the second order differential of the displacement time history from the analysis. The rms amplitude is determined from the acceleration time history.

b. Strain gages   : The amplitude of the dynamic strain was determined from the dynamic bending moment from the analysis divided with the section modulus and the Young's modulus.

The predicted responses of the transducers are summarized in Table 3.3.3-6.

Table 3.3.3-1 Analysis Matrix

(**US-APWR Analysis Conditions**)

Case ID	Configuration	Model Type	Forcing Functions[1]	Key Support Gap[2]	Damping Coefficient
B1	US-APWR with Core	Solid	DC	Open	⎿ ⏌%
B2		Beam System	DC		
B3			DC+LP+UP+V		
B4			RCP	↓	
B5			DC+LP+UP+V	Close	
B6	↓	↓	RCP	Ditto	
C1	US-APWR without Core	Solid	DC	Open	
C2		Ditto	RCP		
C3		Beam System	DC		
C4			DC+LP+UP+V		
C5		↓	RCP		
C6	↓	Single Beam	RCP	↓	↓

Note 1)   DC   : Downcomer Turbulence
LP   : Lower Plenum Cross Flow
UP   : Upper Plenum Cross Flow
V   : Vertical Load
RCP : RCP Pulsation

Note 2)   Boundary conditions at the key supports in the bottom of the core barrel and the top of the neutron reflector

Table 3.3.3-2 US-APWR Reactor Internals Rms Response (FIV)

(US-APWR Analysis Results)

Components	Remarks	Rms Response		
		with core	without core	Ratio
Core Barrel-RV Relative displacement	Bottom (Beam+Shell)			
Neutron Reflector-Core Barrel Relative displacement	Top (Beam)			
	Top (Shell)			
Lower Diffuser Plate Support column	Moment			
Upper Diffuser Plate Support column	Moment			
RCCA Guide Tube	Moment			
Upper Support Column	Moment			
Top Slotted Column	Moment			

Table 3.3.3-3 US-APWR Reactor Internals Response (RCP pulsation, without core)

(US-APWR Analysis Results)

Components	Remarks	0-p response
Core Barrel-RV Relative displacement	Bottom	
Neutron Reflector-Core Barrel Relative displacement	Top (Beam)	
	Top (Shell)	
Lower Diffuser Plate Support column	Moment	
Upper Diffuser Plate Support column	Moment	
RCCA Guide Tube	Moment	
Upper Support Column	Moment	
Top Slotted Column	Moment	

Mitsubishi Heavy Industries, LTD.

Table 3.3.3-4 High Cycle Fatigue Evaluation Based on Analysis Responses
(US-APWR Analysis Results)

Components	Locations or parts	Alternating Stress (ksi)			Limit	Margin of Safety [1]
		Flow	RCP	Total		
Core Barrel	Flange					
Neutron Reflector	Block Alignment Pin					
Diffuser Plate Assembly	Support Column Upper Assembly Lower Assembly				13.6 ksi	
UCS	Flange Skirt					
RCCA GT	Top of Lower GT					
USC						
TSC						

Note

1) Margin of safety = (Allowable Stress Limit) / (Alternating Stress) - 1

Table 3.3.3-5 Interface Loads
(US-APWR Analysis Results)

	Load (lbf, FIV 4.5rms+RCP 0-P)
Core Barrel Radial Key	
Neutron reflector alignment Pin	
Upper core plate Alignment Pin	

Table 3.3.3-6 Estimated Transducers Responses in US-APWR Reactor Internal Vibration Measurement in Hot Functional Testing   (US-APWR Analysis Results)

Subassembly	Location and Transducer Type	Sensitive Direction	Flow Excitation Response (rms)	RCP Pulsation Response (0-peak)
Core Barrel	Flange Strain Gages	axial		
	Middle: ACC	radial		
Lower Core Support Plate	1-D Accelerometers	vertical		
Neutron Reflector	1-D Accelerometers	vertical radial		
	Displacement Transducers	radial		
Upper Diffuser Plate Support Column	Strain Gages	axial		
Lower Diffuser Plate Support Column	Strain Gages	axial		
Upper Core Support	Skirt: Strain Gages	axial		
	1-D Accelerometers	vertical		
Upper Support Column	Strain Gages	axial		
Top Slotted Column	Strain Gages	axial		
Upper Guide Tube	Strain Gages	axial		
Lower Guide Tube	Strain Gages	axial		

Figure 3.3.3-1 CB Bottom / RV Relative Displacement FFT Analysis Results
(US-APWR Analysis Results)

Figure 3.3.3-2 NR Top / CB Relative Displacement FFT Analysis Results
(US-APWR Analysis Results)

Mitsubishi Heavy Industries, LTD.

3.4 Adverse Flow Effects

3.4.1 Evaluation of the Cross Flow Velocity

The cross flow velocity around the structure in the lower and upper plenum of the reactor vessel was evaluated in the manner as described in 3.2.2.2 (1). The maximum flow velocity was referred in the evaluations of vortex shedding and fluid elastic instability.
The calculation results of the cross flow velocities are shown in Table 3.4.1-1 as "U".

3.4.2 Margin for Vortex Shedding Lock-in and Fluid Elastic Instability

For the column structures in the reactor vessel lower plenum and upper plenum, the margin of safety for the cross flow induced vibrations were evaluated based on the FIV guidelines I the ASME Code Section III (Reference (2), Appendix-N1300).

(1) Fluid elastic instability

The critical velocity is estimated with the Conner's equation as below.

$$U_c / f_n D = C (m \delta / \rho D^2)^\alpha$$

Here,

U	: axial flow velocity (in/s)
U_c	: critical flow velocity for fluid elastic instability (in/s)
D	: diameter (in)
m	: mass per unit length (lb/in)
δ	: logarithmic damping ratio
f_n	: fundamental mode frequency of column（Hz）
ρ	: fluid mass density (lb/in^3)
C, α	:coefficients for critical velocity, C=2.4 and α =0.5 are applied as most conservative value which are suggested in FIG.N-1331-4 in the APPENDIX N of Reference (2).

The evaluation results are shown in Table 3.4.1-1. The US-APWR reactor internals have the sufficient margin of safety against the fluid elastic instability.

(2) Vortex shedding lock-in
The design guidelines to avoid vortex shedding lock-in in the ASME Sec. III (Reference (2), appendix N1324) were followed check the column structures in the lower plenum and those in the upper plenum based on the computed natural frequencies. The results of vortex shedding lock-in evaluation are summarized in Table 3.4.2-1. As result, the lock-in of vortex shedding is avoided for all reactor internal structures.

3.4.3 Conclusions of the Assessment for Adverse Flow Effects

It is concluded that the reactor internals of the US-APWR have sufficient margins of safety against the adverse flow effects due to the cross flow, including the lock-in with vortex shedding or fluid elastic instability.

Table 3.4.1-1 Cross Flow Parameters and Margin for Fluid Elastic Instability

(US-APWR Analysis Results)

	U (in/s)	D (in)	fn (Hz)	fs (Hz)	Vr = U/fn D	$m\delta/\rho D^2$	M.S = Uc/U-1
Lower Diffuser Plate Support Column							
Upper Diffuser Plate Support Column							
RCCA Guide Tube							
Upper Support Column							
Top Slotted Column							

M.S: Margin of Safety

Table 3.4.2-1 Evaluation for Vortex Shedding Lock-in

(US-APWR Analysis Results)

ASME Design Guidelines to avoid vortex shedding lock-in	N1324.1-(a) U/fn D<1.0	N1324.1(b) U/fn D<3.3 and $m\delta/\rho D^2$>1.2	N1324.1(d) fn<0.7fs or fn>1.3fs	Evaluation
Lower Diffuser Plate Support Column	—	X	X	Lock-in avoided
Upper Diffuser Plate Support Column	—	X	X	Lock-in avoided
RCCA Guide Tube	X	—	X	Lock-in avoided
Upper Support Column	—	—	X	Lock-in avoided
Top Slotted Column	X	—	X	Lock-in avoided

Mitsubishi Heavy Industries, LTD.

3.5 Acceptance Criteria

Following Regulatory Guide 1.20 and SRP 3.9.2, the data from the pre-operational vibration test described in Subsection 3.9.2.4, including accelerations, amplitudes, strains and component modal frequencies, will be compared with the corresponding predicted and allowable values. The following lists the specific items to be evaluated together with their acceptance criteria. In general, Category 1 criteria are related to the integrity of the components while Category 2 criteria are related to the adequacy of the analysis technique. Contingency plans in case these criteria are not met are given.

a. Modal Frequencies

Category 2 Criterion: The measured frequencies for the fundamental beam mode and the lowest shell modes must not differ from the predicted values by more than 10%.

b. Damping Ratios

Category 2 Criterion: The measured damping ratios, as determined from the half-power point method, must be within a factor of 2.0 of what are used in the prediction analysis.

c. Forcing Function due to Flow Turbulence
Category 2 Criterion: The rms amplitude of measured broad –band random turbulence pressure fluctuation in the downcomer must be within a factor of 2.0 of the corresponding predicted values in the analysis.

d. Forcing Function due to RCP Pulsation

Category 2 Criterion: The measured 0-p amplitude of the RCP induced acoustic loads in the downcomer and the upper plenum must be within +0 or -50% of the corresponding predicted values in the analysis.

e. Stress due to FIV and RCP Loads

f. Similarity of the Dynamic System Model between FIV and Seismic/LOCA

Category 2 Criterion: The dynamic models in the FIV and in the seismic/LOCA analyses are generally similar except in the assumed boundary conditions. Because of the much larger displacements experienced in seismic and LOCA events compared with those experienced in flow induced vibrations, the assumed boundary conditions in the former type of analysis may be different from those in FIV analyses in order to better simulate the larger displacements anticipated.

Mitsubishi Heavy Industries, LTD.

g. Adverse Flow Effects

Category 1 Criterion: No fluid-elastic instability or lock-in vortex induced vibration is experienced in the pre-operational test.

h. Contingency Plans in Case the Acceptance Criteria are not met

Category 1 Criteria
In case any category 1 criterion is not met, the overall impact on the design of the reactor internals will be evaluated. The reactor will not put into operation until it is sure that the design can accommodate the larger than expected vibration responses.

Category 2 Criteria
In case any category 2 criterion is not met, the difference will be resolved by the post-preoperational test analysis.

4.0 VIBRATION AND STRESS MEASUREMENT PROGRAM

In accordance with the United States Nuclear Regulatory Commission Regulatory Guide 1.20 Revision 3, a vibration measurement program is developed for the first US-APWR unit. US-APWR has reactor internals based on well-proven 4-loop plant but the reactor core is enlarged and the new design structures such as the neutron reflector are adopted. As written in section 1, the reactor internals is classified to "Prototype" for first US-APWR, the pre-operational measurement program is planned.

The purpose of the measurement program is to verify the structural integrity of the reactor internals, determine the margin of safety associated with steady-state and anticipated transient conditions for normal operation, and confirm the results of the vibration analysis.

Instrumentation consisting of the strain gages, accelerometers, pressure transducers and displacement transducers are mounted on the selected assemblies and their specified locations. The lead wires of the transducers inside the reactor vessel will be guided to outside the vessel through the ICIS and / or thermocouples penetrations in the vessel head. The ICIS thimbles and thermocouples will not be installed prior to the core loading.

The measurements will be conducted without a core during cold hydraulic test (CHT) and hot functional test (HFT), and with core but pre-critical phase in initial start-up test (IST). However, the measurement in with the core conditions can be eliminated if it can be shown that the conditions in without the core result severe response relative to without the core conditions. In each stage, testing will be done at all steady state and pump startup / shutdown conditions corresponding to normal and part loop operation.

All of the transducers, lead wires and attachments inside the reactor vessel will be removed after the all measurements will be done.

4.1 The Data Acquisition and Reduction System

4.1.1 Transducer Types and Specifications

The environment of preoperational test including a cold hydraulic test and hot functional test is in water and covered by the conditions of the pressure at about 3100 psi and temperature of [ ] °F. All of the transducers installed inside the reactor vessel should endure these conditions. The insulation tests will be conducted for all of the transducers at a test pressure and temperature in water to confirm their integrity. Helium leak test will be also conducted.

(1) Strain Gage

The frequency response should be ± [ ]% in 0Hz -[ ]Hz to cover the secondary blade passing frequency of [ ] Hz, and the dynamic resolution is expected to be better than [ ] micro strain.

"[   ]" high-temperature weldable strain gages will be used. The gages will be attached to the locations described in previous section by the electrical resistance spot welds. The dual head gages which have two sensing units are bundled to one lead wire will be used to reduce the number of wires through the penetration.

(2) Accelerometer

Two types of accelerometers will be used. One is "[   ]" that will be installed inside the flow hole of the neutron reflector. The frequency response should be better than ±[   ]% in [   ] Hz - [   ]Hz. The other type is "[   ]". The frequency response of this should be in "[   ]". The frequency response of this should be ±[   ]% in [   ]Hz-[   ]Hz to cover the secondary blade passing frequency of [   ] Hz, and the resolution is expected to be better than [   ]g.

The frequency response of this should be ±[   ]% in [   ]Hz-[   ]Hz to cover the secondary blade passing frequency of [   ] Hz, and the resolution is expected to be better than [   ]g.

(3) Displacement Transducer

The frequency response should be better than [   ]% in [   ]Hz-[   ]Hz and the dynamic resolution should be better than [   ] mils.
There are two options for the transducer. One is the cantilever type that is mounted on the top of the neutron reflector and its end is contacted to the core barrel inner surface. A pair of the strain gages is attached on the root to measure the bending strain. The relationship between strain and the relative displacement will be obtained prior to the test. The other option is to use non-contacting eddy current type transducer like "[   ] ". The transducer type will be determined in the detail design phase.

(4) Pressure Transducer

The frequency response should be better than [   ]% in [   ]Hz- [   ]Hz to cover the secondary blade passing frequency of [   ] Hz. "[   ]" will be selected.

4.1.2 Transducer Locations

The type, number and locations of the measurement program instrumentation are shown in Table 4.1-1 and Figures 4.1-1 through 4.1-8. The lead wires of transducers will be guided along the reactor internals surface and go through the penetrations on the reactor vessel head.

(1) Core Barrel / Lower Core Support Plate

The core barrel and the lower core support plate are enlarged in their diameters from current The frequency response of this should be ± [   ]% in [   ]Hz - [   ]Hz to cover the secondary blade passing frequency of [   ] Hz, and the resolution is expected to be better than [   ]g.
4-loop plants, which affect to the excitation force and the vibration characteristics of the lower internals assembly.

Three pressure transducers are installed on the outer surface of the core barrel as the inputs to evaluate the forcing function of the down comer.

To confirm the vibration response of beam mode for the lower internals, three strain gages are needed to separate the vibration response of horizontal two directions and a vertical direction; however, total four gages will be installed in considering of the redundancy. These strain gages will be installed on just below the core barrel flange outer surface. Furthermore, two additional gages will be installed on inner surface to confirm the stress caused from local bending of the core barrel flange.

Accelerometers are needed to be installed on outer surface of the core barrel to obtain the shell mode responses. In order to confirm the response against the 1st frequency of the pump pulsation (approx.[   ]Hz), the shell mode natural frequencies up to [   ]Hz should be identified. According to the tentative analysis results, acquisition of 4th mode is corresponding to this target, and thus four accelerometers will be installed.

An accelerometer will also be installed on the center of lower surface of the lower core support plate to acquire the vertical vibration characteristics.

The frequency response of this should be ± [   ]% in [   ]Hz - [   ]Hz to cover the secondary blade passing frequency of [   ] Hz, and the resolution is expected to be better than [   ]g.

(2) Neutron Reflector / Tie Rod

Since a neutron reflector is the new design structure, it is necessary to acquire the basic behavior data and confirm that unexpected vibration does not occur. Four accelerometers in radial direction will be installed to consider the symmetry and redundancy, and an accelerometer in vertical direction will be installed. The relative displacement between neutron reflector and core barrel is also measured. Two displacement transducers will be mounted on the top surface of the neutron reflector.

A tie rod of the neutron reflector is also the new design structure and its natural frequency is predicted to be low, it is planned to acquire the vibration response to confirm the structural integrity. Two strain gages will be installed for a tie rod.

(3) Lower Plenum Structures

In regards to the lower plenum structures, these structures consist of two sub assemblies, the upper diffuser plate assembly and the lower diffuser plate assembly. All of the diffuser plate support columns (here after support columns) are tightly connected by the diffuser plate; so the

expected vibration response of each support column should be similar. In addition, the natural frequency of the assembly and the stress of support columns can be confirmed by the strain measurement on a support column for the each assembly. Considering the original design of these structures, the strain on two support columns will be measured for each assembly to maintain sufficient redundancy. Six strain gages are installed to the upper diffuser plate support columns to evaluate the horizontal, rotation and oval motions, and five strain gages are installed to the lower diffuser plate support columns to evaluate the horizontal, vertical and rotation motions.

(4) Upper Core Support / Upper Core Plate

The upper core support and the upper core plate are enlarged in their diameters from current 4-loop plant, which affect to the forcing function of the upper plenum. To obtain the forcing function, a pressure transducer is installed on lower surface of the upper core support plate rim.
The design difference also affects the vibration characteristics of the upper internals assembly. To confirm the vibration response of beam mode for the upper internals, strain gages will be installed on the top end of upper core support skirt. Two strain gages are needed to confirm two directional behaviors. An accelerometer will also be installed on the center of upper surface of the upper core support plate to acquire the vertical vibration characteristics.

(5) Upper Plenum Structures

A top slotted column is a first-of-a-kind design in US-APWR. For this component, three strain gages are installed to obtain horizontal two directional responses and for the redundancy. Although the upper support column design is almost the same as that of the current 4-loop plant, it is planned to measure since the flow pattern in the upper plenum will be changed from the current 4-loop plant. Two strain gages are installed for this component.
The mixing device and the level instrumentation support tube are not instrumented because these components are located where the cross flow velocity is not so high, and have been successfully used in the conventional plants.

(6) RCCA Guide Tube

The guide tube design in the US-APWR has been changed from that of current 4-loop plant as following points;
- Adoption of square pipe for the lower guide tube enclosure,
- Extension of the upper guide tube.
Therefore, strain gages will be installed to confirm the vibration characteristics and the response on both top end of the lower guide tube and bottom end of the upper guide tube. Three strain gages will be installed to obtain three directional responses for one specific lower guide tube. For the same guide tube, two strain gages will be installed in upper guide tube. In addition to that, two strain gages will be installed on another lower guide tube in consideration of the redundancy

since guide tube has a safety related function and one of the most important subassembly of the reactor internals. The guide tube closest to outlet nozzle will be selected to the measurement.

(7) Head Plenum Structures

The excitation force in head plenum is predicted not to be severe because the flow velocity in this area is not so high. Therefore, the measurement for head plenum structures such as the thermocouple conduit support columns and the ICIS thimble assemblies are unnecessary.

(8) The transducers exterior the reactor vessel

Accelerometers will be mounted on the bottom and head vessel in order to monitor the base motion.

4.1.3 Precautions to Ensure Acquisition of Quality Data

All of the transducers are tested before they are installed to the components. Autoclave test at each test temperature and pressure for 24hours, and the sensitivity, background noise level and resistance of each transducer is confirmed after the test. The calibration test for all transducers will be also performed in this phase.
The frequency band from [   ] Hz to [   ] Hz, which covers second blade passing frequency of RCP, should be recorded. Theoretically the upper frequency limit is a half of the sampling rate, and then the sampling rate should be over [   ] Hz. In this program, the sampling rate is set to [   ] Hz considering some margin.

4.1.4 Online Data Evaluation System

The data recording system is designed to record the time historical electrical signals from the transducers on the data storages of the personal computer as the digital data.
The transducers hard cable (mineral insulation cable) will be terminated at a junction box. The signal is connected to the data acquisition system via the soft cable. The charge signals from the accelerometers and pressure transducers will be input to charge amplifiers, while strain gages will be connected to dynamic strain amplifiers to convert to the voltage signal. These voltage signals will be lead to the personal computer via the frequency filters and the analog-digital (A/D) converters.
The signal level of each transducer will be checked prior to the test to adjust the gains of the charge amplifiers for the accelerometers and pressure transducers. The dynamic strain amplifiers will be balanced and their sensitivities will be selected.
The spectrum of each signal will be monitored through the test to verify the recording process and adequacy of the level of data signals.

4.1.5 Procedure for Determining Frequency, Modal Content and Maximum Values of Responses

Reduction of the data will be done during the test to determine whether the responses are within the acceptable or not. The spectrum analyzer will be used to analyze the natural frequencies of each component, and the vibration characteristics obtained from the measurement results will be compared with the prediction analysis results described in section 3.4. The maximum stress values will be also calculated to confirm the structural integrity.

4.1.6 Bias Errors and Random Uncertainties

Acceptance criteria, described in section 3.5, are the maximum values. These values do not reflect the effect of bias errors and / nor uncertainties due to errors in the measured values. Bias error and uncertainty depend on the accuracy of both the acquisition and reduction of the data. The accuracy of the data acquisition is primarily a function of instrument error, and the accuracy of the data reduction is a function of the number of data samples, the bandwidth, etc. Thus the all bias errors and random uncertainties are defined after the specification of data acquisition systems is determined.

Table 4.1-1 Reactor Internals Transducers Arrangement

| Subassembly	Transducer Type	Number	Sensitive Direction
Core Barrel	Strain Gages	6	axial
	1-D Accelerometers	4	radial
	Pressure Transducers	1	-
Lower Core Support Plate	1-D Accelerometers	1	vertical
Neutron Reflector	1-D Accelerometers	5	vertical: 1 radial: 4
	Displacement Transducers	2	radial
Tie Rod	Strain Gages	2	axial
Upper Diffuser Plate Support Column	Strain Gages	6	axial
Lower Diffuser Plate Support Column	Strain Gages	5	axial
Upper Core Support	Strain Gages	2	axial
	1-D Accelerometers	1	vertical
	Pressure Transducers	1	-
Upper Support Column	Strain Gages	2	axial
Top Slotted Column	Strain Gages	3	axial
Upper Guide Tube	Strain Gages	2	axial
Lower Guide Tube	Strain Gages	5	axial
Sub Total	Strain Gages	33	-
	1-D Accelerometers	11	-
	Displacement Transducers	2	-
	Pressure Transducers	4	-
Total		50	-
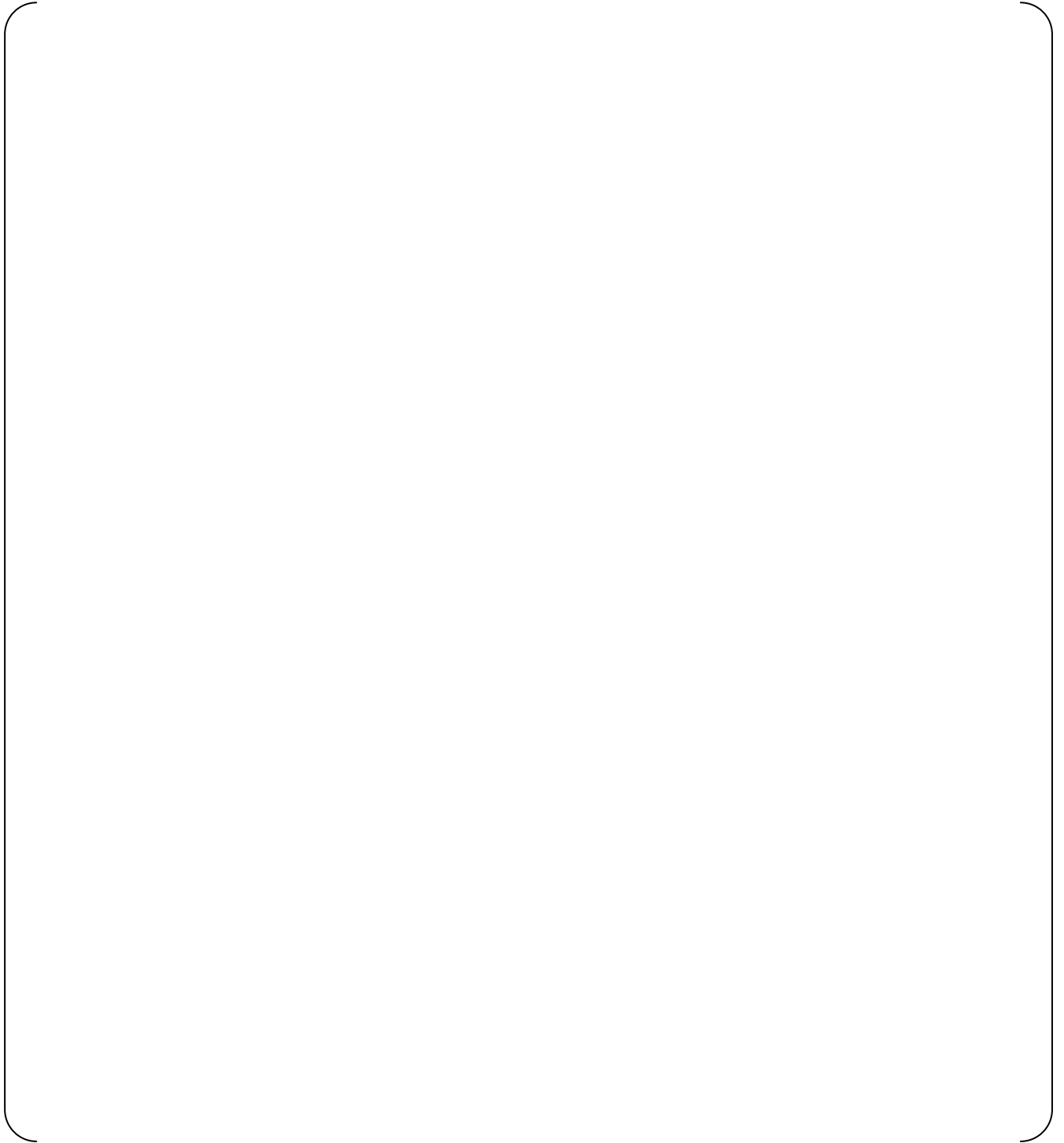
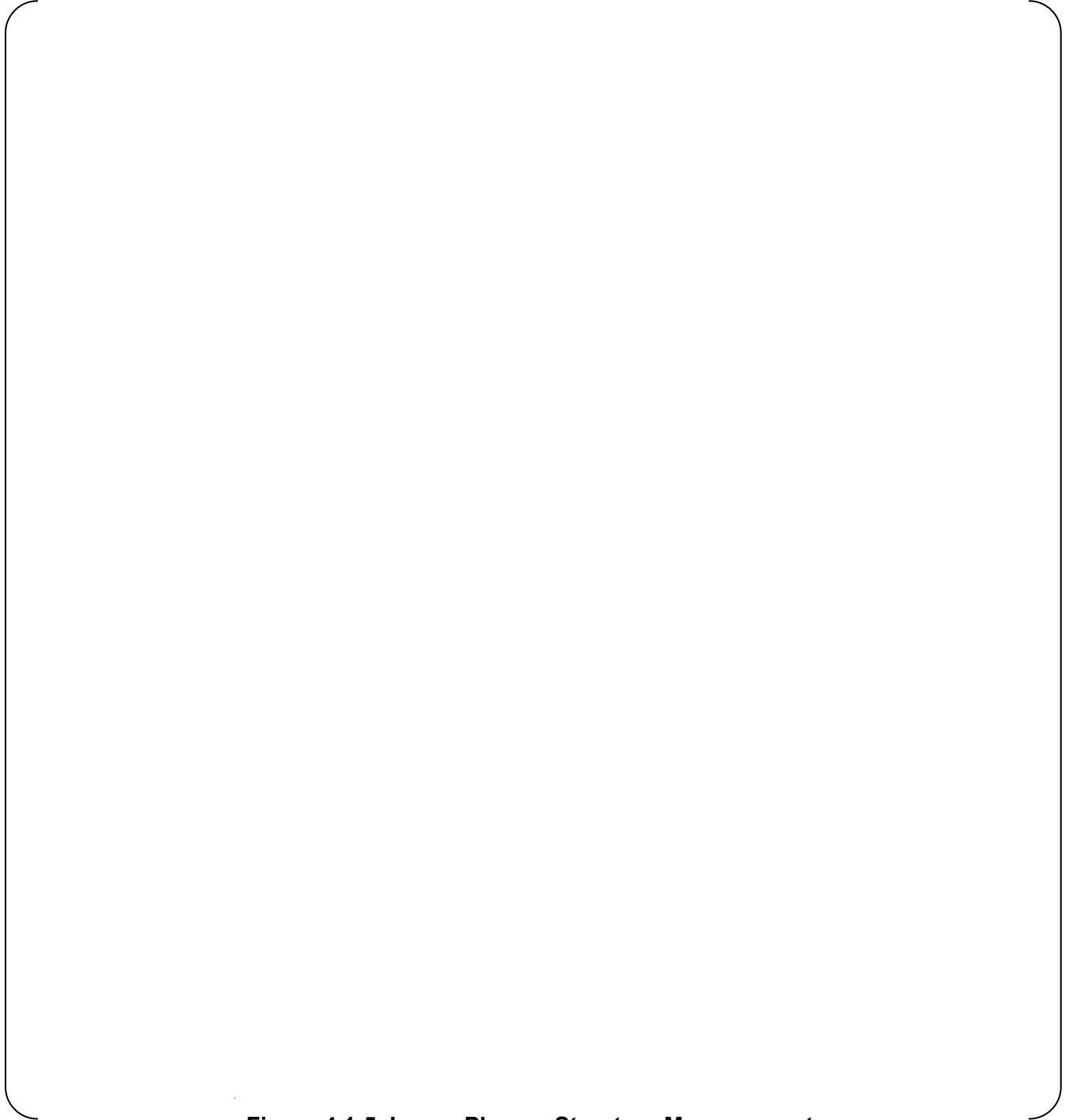**Figure 4.1-1 Schematic View of Transducers Arrangement**
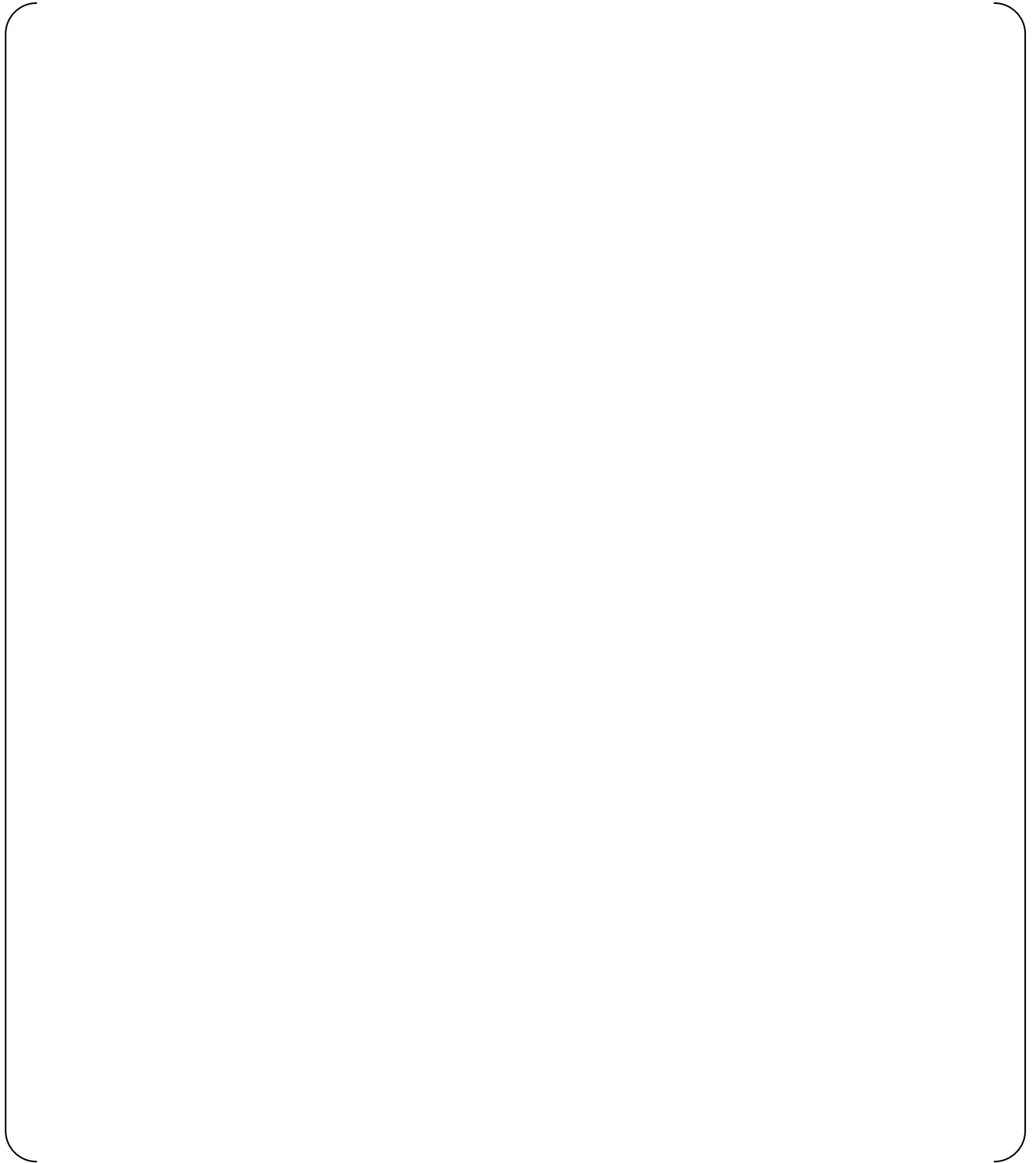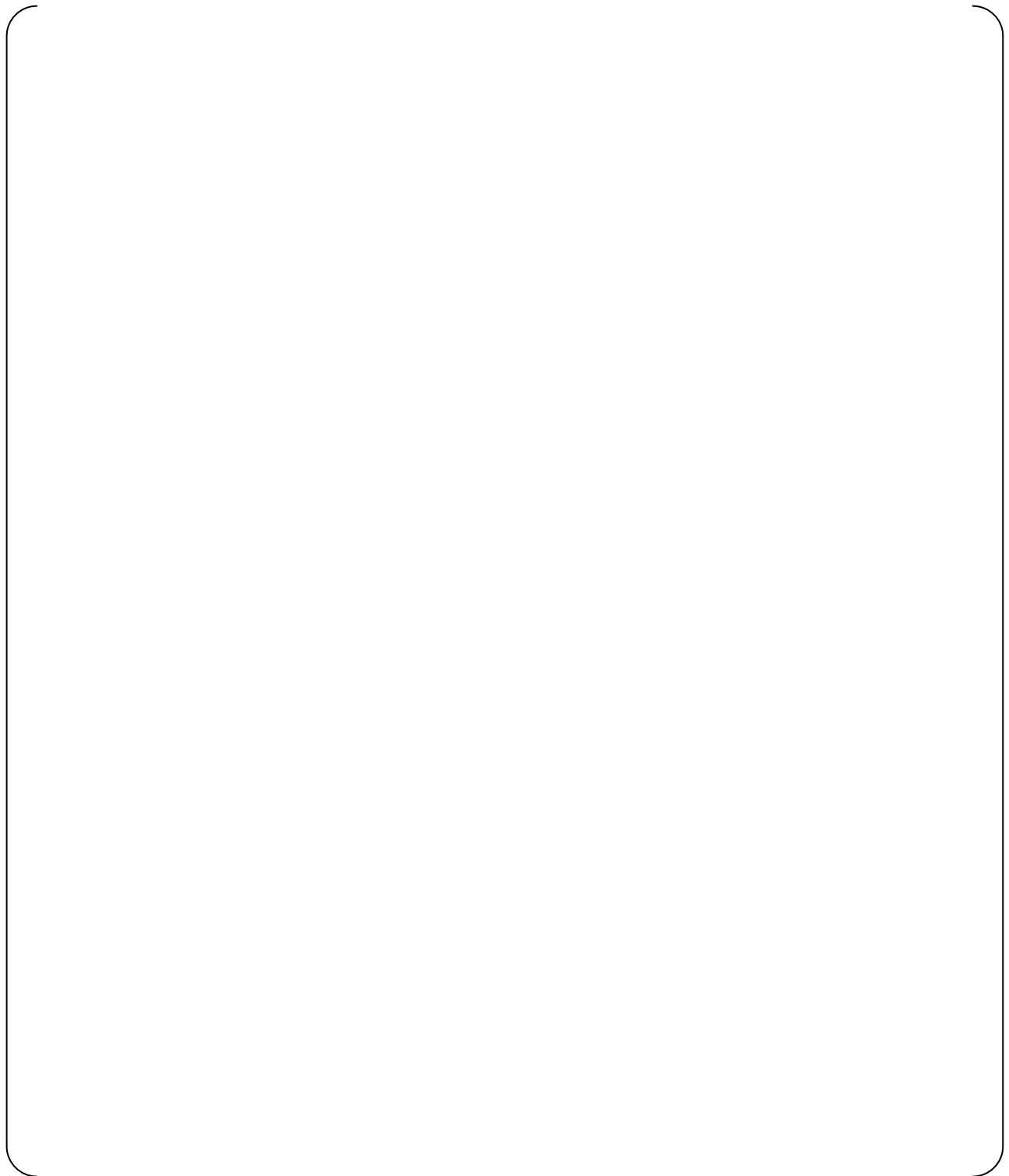
Figure 4.1-2 Core Barrel Measurement
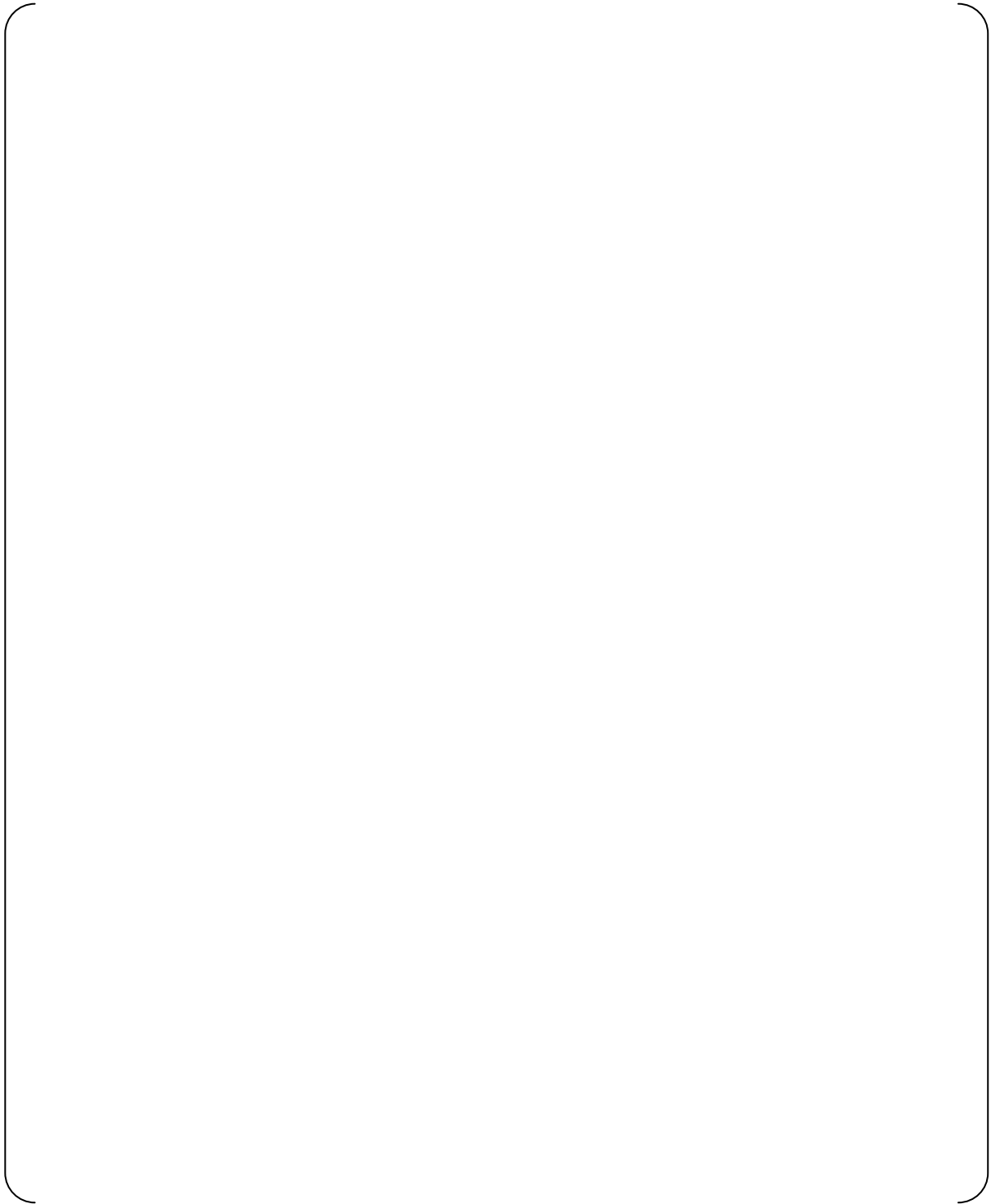
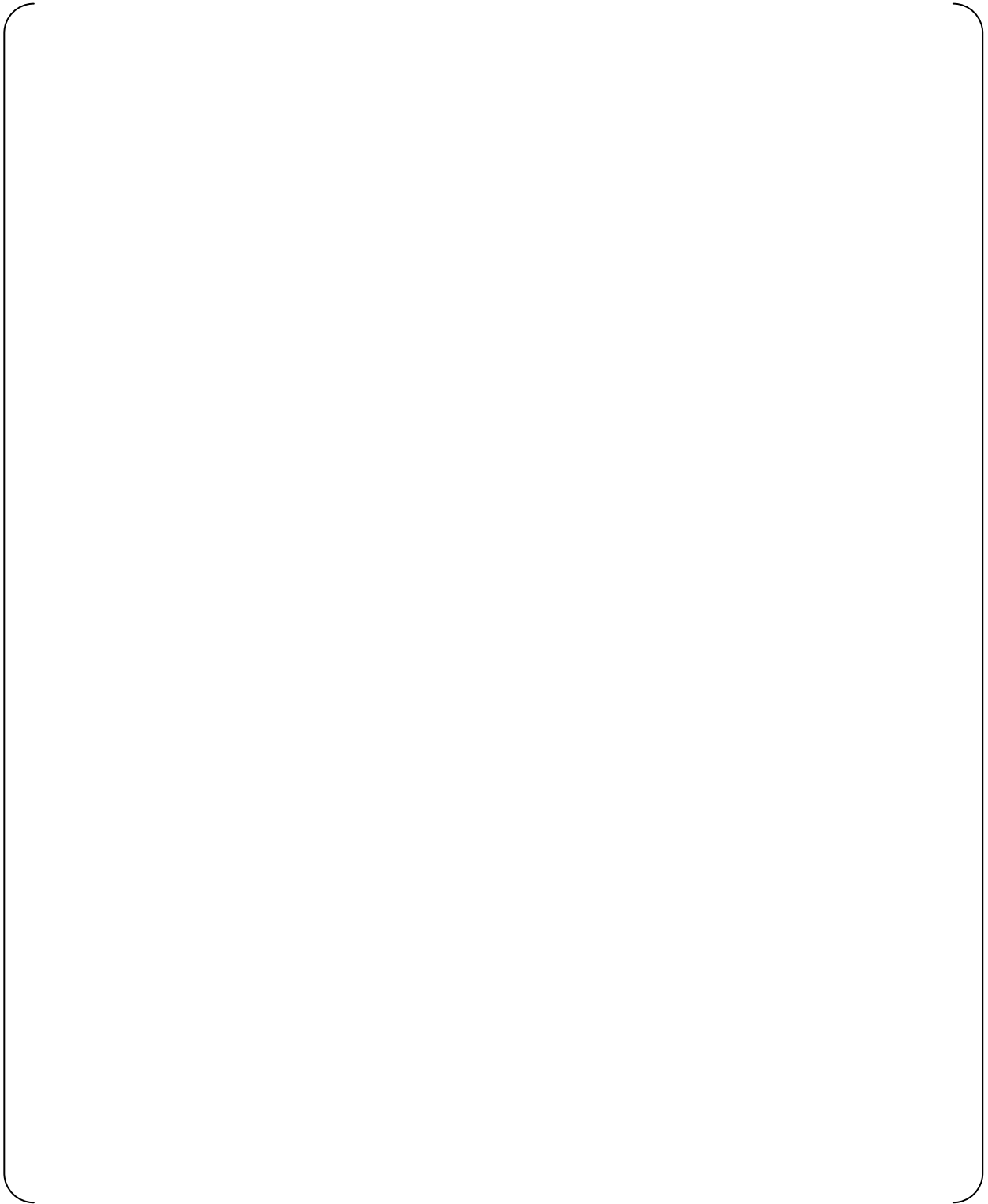**Figure 4.1-3 Neutron Reflector Measurement**
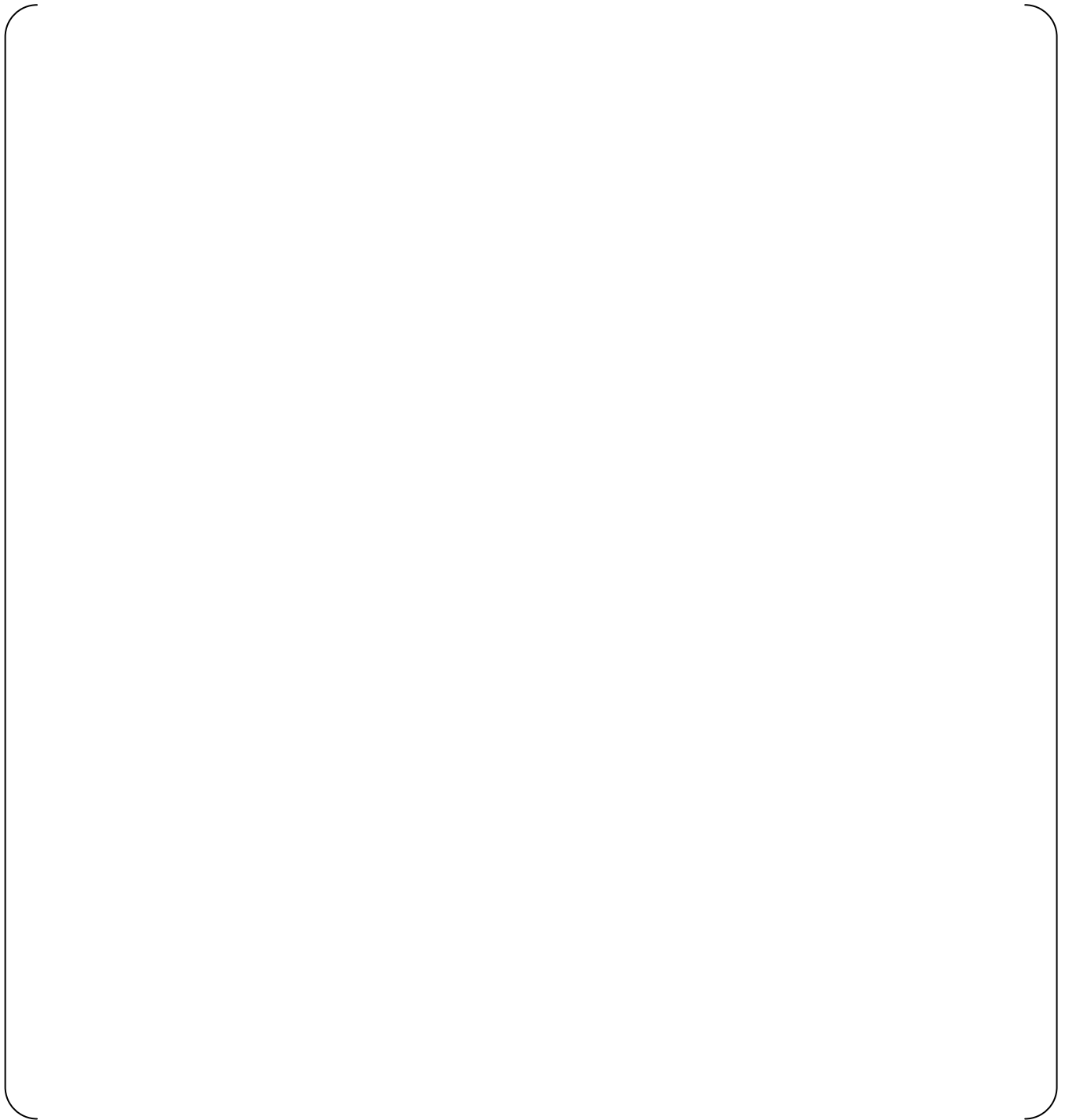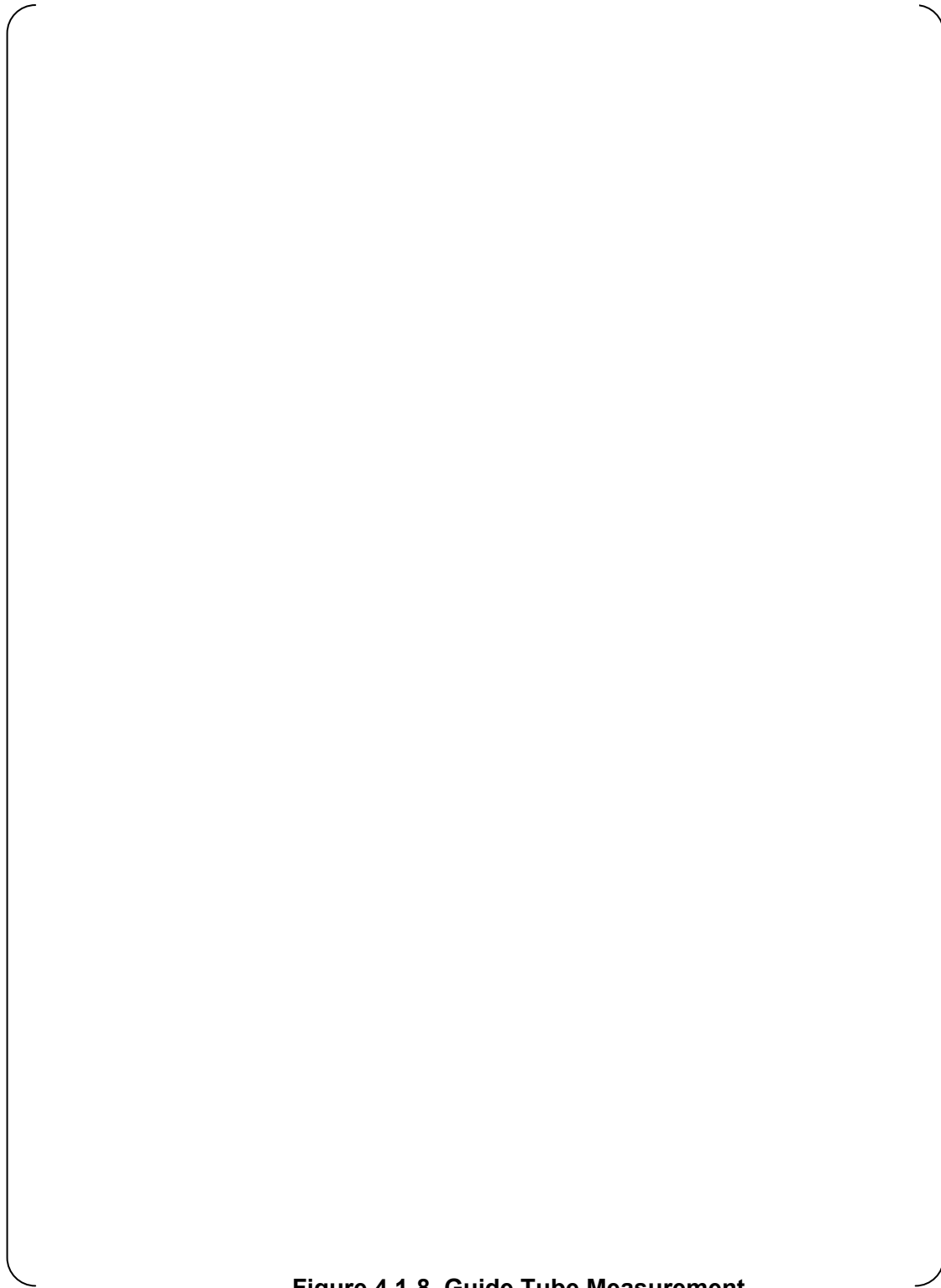
Figure 4.1-4 Tie Rod Measurement

Figure 4.1-5 Lower Plenum Structure Measurement

Figure 4.1-6 Upper Core Support Measurement

Figure 4.1-7 Upper Support Column Measurement

Figure 4.1-8 Guide Tube Measurement

4.2 Test Conditions

4.2.1 Operating Modes

Measurements will be conducted during the cold hydraulic test (CHT) and the hot functional test (HFT). The flow rate and the temperature is changed in these test phases, the responses will be varied depending on these conditions, i.e. as a function of dynamic pressure. Since the fluid density is larger in lower temperature, it is expected that the vibration response in a cold full flow condition is the maximum.

The data will be recorded at no pump operation condition to obtain background noise, startup and shutdown transient to record mean strains and transient vibration behavior that, and steady-state operations condition of the possible pump combinations to obtain vibration response of the instrumented components during various flow conditions.

4.2.2 Duration of Tests

Recording time for each steady pump operation condition will be determined to allow for proper signal averaging in later analysis.

4.2.3 Disposition of Fuel Assemblies

Since dynamic response of each structure depends on the excitation force and vibration characteristics of itself, in general, the excitation force which is close to a natural frequency of the structure will produce a larger response. In this section, the effects of the core on the vibration characteristics of the components and the hydraulic loading are discussed to determine the more conservative test conditions.

The presence of the core has following effects;
  -change in the flow rate due to the increase of the pressure drop in the core region,
  -changes in pump pulsation loads due to the flow resistance in the core region,
  -changes in the natural frequencies of structures due to the additional mass of the fuel
    assemblies and reaction force caused by the hold down springs

Analyses have been done for both without and with the core conditions considering the differences mentioned above as written in section 3.4.3. The results show that the amplitudes of vibration response due to the flow turbulence were decreased in with the core conditions at all components and locations. This is mainly because the flow rate without core is larger relative to with the core conditions, while the natural frequencies of beam and shell modes of each component were almost unchanged as shown in section 3.2.2. Pump pulsation loads with core conditions will be lower due to the acoustic damping in core region so that the vibration responses will be decreased from without the core conditions.

In conclusion, without the core conditions will result in higher response than with the core conditions, and thus the test is conducted only during HFT without the core.

5.0 INSPECTION PROGRAM

The internal components of all US-APWR plants will be inspected before and after the hot functional test. The reactor internals will not be considered adequate and pass the comprehensive vibration assessment program unless no indication of harmful sign, abnormally large vibration amplitudes or excessive wear is detected.

- Acceptance Criteria

  Broken components and / or excessive wear or deformation is not observed in the post-hot functional test inspection.

6.0 EVALUATION

The results of the vibration and stress analysis, measurement, and inspection programs will be reviewed and correlated to determine the extent to which the test acceptance criteria as described in Subsection 3.5 are satisfied.

7.0 CONCLUSIONS

- The US-APWR reactor internals represent a unique, first of a kind design because of its design, size, arrangements and operating conditions. Therefore, the first US-APWR will be classified as a Prototype in accordance with the United States Nuclear Regulatory Guide 1.20 Rev.3 (Reference (1)).

  Upon qualification of the first US-APWR as a valid prototype, subsequent plants will be classified as Non-Prototype Category I.

- Alternating stress levels of reactor internals due to flow induced vibrations are acceptably low in comparison with the limit for high cycle fatigue that is specified in the ASME Code.

- The difference in reactor internals vibration characteristics, such as the natural frequency of the core barrel, is very small with or without the core. The vibration responses without the core are the same or slightly larger than those with the core. These are because of the flow rate increase with the elimination of fuel assemblies and the subsequent pressure loss. Thus, in the preoperational test of the prototype plant, the results of vibration measurements after the core loading are bounded by the measurements before the core loading and only measurements before the core loading will be necessary.

- Measurements will be performed during the pre-operational test to confirm the vibration characteristics and structural integrity of the Prototype US-APWR reactor internals.

- The reactor internals of all US-APWR plants will be inspected before and after the hot functional test. The reactor internals will not be considered adequate and pass the comprehensive vibration assessment program unless no indication of harmful sign, abnormally large vibration amplitudes or excessive wear is detected.

8.0 REFERENCES

(1) Preoperational Vibration Assessment Program for Reactor Internals during Preoperational and Initial Startup Testing. Regulatory Guide 1.20, Rev.3, U.S. Nuclear Regulatory Commission, Washington, DC, March 2007.

(2) "Nuclear Power Plant Components," ASME Boiler and Pressure Vessel Code. Section III, Division 1, American Society of Mechanical Engineers. Includes: NCA, NB, NC, ND, NF, NG, Code Cases and Appendices including Appendix I, F, and N, 2001 edition thru 2003 Addenda.

(3) ANSYS, Finite Element Structural Analysis Program, Release 11.0, ANSYS, Inc., Canonsburg, PA, 2007.

(4) "Flow-Induced Vibration of Power and Process Plant Components: A Practical Workbook", M.K.Au-Yang ,2001, ASME Press.

(5) Au-Yang, M.K. and Connelly, W.H. A Computerized Method for Flow-Induced Random Vibration Analysis of Nuclear Reactor Internals. Nuclear Engineering and Design 42, 1977, pp 277-263.

(6) Au-Yang, M.K, "FLOW INDUCED VIBRATION TEST OF AN ADVANCED WATER REACTOR MODRL PART1 TURBULENCE –INDUCED FORCING FUNCTION", PVP Vol.273, pp43-69, Flow Induced Vibration ASME 1994.

(7) APWR Reactor Internals 1/5 Scale Model Flow Test Report. MUAP-07023, Mitsubishi Heavy Industries, Ltd. December 2007.

(8) "Pressure spectra in turbulent free shear flows", Journal of Fluid Mechanics, 1984, vol. 148, pp. 155-191

(9) A.W.Guess 1975 Journal Sound and Vibration 40(1), pp119-137 Calculation of Perforated Plate Liner Parameters from Specified Acoustic Resistance and Reactance

(10) "Flow-Induced Vibration of Power and Process Plant Components: A Practical Workbook", M.K.Au-Yang ,2001, ASME Press

Appendix-A Comparison of US-APWR with J-APWR and J-APWR SMT

The data in the J-APWR scale model test (SMT) was used to confirm the adequacy of MHI's flow-induced vibration analysis methodology and as a comparison reference for the response level of reactor internals. The results of structural integrity evaluations for reactor internals flow induced vibration in the J-APWR SMT benchmark analysis were not directly applied to the US-APWR vibration assessment, as explained below.

As shown in the analysis flow diagram, Figure 3.1-1 of MUAP-07027-P, Revision 1, the measured natural frequencies and the vibration response levels were used as reference data for the validation of the analysis methodology through the benchmark flow-induced vibration analysis of the scale model used in the J-APWR SMT. In addition, the normalized pressure power spectral densities (PSDs) measured in the downcomer of the J-APWR SMT were used in both the J-APWR SMT benchmark analysis and the US-APWR prototype flow-induced vibration analysis. This was based on the similarity of the downcomer geometrical dimensions and flow rate as discussion in answer (a) (below).

Responses to the pertinent RAIs are given in (a) through (f) below:

 (a) Comparison of the Reactors - Current 4-loop/J-APWR/US-APWR Plants:
 The key specifications of the reactors for the current 4-loop, J-APWR, and US-APWR are summarized in Table A-1 (below).

The core lengths in the J-APWR and US-APWR are different, but the number of fuel assemblies is the same. The dimensions of the reactor vessel and the core barrel are also the same as is the flow rate. These parameters do differ from the current 4-loop plants with the exception of the core barrel (downcomer) length.

Therefore, the flow-induced vibration response characteristics of the US-APWR reactor internals are similar to those of the J-APWR.

(b) Comparison of dimensionless parameters between the J-APWR SMT and the US-APWR

   plant:

The dimensionless parameters related to the flow-induced vibrations, the Reynolds number (Re), and the reduced velocity (Ur) for the J-APWR SMT, J-APWR plant, and US-APWR plant are shown in the Table A-2. In addition, the Strouhal numbers (St) are also summarized in the same table for structures exposed to cross-flow in the lower and upper plenums.

i)   Reynolds number

 Under operating conditions of a PWR, the coolant flow inside the reactor vessel will be in the turbulent flow regime. It is considered that the flow characteristics would remain the same in sufficiently developed turbulent flow regime. The transition from laminar flow to turbulent flow

occurs at Reynolds number (Re = U D / ν) around 10^3 in general. For this reason, we selected the scale model test condition to keep the Reynolds number greater than 10^4.

As shown in the TableA-2, sufficiently high Reynolds number was maintained in the downcomer, lower plenum and upper plenum under the test conditions of the J-APWR SMT. This is also true under plant operating conditions.

ii)   Reduced velocity

The reduced velocity (Ur = U / (fn D)) is generally used in dimensional analysis of flow-induced vibration. Ur represents the ratio of the path length per cycle (U / fn) to the model width (D). From another view point, Ur represents the ratio of the fluid force frequency (proportional to U / D, the vortex shedding frequency (fs) is a typical example) to the natural frequency of the model. As shown in Table A-2, the reduced velocities in the J-APWR SMT were close to those under the J-APWR plant operating conditions and were also similar to those of the US-APWR plant.

iii)   Strouhal number

The Strouhal number (St = fs D / U) is the non-dimensional parameter for the vortex shedding frequency. As is well known, St of a cylinder in cross-flow is almost constant (around 0.2) below the critical Re number based on the cylinder diameter. As shown in Table A-2, St in the SMT, at room temperature, was also around 0.2. But under plant operating conditions, St will be around 0.3 because the Re will be in the super critical region. So the evaluation based on the analysis as shown in the Table 3.2-4 of MUAP-07027-P, Revision 1, is also required for checking vortex shedding lock-in, even though lock-in was not observed in the SMT.

(c)   Effect of fuel assemblies on the flow

The fuel assemblies have little effect on the reactor vessel flows, including cross flows in the lower and upper plenums, for reasons given below.

The maximum cross-flow distribution in the upper plenum depends on the outlet nozzle flow velocity and geometries of structures near the outlet. It does not depend on the core outlet flow distribution into the upper plenum. And because of a small increase of total flow rate with a lower pressure loss in the core, the maximum cross flow velocity in the upper plenum during the hot functional test without the core will be higher than that under normal operating condition.

The maximum cross flow distribution in the lower plenum depends on the flow velocity in the downcomer and the geometries of structures in the peripheral region of the lower plenum. It does not depend on the core inlet flow distribution in the downstream side. And because of the increase of total flow rate with lower pressure loss in the core, the maximum cross flow velocity in the lower plenum during the hot functional test without the core will be higher than that under normal operating conditions.

Therefore, the mechanical integrity of structures subjected to cross-flow in the lower and upper plenums can be conservatively verified without the fuel assemblies.

(d)   The bypass flow rate from the outlet nozzle gap between the Core Barrel/RV under plant operating conditions will not be larger than that during the pre-operational test, because the gap clearance is designed to be minimum under normal operating conditions as a result of core barrel thermal expansion.

In any case, the bypass flow through the outlet nozzle gap has little effect on the core barrel vibration because both the flow rate and the surface area of the flow channel are much smaller than those of the downcomer flow.

The difference of operating point on the reactor coolant pump (RCP) Q-H curve has been considered in the estimation of test flow rate from that under normal operating conditions with the fuel loaded.

(e) There is little need for fuel assembly vibration measurement in the pre-operational or start – up test because of following reasons.

i)   Flow induced vibration response of the fuel assembly will be confirmed in a full size mock-up test.
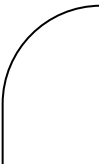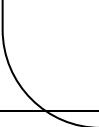
ii)   Vibration of the fuel assemblies in the core can be checked by spectral analysis of the ex-core nuclear instrumentation signals in the start-up test, if needed.

Table A-1 Comparison of Reactor of Current 4-loop /J-APWR / US-APWR

	Current 4-loop	J-APWR	US-APWR
Number of RC Loops	4	4	4
Numbers of Fuel Assemblies	193	257	257
Core length (ft)	12	12	14
Downcomer length (inch)	[ ]	328	328
Vessel Inside Diameter (inch)		202.8	202.8
Numbers of RCCA/GT	53	69 / 77 / 85	69
Loop flow rate for Mechanical Design (GPM)	[ ]	129,000	130,000
Structure around the core	Core Baffle	Neutron Reflector	Neutron Reflector

Table A-2 Comparison of Dimensionless Parameters between J-APWR SMT, J-APWR plant, and the US-APWR Plants

	J-APWR plant	J-APWR 1/5 SMT	US-APWR plant

Downcomer /Core Barrel
  Flow Velocity U (m/s)
  Annulus width h (m)
  Core barrel fn (Hz)			

Re=Uh/ν Vr=U/fnh			

Lower plenum / Lower Diffuser Plate Support Colum
  Flow Velocity U (m/s)
  Column diameter D (m)
  Column fn (Hz)			

Re=Uh/ν
   Vr=U/fnD
   St =fs D/U			

Upper Plenum / Top Slotted Colum
  Flow Velocity U (m/s)
  Column diameter D (m)
  Column fn (Hz)			

Re=Uh/ν
   Vr=U/fnD
   St =fs D/U			

Appendix–B Conversion of Forcing Functions from the Scale Model Test to those under Plant Operating Conditions

1. Analysis procedure, modeling and forcing functions

The analysis procedure, modeling and forcing functions for the US-APWR prototype are discussed below.

As described in Subsection 3.1.1 of the vibration assessment program report MUAP-07027-P, Revision 1, the FIV analysis program consists of two separate tasks. One was to validate the analysis method by calculating the responses of the model used in the J-APWR scale model test (SMT) and the other was the prototypical analysis of the US-APWR. The structural model and the forcing functions were customized for each task as follows.

Task 1: J-APWR SMT benchmark analysis

This task was performed to validate the analysis method.

All properties in the scale model benchmark analysis were adjusted to 1/5 scale. The structural model of the reactor internals was developed based on the full scale J-APWR drawings and scaled down following the scaling laws for each parameter. The stiffness of the test vessel support, which did not simulate that in the actual plant, was determined based on the measured natural frequency in the tapping test.

The forcing functions for the scale model benchmark analysis were determined at the test flow rate at room temperature consistent with the SMT conditions.

Task 2: Analysis for the US-APWR prototype

The analysis of the US-APWR was performed with a full scale model and forcing functions for the US-APWR. Tables B-1 give a side-by-side comparison of the US-APWR and the J-APWR SMT benchmark analyses.

In the US-APWR analysis, the model properties were developed based on the drawings of US-APWR in the same manner as in the J-APWR SMT benchmark analysis.

The flow-induced forcing functions in the horizontal direction were scaled from the J-APWR SMT as shown in Table B-2.

For the downcomer turbulence and the cross flow loads in the upper plenum, the force time history data generated for the 1/5 SMT in the J-APWR analysis were directly converted to those

of the US-APWR prototype in the following manner. Conversion ratios C1, C2 and C3 were factors for the force area, the dynamic pressure and time (or frequency), as shown in Table B-2. Here, the constants of proportionality are assumed to be the same because the structural configurations and flow conditions are the same in these regions in both plants. .

$$Fuspro (t) = C1 \, C2 \, F \, jsmt(\, t/C3)$$

Here,

      Fuspro: force for analysis of the US-APWR prototype
      Fjsmt : force for the benchmark analysis of the 1/5 scale model of the J-APWR
      t   : time

This scaling process has been validated by comparison of the normalized PSDs measured in a PWR scale model test under room temperature and that of plant field data by Au-Yang as shown in the Figure 8.17 in Reference (B1). Similarity between the US-APWR SMT and the Au-Yang data was also shown in Figure B-2.

For the lower plenum cross flow loads, the original forcing functions in the US-APWR prototype were re-constructed for the diffuser plate columns, because the diameters of these columns are different from those of the BMI columns in the J-APWR.

The vertical loads and the RCP pulsation loads were also developed specifically for the US-APWR prototype.

2. Validation of the analysis method

The validation of the method of structure modeling was conducted by the comparing the computed natural frequencies of the J-APWR SMT with the measured data, as discussed in Subsection 3.2.1 of the Vibration Assessment Program Report MUAP-07027-P, Revision 1.

The validation of the forcing functions was confirmed by comparing the computed responses of the model in the J-APWR SMT with the measured responses as discussed and verified in Subsection 3.2.3 of the Vibration Assessment Program Report MUAP-07027-P, Revision 1. In addition, the scaling of the forcing function from a SMT to that in a PWR under operating condition has been validated through the comparison of the normalized PSD measured in a PWR scale model test and the corresponding field test data from a full scale plant by Au-Yang as shown in Figure B-1 (Figure 8.17 in Reference(B1)). Agreement between the normalized data from the US-APWR SMT and the Au-Yang data is also shown in Figure B-2, with the exception of the J-APWR SMT data at 90 degrees in the upper and middle locations of the reactor. It is not surprising that these last two data sets showed larger forcing function than the others because these two measurement points were close the inlet nozzle.

Reference

(B1)   "Pressure spectra in turbulent free shear flows", Journal of Fluid Mechanics, 1984, vol. 148, pp. 155-191

Table B-1 Comparison of the models in the benchmark analysis of the J-APWR SMT and the US-APWR prototype vibration assessment

	J-APWR SMT model	US-APWR Proto-type model
Configurations and dimensions	1/5 of J-APWR	1/1 of US-APWR
Properties of Vessel support stiffness	Test vessel support	Plant design value
Reference temp. for metal / fluid material properties	Room temp.	Temp. in normal operation
Vessel Inlet Flow rate for flow velocity definition	28,200 / 25 m^3/h/loop (=test condition)	29,600 m^3/h/loop

Table B-2 Conversion of Flow- Induced Forcing Functions from the J-APWR SMT into US-APWR prototype

	Fjsmt: Forcing function for J-AWR SMT	C1: Scale effect on force area	C2: Ratio of ρv^2	C3: Scale effect on time
Down comer Turbulence	Measured data in J-APWR 1/5 SMT	25	[ ]	5
Cross flow loads in Lower Plenum	Reference (B1) Figure 9-5	Defined with the US-APWR configuration		
Cross flow loads in Upper Plenum structures	Reference (B1) Figure 9-5	25	[ ]	5

Figure B-1 Comparison of empirical normalized PSD equation with field measured data (Au-Yang and Jordan,1980, Figure 8-17 in Reference (B1)
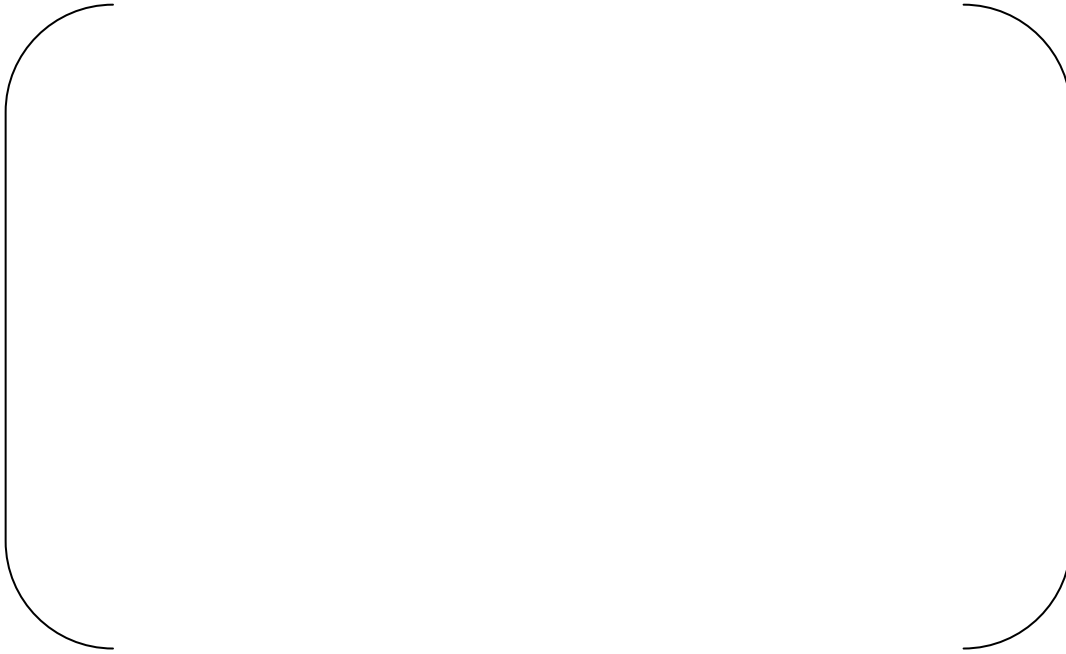
Figure B-2 J-APWR 1/5 SMT D/C NORMARIZED PSD with Au-Yang's empirical equation

Appendix-C   Substituting the downcomer turbulent forcing function with updated data

1. Introduction

 In MUAP-07027-P, Revision1, the downcomer turbulent forcing functions from the data measured in the J-APWR 1/5 scale model test (J-APWR SMT) were substituted with those measured in the US-APWR 1/7 scale model lower plenum test (US-APWR LPT). This document explains the reason of this substitution and its impact on the evaluation results.

2. Back ground

The US-APWR LPT was performed in 2008 after the DCD and MUAP-07027-P, Revision 0, were submitted to NRC. MHI performed a sensibility analysis with the new forcing function replacing that derived from the J-APWR SMT data. As a result, it was confirmed that the new downcomer forcing functions were similar to those derived from J-APWR SMT. On the other hand, re-analyses of reactor internals vibration were needed to obtain input to the stress analyses of the core support structures in 2009.

3. Discussion

It was decided to replace the downcomer forcing functions with the new one from the US-APWR LPT for the following reasons.

a. In general, data from the US-APWR scale model test is more appropriate for analyzing the response of the US-APWR. If the data is available there is no special reason to select other data sets.

b. Comparing the pressure fluctuation PSDs, the difference between the two test data sets was not large as shown in Figures C-1 and C-2, although a more smooth spectrum was obtained in the US-APWR LPT in Figure C-2. A possible reason for the difference was the effect of wiring for the data acquisition system, which was on the outside surface of the core barrel in the J-APWR SMT. This was necessary because there was little free space between the fuel assemblies and the neutron reflector. In the US-APWR LPT, wiring for the data acquisition system was able to be set inside of the core barrel because the fuel assembly and the radial reflector were not included in the scale model.

c. Some improvements in the accuracy of the benchmark analysis with the US-APWR LPT data are identified as shown in Table C-1.

4. Impact on the analysis results and the measuring plan

The effects of substituting the downcomer forcing function with that derived from the US-APWR LPT on the vibration responses were around 2% on both the core barrel and the neutron reflector. So there is little impact on the prediction results for the US-APWR and the measurement plan.

Table C-1 Effect of the difference of downcomer forcing function on the CB / NR Response(J-APWR 1/5 SMT benchmark scaled to actual dimensions)

Components	RMS Response、mil （Ratio to measured results）			Effect of downcomer force change
	Measured*	Analysis* based on J-APWR SMT data	Analysis* based on US-APWR-LPT data	
CB bottom –RV relative displacement				
NR top –CB relative displacement				

*Converted to actual plant scale.

Figure C-1 Down comer pressure PSD measured in J-APWR 1/5 scale model test

Figure C-2 Down comer pressure PSD measured in US-APWR 1/7 scale lower plenum test

Appendix-D   RCP Pulsation Forcing Functions

1. Introduction

The forcing functions of the RCP-induced pressure pulsations for the US-APWR reactor internals were determined from scale model tests of both generic and APWR-specific RCPs.

2. Studies based on the RCP model tests data

The RCP scale model flow tests of generic and APWR-specific types (J-APWR/ US-APWR) were performed. In each test, measured pressure fluctuations were normalized with the total hydraulic head of the RCP. In Table D-1, the measured pressure fluctuation data are summarized.

(1) Total Pressure fluctuations at the RCP outlet
The pressure fluctuations at the RCP outlet including the local turbulence were obtained in all of the tests. The value for the APWR ([ ]% of hydraulic head) was the same or lower than that for the generic RCP ([ ]%).

(2) RCP pulsations related to the rotation speed
In the generic RCP test, amplitudes of the pressure pulsations generated by the RCP shaft rotation and the blade passing frequency were confirmed with spectral analysis as shown in Figure D-1. The largest amplitude was about [ ]% of the total head at the first blade passing frequency NZ. At the RCP shaft rotational(N) and the 2nd harmonic of the blade passing frequencies the amplitudes were about 1/5 of that at NZ.

3. Forcing functions for the US-APWR

The amplitude of the RCP pulsation in the US-APWR were assumed to be the same as that generated by the generic RCPs, rationed by the total hydraulic heads to be conservative. The absolute amplitude is defined with the total head of the US-APWR RCP as shown in Table D-2.

Table D-1 RCP pulsation amplitudes in 1/2 scale model tests

	Over-all fluctuation(0-p) /hydraulic head	Shaft Rotational Speed	Blade Passing Frequency(0-p) /hydraulic head	2nd harmonic of blade Passing
Generic				
APWR				

Table D-2   US-APWR RCP pulsation amplitude for the vibration Analysis

	Shaft Rotational Speed	Blade Passing Frequency	2nd harmonic of the blade passing
Frequency(Hz)			
d H 0-peak / H			
Amplitude(Pa 0-peak)			

Figure D-1 The pressure pulsation spectrum of generic RCP.

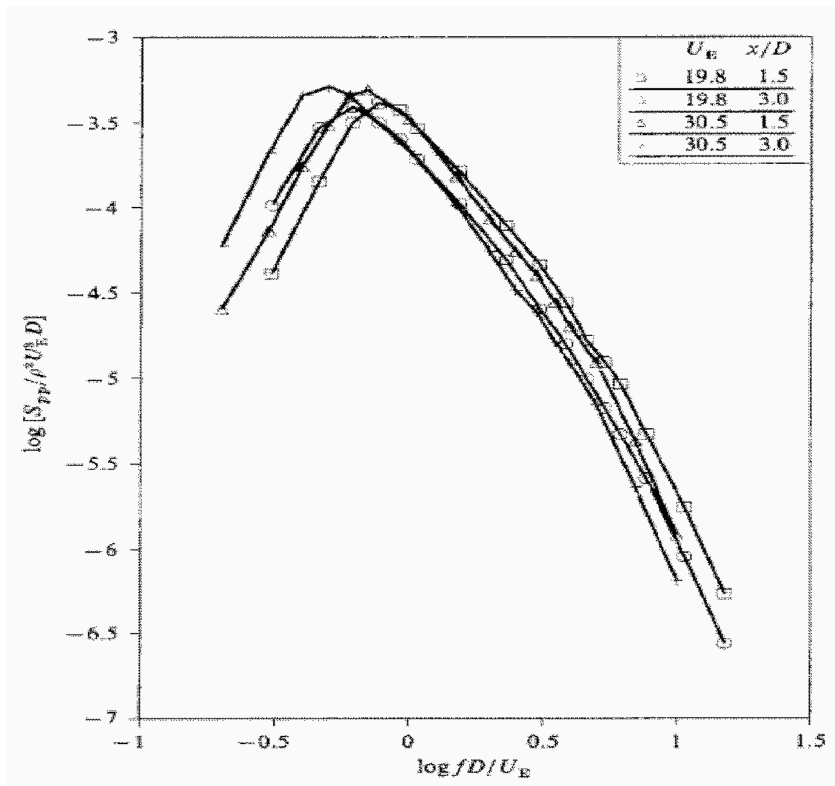**Figure E-1   Normalized pressure PSD for US-APWR UCP/CSP**

Figure E-2 Normalized pressure PSD measured in a jet flow (Reference E1)